European Erasmus Mundus Master

Sustainable Constructions under natural hazards and catastrophic events

Investigation of performance of MRF EBF dual frames with removable links during and after seismic events

Author: Natarajan Aravind

Supervisor: Prof. Ph.D. Raffaele Landolfo, Assist. Prof. Ph.D. Mario D'Aniello

University of Naples Federico II

European Commission

ERASMUS MUNDUS

STATEMENT OF THESIS APPROVAL

This thesis prepared by Natarajan Aravind entitled 'Investigation of performance of MRF EBF dual frames with removable links during and after seismic events' is approved in partial fulfillment of the requirements for the degree of Master of Science by the following faculty members served as the supervisory committee chair and members.

_____,Chair_____

(Date Approved)

_____,Member_____

(Date Approved)

_____,Member_____

(Date Approved)

Student's signature _____

Date of Submission _____

Abstract

KEYWORDS: Dual frames, Seismic Design of frames, Seismostruct, SAP2000, Moment resisting frames, eccentrically braced frames, earthquake, recentering, pushover analysis, time history analysis.

Moment resisting frames and braced frames are both being used extensively as lateral force resisting systems in multi-storey buildings nowadays. While moment resisting frames are known for being ductile, the eccentrically braced frame alternatives provide increasing stiffness but reduced ductility while retaining high energy dissipation capacity. The thesis focusses primarily on the possibility of combining the two systems (MRF and EBF) in order to achieve the best of both worlds (an increased initial stiffness and high energy dissipation at moderate earthquakes with enough reserve ductility for severe earthquakes). This ensures non-collapse of structures at severe ground displacements with easy repair and rehabilitation measures at frequent less severe seismic demands.

A case study is also presented where buildings of different heights (2, 4 and 8 storeys) are designed as dual frames according to the Eurocodes (EC3 and EC8) using moment resisting frames and eccentric bracings with short links. The performance of the frames under seismic loading is observed in order to verify the superiority of such dual frames over both its constituents.

Table of Contents

List of Figures vi
List of Tables ix
Acknowledgements x
Abbreviations xi
Chapter 1 - Introduction 1
1.1 Objectives 2
1.2 Scope and limitations 2
Chapter 2 - Literature Review 3
Chapter 3 - Design of dual frames 10
3.1 Design Methodology 11
3.1.1. Moment resisting frame design overview 11
3.1.2. Eccentrically braced frame design overview 12
3.2 Conceptual design for dual behavior 13
3.2.1. Check for elasticity of beams and columns 14
3.2.2. Check for strength of MRF 19
3.2.3. Reduction in residual displacements 20
Chapter 4 - Case Study 22
4.1 Seismic design of case study frames 24
4.2 Design summary of case study frames (8 storey) 27
4.2.1. 8 Storey frame (case A1) 27
4.2.2. 8 Storey frame (case A2) 29
4.2.3. 4 Storey frame (case A1) 31
4.2.4. 4 Storey frame (case A2) 32
4.2.5. 2 Storey frame (case A1) 33
4.2.6. 2 Storey frame (case A2) 34
4.3 Design summary of variations in case study frames 35
Chapter 5 - Non-linear Analysis 40
5.1 Analytical tool 40

5.2 Modelling the link element 41
5.2.1. Description of link model 41
5.3 Non-linear Static Analysis (pushover) 44
5.3.1. Axial forces in the links 54
5.4 Non-linear Dynamic Analysis (THA) 55
5.4.1. 8 storey frame (THA – links removed from top to bottom) 57
5.4.2. 8 storey frame (THA – links removed from bottom to top) 59
5.4.3. 4 storey frame (THA – links removed from top to bottom) 61
5.4.4. 4 storey frame (THA – links removed from bottom to top) 63
5.4.5. 2 storey frame (THA – links removed from top to bottom) 65
5.4.6. 2 storey frame (THA – links removed from bottom to top) 66
Chapter 6 - Conclusions 69
Bibliography 71
Appendix A - Design checks for 8 storey frame (Case A) 73

List of Figures

Figure 2.1 Test setup showing various stages in the experimental verification of removable links [6] 5
Figure 2.2 Deformed shape of the structure during various stages of link removal [6] 6
Figure 2.3 Base shear-Roof displacement relation during link removal procedure [6] 6
Figure 2.4 Elements of the link section [20] 8
Figure 2.5 Simplified kinematic bilinear shear spring model [20] 9
Figure 2.6 Comparison of residual drifts from reference model and simplified models [20] 9
Figure 3.1 Conceptual description of dual frames 10
Figure 3.2 Equal displacement condition (rigid diaphragm effect of slab) 13
Figure 3.3 Roof displacements in relation to link rotation 14
Figure 3.4 One storey – One bay Moment resisting frame 15
Figure 3.5 Residual drifts in a storey (due to EBF link plastic rotation) 19
Figure 4.1 Plan configuration of the case study buildings 22
Figure 4.2 Side view (Elevation) of the case study buildings 23
Figure 4.3 Arrangement of lateral load resisting system 24
Figure 4.4 Response spectrum for the case study buildings (q=6) 25
Figure 4.5 Design sections for 8 storey frame (case A1) 28
Figure 4.6 Design sections for 8 storey frame (case A2) 30
Figure 4.7 Design sections for 4 storey frame (case A1) 31
Figure 4.8 Design sections for 4 storey frame (case A1) 32
Figure 4.9 Design sections for 2 storey frame (case A1) 33
Figure 4.10 Design sections for 2 storey frame (case A2) 34
Figure 5.1 Menegotto-Pinto steel model (Seismostruct) 40
Figure 5.2 Link modelling in Seismostruct (initial and deformed shapes) 42
Figure 5.3 Link element (shear spring) model in Seismostruct 43
Figure 5.4 Pushover curves (case A1) for the 8 storey building 44
Figure 5.5 Pushover curves (case B1) for the 8 storey building 44
Figure 5.6 Pushover curves (case C1) for the 8 storey building 45
Figure 5.7 Pushover curves (case A2) for the 8 storey building 45

Figure 5.8 Pushover curves (case B2) for the 8 storey building 45
Figure 5.9 Pushover curves (case C2) for the 8 storey building 46
Figure 5.10 Pushover curves (case A1) for the 4 storey building 46
Figure 5.11 Pushover curves (case B1) for the 4 storey building 46
Figure 5.12 Pushover curves (case C1) for the 4 storey building 47
Figure 5.13 Pushover curves (case A2) for the 4 storey building 47
Figure 5.14 Pushover curves (case B2) for the 4 storey building 47
Figure 5.15 Pushover curves (case C2) for the 4 storey building 48
Figure 5.16 Pushover curves (case A1) for the 2 storey building 48
Figure 5.17 Pushover curves (case B1) for the 2 storey building 48
Figure 5.18 Pushover curves (case A2) for the 2 storey building 49
Figure 5.19 Pushover curves (case B2) for the 2 storey building 49
Figure 5.20 Pushover curves (case 1- Triangular) for the 8 storey building 50
Figure 5.21 Pushover curves (case 1- Uniform) for the 8 storey building 50
Figure 5.22 Pushover curves (case 1- Triangular) for the 4 storey building 51
Figure 5.23 Pushover curves (case 1- Uniform) for the 4 storey building 51
Figure 5.24 Pushover curves (case 1- Triangular) for the 2 storey building 52
Figure 5.25 Pushover curves (case 1- Uniform) for the 2 storey building 52
Figure 5.26 Development of axial forces in the shear links 54
Figure 5.27 Artificial accelerogram (scaled to 0.2g PGA) 55
Figure 5.28 Response spectrum (design vs accelerogram) 56
Figure 5.29 THA 8 storey frame case A1 (Links removed from Top) 57
Figure 5.30 THA 8 storey frame case A2 (Links removed from Top) 57
Figure 5.31 THA 8 storey frame case B1 (Links removed from Top) 57
Figure 5.32 THA 8 storey frame case B2 (Links removed from Top) 58
Figure 5.33 THA 8 storey frame case C1 (Links removed from Top) 58
Figure 5.34 THA 8 storey frame case C2 (Links removed from Top) 58
Figure 5.35 THA 8 storey frame case A1 (Links removed from Bottom) 59
Figure 5.36 THA 8 storey frame case A2 (Links removed from Bottom) 59
Figure 5.37 THA 8 storey frame case B1 (Links removed from Bottom) 59
Figure 5.38 THA 8 storey frame case B2 (Links removed from Bottom) 60

Figure 5.39 THA 8 storey frame case C1 (Links removed from Bottom)..... 60
Figure 5.40 THA 8 storey frame case C2 (Links removed from Bottom)..... 60
Figure 5.41 THA 4 storey frame case A1 (Links removed from Top)..... 61
Figure 5.42 THA 4 storey frame case A2 (Links removed from Top)..... 61
Figure 5.43 THA 4 storey frame case B1 (Links removed from Top)..... 61
Figure 5.44 THA 4 storey frame case B2 (Links removed from Top)..... 62
Figure 5.45 THA 4 storey frame case C1 (Links removed from Top)..... 62
Figure 5.46 THA 4 storey frame case C2 (Links removed from Top)..... 62
Figure 5.47 THA 4 storey frame case A1 (Links removed from Bottom)..... 63
Figure 5.48 THA 4 storey frame case A2 (Links removed from Bottom)..... 63
Figure 5.49 THA 4 storey frame case B1 (Links removed from Bottom)..... 63
Figure 5.50 THA 4 storey frame case B2 (Links removed from Bottom)..... 64
Figure 5.51 THA 4 storey frame case C1 (Links removed from Bottom)..... 64
Figure 5.52 THA 4 storey frame case C2 (Links removed from Bottom)..... 64
Figure 5.53 THA 2 storey frame case A1 / C1 (Links removed from Top)..... 65
Figure 5.54 THA 2 storey frame case A2 / C2 (Links removed from Top)..... 65
Figure 5.55 THA 2 storey frame case B1 (Links removed from Top)..... 65
Figure 5.56 THA 2 storey frame case B2 (Links removed from Top)..... 66
Figure 5.57 THA 2 storey frame case A1 / C1 (Links removed from Bottom)..... 66
Figure 5.58 THA 2 storey frame case A2 / C2 (Links removed from Bottom)..... 66
Figure 5.59 THA 2 storey frame case B1 (Links removed from Bottom)..... 67
Figure 5.60 THA 2 storey frame case B2 (Links removed from Bottom)..... 67

List of Tables

Table 4.1 Eigenvalue results for 8 storey frame (case A1) 27
Table 4.2 Design cross sections - 8 storey frame (case A1) 27
Table 4.3 Eigenvalue results for 8 storey frame (case A2) 29
Table 4.4 Design cross sections - 8 storey frame (case A2) 29
Table 4.5 Eigenvalue results for 4 storey frame (case A1) 31
Table 4.6 Design cross sections - 4 storey frame (case A1) 31
Table 4.7 Eigenvalue results for 4 storey frame (case A2) 32
Table 4.8 Design cross sections - 4 storey frame (case A2) 32
Table 4.9 Eigenvalue results for 2 storey frame (case A1) 33
Table 4.10 Design cross sections - 2 storey frame (case A1) 33
Table 4.11 Eigenvalue results for 2 storey frame (case A2) 34
Table 4.12 Design cross sections - 2 storey frame (case A2) 34
Table 4.13 Design cross sections - 8 storey frame (case B1) 35
Table 4.14 Design cross sections - 8 storey frame (case B2) 36
Table 4.15 Design cross sections - 4 storey frame (case B1) 36
Table 4.16 Design cross sections - 4 storey frame (case B2) 36
Table 4.17 Design cross sections - 2 storey frame (case B1) 37
Table 4.18 Design cross sections - 2 storey frame (case B2) 37
Table 4.19 Design cross sections - 8 storey frame (case C1) 37
Table 4.20 Design cross sections - 8 storey frame (case C2) 38
Table 4.21 Design cross sections - 4 storey frame (case C1) 38
Table 4.22 Design cross sections - 4 storey frame (case C2) 38
Table 4.23 Design cross sections - 2 storey frame (case C1) 39
Table 4.24 Design cross sections - 2 storey frame (case C2) 39

Acknowledgements

I would like to take this opportunity to express my deep gratitude to my adviser, **Assistant Professor Mario D'Aniello,** Department of structural engineering and architecture, University of Naples Federico II, for his valuable insights, guidance, motivation and support in overcoming challenges at various stages and levels which ultimately led to the successful completion of the project.

I express my sincere gratitude to **the faculty**, Department of structural engineering and architecture, University of Naples Federico II for their valuable comments and useful suggestions during the course of the project.

I also take up this opportunity to thank **Prof. Raffaele Landolfo**, Department of structural Engineering and Architecture, University of Naples Federico 2 for welcoming us to the department, providing us with access to the departmental facilities and work space. I also thank the staff for their timely guidance on numerous activities which helped me get settled in a completely new place with ease and in completing all formalities.

Special thanks to **Professor Frantisek Wald**, **Professor Luis Simoes Da Silva**, **Professor Raffaele Landolfo** and the rest of the coordinators of the SUSCOS_M program. I thank all the professors who taught me invaluable things during the course of the program to develop me professionally and personally. I also thank **Miss Barbora Skalova** and **Miss Vera Klatova** for their immense support during administrative and visa issues. I also thank all my friends, colleagues and classmates for making this experience an amazing and unforgettable one.

I thank my parents for their whole hearted love, support and guidance without which this endeavor would have been impossible to complete.

Abbreviations

MRF	:	Moment Resisting Frame
EBF	:	Eccentrically Braced Frame
L_c	:	Length of column (storey height)
h	:	Height of column (storey height)
L_b	:	Length of beam / bay for both MRF and EBF
e	:	Link length
θ	:	Interstorey drift angle
γ	:	Link rotation angle
ε	:	Strain (steel)
χ	:	Reduction factor (to calculate shear area)
Δ	:	Interstorey drift (displacement)
E	:	Young's Modulus of steel
G	:	Shear Modulus of steel
A	:	Area of steel section under consideration
A_{sh}	:	Shear area of steel section under consideration
D	:	Depth of section under consideration
I	:	Moment of inertia (major axis) of section under consideration
q	:	Behavior factor

Chapter 1 - Introduction

It is a well-known fact that steel (both structural and reinforcing) play crucial and extensive roles in the present construction industry. In the building sector, earthquakes form a major chunk of destruction of structures due to force majeure events. This resulted in the development of design technology to create building systems that can resist such events with minimal human casualty. Structural steel, having a huge strength/weight ratio is already one of the best and most used materials for such systems. But it is not cheap. Repair / replacement of steel structures has always been considered to be cost and labour intensive. This resulted in a shift in research interests from designing lateral force resisting frames to lateral force resisting frames with easy reparability. It is in this aspect that one can highlight the advantages that eccentrically braced frames provide over other types of systems.

Eccentrically braced systems have a 'structural fuse' which is the link element, usually present in between the braces, which is the primary and usually the only source of energy dissipation in the system by means of yielding. This led to research on the possibilities of replacing the damaged links with new ones in hopes of a renewed lateral load resisting system. Unfortunately the yielding of links is associated with a permanent residual drift in the structure and replacing the links does not undo that. Hence replacing the links might replenish the structure's energy dissipation capacity, but the drifts and displacements would only pile up resulting in costly repairs down the line.

This has led to a recent development of interest towards finding systems which can not only replenish their energy dissipation capacity but also re-center themselves after a seismic event. It is in this stage that possibilities of dual frames and its advantages come to highlight. The current thesis is also aimed towards the possibilities of designing a dual frame which can 'literally' be as good as new after a quick intervention following an earthquake.

1.1 Objectives

The objective of the endeavor is to embark upon the possibility of having two completely different seismic systems (MRFs and EBFs) to act together in unison to achieve the most optimal performance of structures under various seismic scenarios (seismic events with different return periods). This involves

1. Design of dual frames as per EC3 and EC8
2. Quick assessment of the performance of said frames using non-linear static analysis (Pushover)
3. Confirmation of the desired behavior under various events (Time history Analysis)

1.2 Scope and limitations

The scope of research work undertaken in the project, to study the global seismic behavior of framed systems, is limited to

1. 2 D frames (or 3 D frames with symmetry which can be reduced to independent 2 D behavior in the X and Y directions)
2. Inverted V bracings for the EBF system
3. Short links for the eccentrically braced frames
4. Design guidelines specified in Eurocodes (for MRF and EBF as explicit systems).

The limitations of the assumptions made in the project are explained in greater detail in the relevant sections.

Chapter 2 - Literature Review

In the recent decades, research on the implementations of removable links has been gaining attention with regards to both structural performance (optimal over-strength values) and cheaper rehabilitation after frequent earthquakes. The use of dual frames has also been researched upon in the recent years for its significant superiority in seismic performance. **Sina KA and Topkaya C (2017)** [4] present a review on the majority of recent literature published on the design of eccentrically braced frames. **Nabil Mansour (2010)** [5], amongst others, present a detailed research on the connections and local aspects of replaceable links. Experimental tests on replaceable shear links are also reviewed by **Fussell AJ et al (2014)** [17] covering recent research work done in Canada and New Zealand and also a finite element verification of the replaceable links attaining required rotation capacity as per codes. The literature pertaining to the design of dual frames and those related to implementation of replaceable links are briefly outlined in the sections below.

Design guidelines in Eurocode 8

Recent years have seen attention being given to further the provisions in the Eurocodes to incorporate dual frames in addition to moment resisting and braced frames. Currently there is no provision for MRF-EBF dual frames in the Eurocodes but only the recommendation that a single behavior factor (q) to be used for the design which is the lesser of the dual frame constituents.
In recent years, it has been found (eg: **Bosco et al (2014)** [8]) that the code provided value for eccentrically braced frames ($5\alpha u/\alpha 1 = 6$) in the Eurocodes is a bit high and a lesser value of 5 is proposed.

In the paper published by **Bosco et al (2017)** [13], the authors conducted a series of incremental dynamic analyses on MRF-EBF dual frames in order to find a better estimate of the ductility factor (q). They observed that the dual systems were not able to display the ductility which they were expected to (even as lesser of the constituents i.e. MRF and EBF), as is the current guideline in the Eurocodes and so proposed the following equation

$$q = \begin{cases} 5 & \varphi_u^m \geq 0.06 \text{ rad} \\ 37.5 \cdot (\varphi_u^m - 0.02) + 3.5 & \varphi_u^m < 0.06 \text{ rad} \end{cases}$$

However, it is noted that in the current study, the MRFs are designed to remain elastic (unlike the case study performed by the authors) and also the utilization of the removable links feature ensures a more uniform over-strength factor distribution in the link shear forces across all storeys and therefore, better dissipation. Since the building frames considered by the authors did feature removable links, considerably higher over-strengths were attained in upper stories where storey shears are lesser and MRFs more dominant. This might also have been one of the causes for the buildings to have the damage concentrated in few stories.

Further, as proposed by **Elgazouli (2009)** [12] and also noted by **Bosco et al (2014)** [8], it would be best for the over-strength factor for the MRF frame to take into account the effects of gravity loads. In other words,

Instead of

$\Omega^{MRF} = \frac{M_{pl.Rd}}{M_{Ed}}$,

$\Omega^{MRF} = \frac{M_{pl.Rd} - M_{Ed.G}}{M_{Ed.E}}$ is proposed.

This makes much sense and is also very influential in the design principles because in the dual frames, the EBFs are much stiffer when compared to the MRFs and as a result, the sharing of lateral load is heavily biased towards the EBFs and therefore can actually even make ULS (1.35 DL + 1.5 LL) the governing load combination in the design of the MRF beams.

Recentering of dual frames

Dubina et al (2011) [6] investigated the possibilities in recentering of dual frames of different configurations, one of which involved an MRF EBF dual frame with links being removed after seismic events.

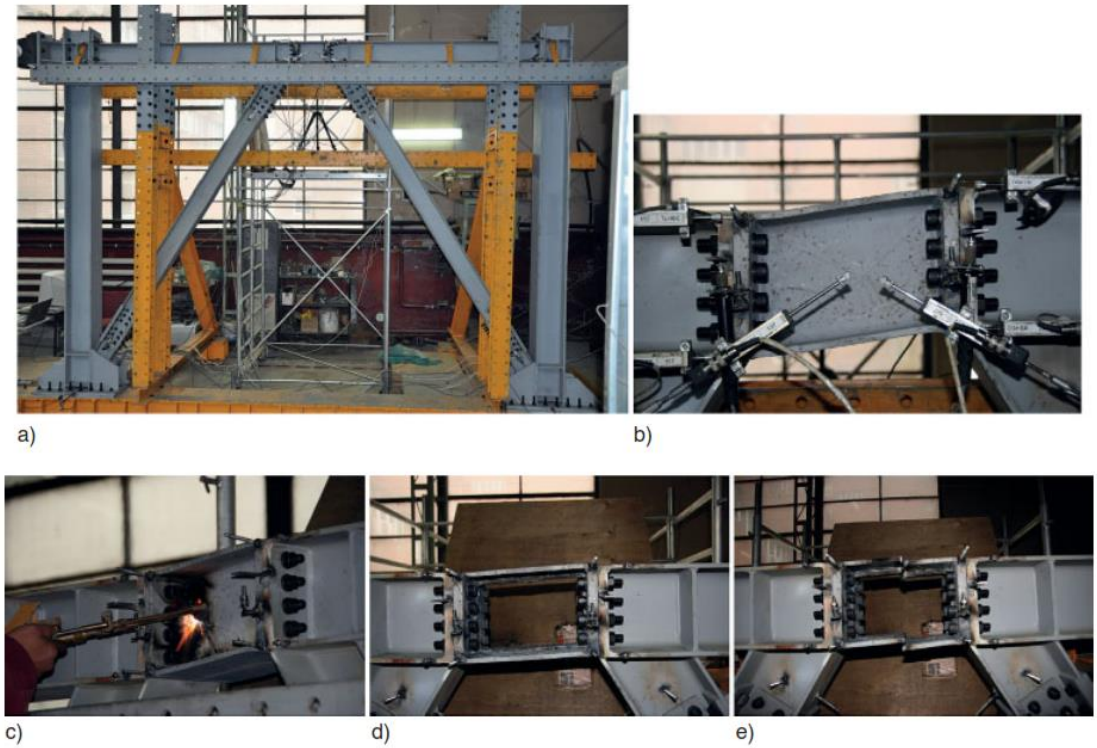

Figure 2.1 Test setup showing various stages in the experimental verification of removable links [6]

It is noteworthy to mention the following design aspects adopted by the authors

- All columns of the MRF components were made from high strength steel (S460)
- The system was completely symmetric
- Behavior factor (q) = 4 was adopted during the design stage.

The authors observed that the dual frames were able to restore themselves completely to their initial positions after being pushed till the target displacements are reached once the links are cut, as shown below.

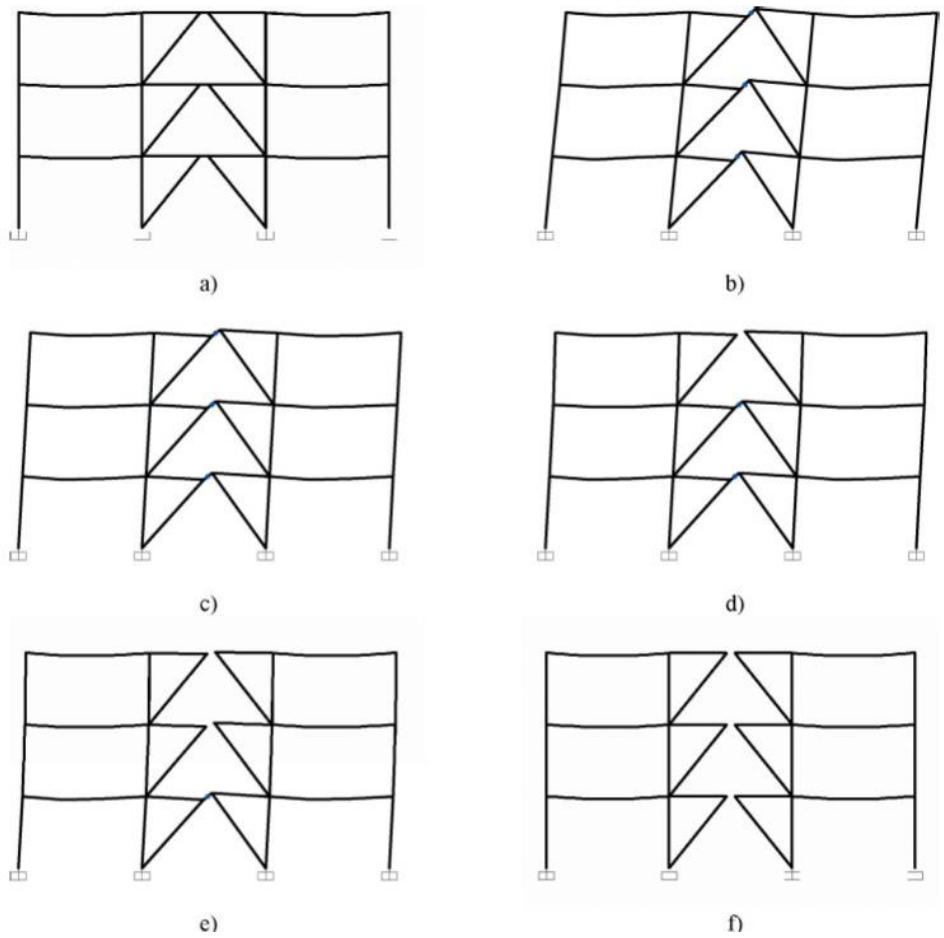

Figure 2.2 Deformed shape of the structure during various stages of link removal [6]

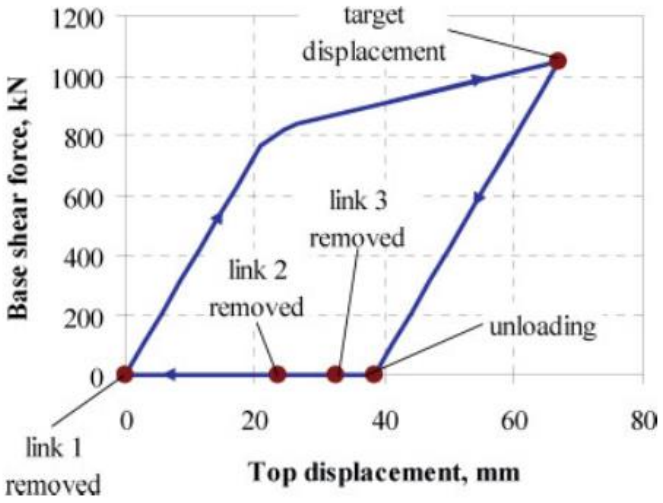

Figure 2.3 Base shear-Roof displacement relation during link removal procedure [6]

Dubina et al (2016) [7] also made numerical investigations into the dual MRF EBF systems with link removal procedures (with a symmetric configuration as above) but with different structural configurations (MRF + EBF + MRF or EBF + MRF + EBF) and also found that it was better for links to be removed from the least loaded towards the most.

Stratan A et al (2013) [8] performed numerical investigations into the procedure of link removal in both horizontal and vertical directions in multi-storey dual MRF EBF frames and made several proposals. The authors proposed the use of temporary tension only rods to act as braces to ensure that the system is stable during the time of link cutting. Also they found that removing the links from top down (least loaded towards most loaded) worked best for lesser transfer of forces. In plan, they propose to remove all links in one direction simultaneously (in order to avoid torsional effects).

Modeling the behavior of shear links

The recent years has seen a shift in focus in the research towards identifying and better modeling of link elements. One of the major modeling parameters in the behavior of shear links is the link over-strength factor. A number of experimental studies (eg: **Hjelmstad KD et al (1983)** [10], **Duscika P et al (2010)** [14], **Mazzolani FM et al (2009)** [15]) have all reported a link over-strength factor of 1.5 or higher (although some found it to be a bit lower, for example **Okazaki et al (2005)** [16]) for short links and have also observed maximum link rotations higher than 0.08 radians which Eurocode recommends. Therefore the material link over-strength and maximum rotation capacity are conservatively taken as the ones given in the Eurocodes.

D'Aniello M et al (2013) [18] investigated the effects of link axial force on the link overstrength, in addition to the effects of flanges and link geometry, and observed that axial forces developed in the links due to the restraints on it from the surrounding frame and the tensile forces so developed result in an increased overstrength of the link, depending on the degree of axial restraint. The authors also found minimum 1.5 overstrength at 0.08 radians of link rotation for short links which may go up to 2 for very short links.

Performing dynamic analyses on models with refined hysteretic rules for shear and flexural non-linearities can be very demanding on time and resources. Hence researchers took to proposing relatively accurate and simplistic models to capture the non-linearity by means of both analytical (finite element modeling approach) and experimental procedures.

Modeling of the complex hysterical behavior of the shear links using simplified methods, by concentrating plasticity at the ends, were proposed by **Ramadan et al (1995)** [19] and **Bosco et al (2016)** [20], the latter of which is described below.

According to the simple but refined model proposed by [20, 21, 22], the non-linearities are modeled by concentrating them as shear and flexural springs (zero length members) at the ends of an elastic link element.

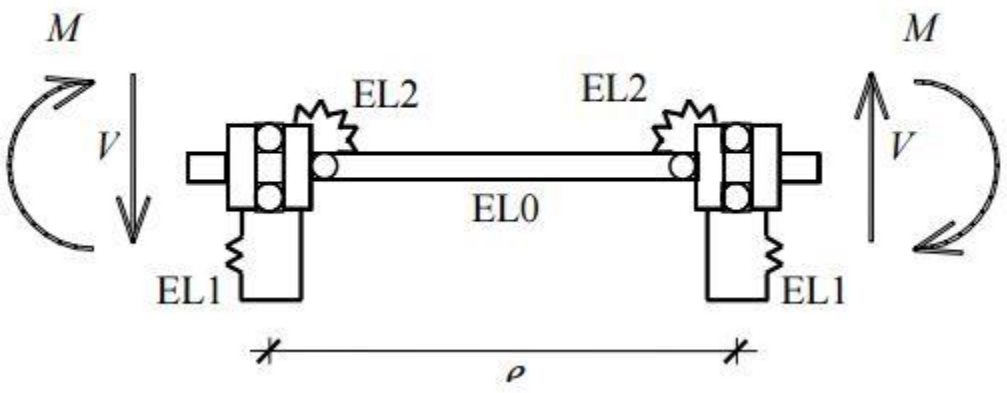

Figure 2.4 Elements of the link section [20]

The main advantage in this model is that the modelling of shear springs includes both isotropic and kinematic hardening which is very important under dynamic / cyclic loading. Various simplifications have been proposed where isotropic and kinematic hardening aspects are captured using

- An increased equivalent kinematic hardening (method #1)
- An increased yield force (isotropic) and normal kinematic hardening (method #2)
- A piece-wise linear multi-linear force displacement curve (Ramadan model)

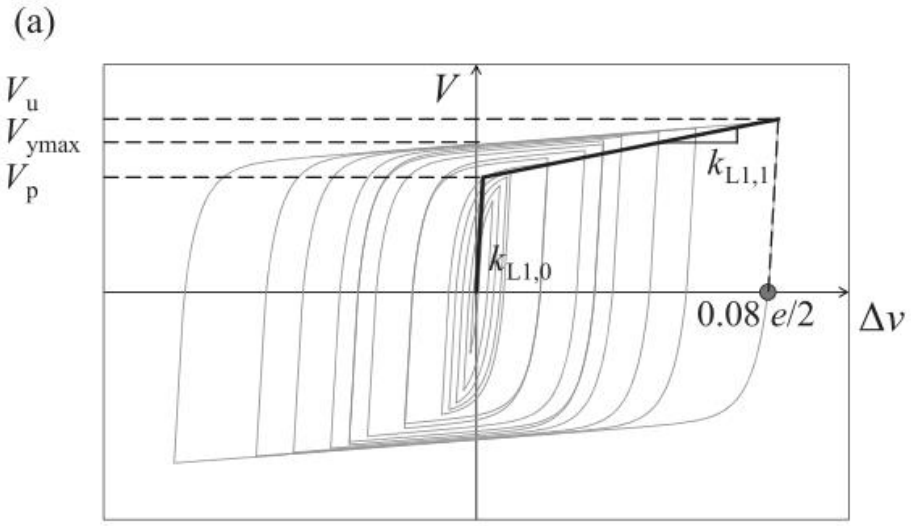

Figure 2.5 Simplified kinematic bilinear shear spring model [20]

Maximum residual drifts predicted by model M1 ($\delta_{r,1}$).

	e/L = 0.10		e/L = 0.30	
	MRSA	LFMA	MRSA	LFMA
Designed according to procedure #1				
n = 4	0.289%	0.289%	0.324%	0.246%
n = 8	0.293%	0.303%	0.215%	0.331%
n = 12	0.243%	0.228%	0.220%	0.250%
Designed according to procedure #2				
n = 4	0.289%	0.289%	0.328%	0.171%
n = 8	0.248%	–	0.365%	–
n = 12	0.232%	–	0.312%	–

– Cases not included in the investigation.

Figure 2.6 Comparison of residual drifts from reference model and simplified models [20]

Similarly, other aspects such as predicted Δag/ag.1, normalized link plastic rotation, variability of response for different ground motions etc, were analyzed and compared with a more rigorous hysteretic reference model created with analytical and experimental results (model M1) for short, medium and high rise buildings for short, intermediate and long links resulted in the authors concluding that the optimal way to model the links was to use the model with an increased equivalent kinematic hardening. Therefore, the same approach is adopted for the current study.

Chapter 3 - Design of dual frames

The design methodology adopted for seismic resistant dual frames is based on the ability of the structure to restore its original shape after the earthquake requiring minimal structural intervention for its restoration. Two kinds of seismic frames, i.e. moment resisting frames and eccentrically braced frames are used which act in unison in resisting lateral loads. Only short links are considered for the eccentrically braced frames due to their superior ductility based on shear yielding of the links. It's counterpart, the moment resisting frame is designed to remain elastic throughout the ground motion so that it facilitates the structure in restoring its original configuration once the damaged links are removed. The dual behavior of such a frame is shown in the picture below.

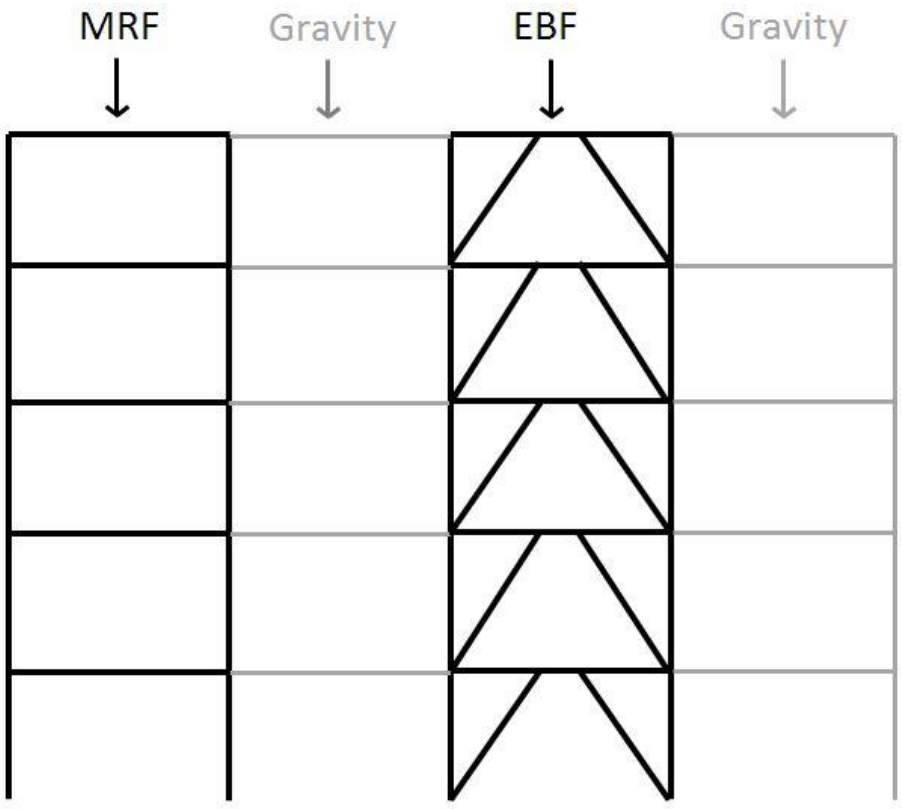

Figure 3.1 Conceptual description of dual frames

3.1 Design Methodology

For the design of moment resisting frame and eccentrically braced frames, the Eurocode framework (EC3, EC8) is followed. The two frames are designed independently but by using a common behavior factor 'q' as that of eccentrically braced frames since the ductility is expected to arise only from the EBF. It should be noted that although the span lengths of MRF and EBF can be different, for the current scenario (theoretical) and the case study performed, the bay lengths are the same and hence denoted using the same term (L_b).

3.1.1. **Moment resisting frame design overview**

In the moment resisting frame bay, the beams are the critical elements and are designed to resist the lateral loads. Based on the capacity design principles, columns are designed for moments that are magnified corresponding to beam element plasticity (in other words, columns are designed for those forces which would cause plasticity in the beams, ensuring that columns are stronger than the beams at all cases).

Design of dissipative elements (Beams) is carried out for

$G_k + 0.3\ Q_k + \delta\ A_{Ed}$

Where

G_k: Permanent actions

Q_k: Variable actions

A_{Ed}: Seismic action

δ: Accidental torsional effects (taken conservatively as the max = 1.6)

Design of non-dissipative elements (columns) is carried out for

$G_k + 0.3\ Q_k + 1.1\ \Omega\ \gamma_{ov}\ \alpha\ \delta\ A_{Ed}$ where

α: P-Δ effects (calculated as 1 due to very low interstorey drifts)

γ_{ov}: Material overstrength (taken as 1.25)

Ω: Member overstrength (calculated as min ($M_{Pl.Rd}$/ M_{Ed}) for all the dissipative elements aka beams)

The above procedure ensures that even in the case where an increased seismic load causes plasic hinges to form in the beams, the columns are still able to withstand the load, thereby not resulting in any collapse.

Local hierarchy criterion as per EC Cl. 4.4.2.3, EN 1998-1-1 is also checked, which states
At all joints of primary seismic columns,

$$\frac{\sum M_c}{\sum M_b} \geq 1.3$$

Interstorey drifts are limited to 0.75% of storey height (assuming ductile non-structural components).

3.1.2. **Eccentrically braced frame design overview**

The eccentrically braced frames are designed very similar to moment resisting frames, pertaining to
Design of dissipative elements (links) is carried out for

$G_k + 0.3\ Q_k + \delta\ A_{Ed}$

Whereas design of non-dissipative elements (beams outside links, braces, columns) is done for

$G_k + 0.3\ Q_k + 1.1\ \Omega\ \gamma_{ov}\ \alpha\ \delta\ A_{Ed}$

Where everything is the same, except the overstrength factor Ω, which is calculated as

$\Omega = \min\left(\frac{1.5\ V_p}{V_{Ed}}\right)$ of all links (for "short links")

It must be noted that since the study focuses primarily on "short links", the link lengths are also limited to

$$e \leq 1.6\frac{M_p}{V_p}$$

It is very important to note that for the seismic design of a frame containing MRF and EBF (each having a different behavior factor, as per the EC), the EC permits to use a single behavior factor, taken as the lesser of the two.
Since behavior factor for EBF is 6 ($5\alpha_u/\alpha_1 = 5*1.2 = 6$) which is smaller than that of MRF ($5\alpha_u/\alpha_1 = 5*1.3 = 6.5$), a single behavior factor of 6 is taken for the seismic design of the dual frame.

3.2 Conceptual design for dual behavior

During the seismic activity, the MRF component of the dual frame is ideally expected to remain completely elastic thereby facilitating the structure restoring its original shape after the shear deformed link sections are removed during rehabilitation. For this, three conditions are expected to be satisfied (ideally),

- The columns of the MRF should be elastic even at the maximum inter-storey drift possible due to plastic yielding in the EBF shear link.
- The beams of the MRF should also be elastic with no plastic hinges.
- The columns of the MRF should be strong enough to pull back the weight of the floor in order to restore the original configuration.

The three conditions are achieved (as a simplification) by considering each storey to act as independently. In other words, the moment resisting frame in each storey should be ductile enough to remain elastic at the maximum interstorey drift in that storey, and yet strong enough to have the elastic capacity to restore the permanent drifts due to plastic deformations in the shear links. The calculations are shown in greater detail in the following sections

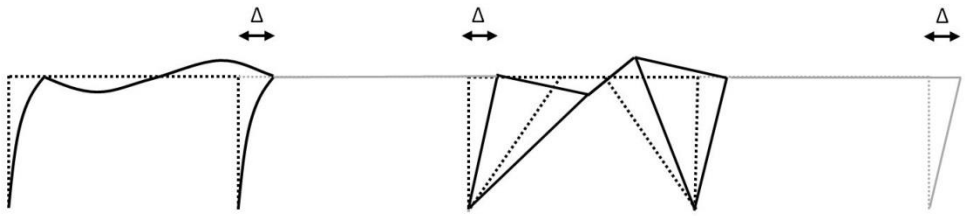

Figure 3.2 Equal displacement condition (rigid diaphragm effect of slab)

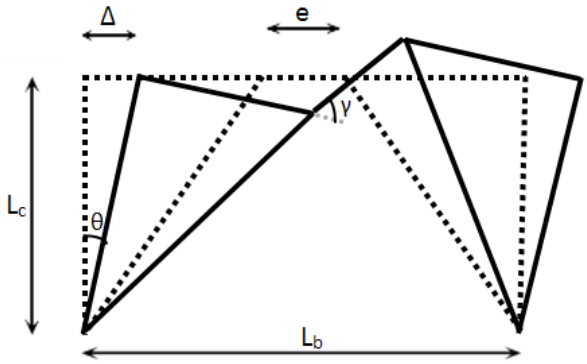

Figure 3.3 Roof displacements in relation to link rotation

As per EC8, maximum allowable chord rotation for short links (γ) is 0.08 radians. As shown in the figure below, this chord rotation corresponds to an interstorey drift of

$$\theta = \frac{\gamma * e}{L_b}$$

$$u_{max} = \Delta = \theta * L_c = \frac{\gamma * e * L_c}{L_b} \qquad (eq\ 3.1)$$

The MRF's of each floor are therefore ensured to remain elastic under a maximum top displacement of u_{max} which can occur before failure of the shear link in the eccentrically braced frame bay. Once the initial seismic design of the building frame is completed, one has working knowledge of the cross section and geometry of the links, thereby enabling us to find out the maximum interstorey drift that could possibly occur in each storey.

3.2.1. **Check for elasticity of beams and columns**

Although it is best to check the elasticity of the single MRF bay using a modeling tool like SAP2000 (as was done in the case study as a verification), a preliminary assessment using hand calculations was also performed to have an idea of the possibilities of achieving an elastic MRF even at the failure level of EBF.

The basic one storey one bay MRF considered for hand calculations is shown below (with the kinematic degrees of freedom considered).

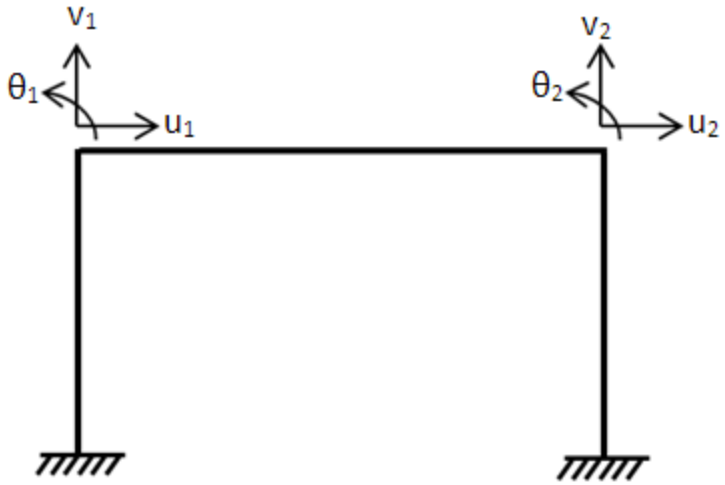

Figure 3.4 One storey – One bay Moment resisting frame

The stiffness matrix of the beam (global coordinates) corresponding to the 6 degrees of freedom is shown below.

$$K_{G.b} = \begin{bmatrix} \frac{EA_b}{L_b} & 0 & 0 & -\frac{EA_b}{L_b} & 0 & 0 \\ 0 & \frac{12EI_b}{L_b^3} & \frac{6EI_b}{L_b^2} & 0 & -\frac{12EI_b}{L_b^3} & \frac{6EI_b}{L_b^2} \\ 0 & \frac{6EI_b}{L_b^2} & \frac{4EI_b}{L_b} & 0 & -\frac{6EI_b}{L_b^2} & \frac{2EI_b}{L_b} \\ -\frac{EA_b}{L_b} & 0 & 0 & \frac{EA_b}{L_b} & 0 & 0 \\ 0 & -\frac{12EI_b}{L_b^3} & -\frac{6EI_b}{L_b^2} & 0 & \frac{12EI_b}{L_b^3} & -\frac{6EI_b}{L_b^2} \\ 0 & \frac{6EI_b}{L_b^2} & \frac{2EI_b}{L_b} & 0 & -\frac{6EI_b}{L_b^2} & \frac{4EI_b}{L_b} \end{bmatrix}$$

Adding the stiffness components of the columns, the global (reduced) stiffness matrix of the MRF frame can be written as

$$K_G = \begin{bmatrix} \frac{EA_b}{L_b}+\frac{12EI_c}{L_c^3} & 0 & 0 & -\frac{EA_b}{L_b} & 0 & 0 \\ 0 & \frac{12EI_b}{L_b^3}+\frac{EA_c}{L_c} & \frac{6EI_b}{L_b^2} & 0 & -\frac{12EI_b}{L_b^3} & \frac{6EI_b}{L_b^2} \\ \frac{6EI_c}{L_c^2} & \frac{6EI_b}{L_b^2} & \frac{4EI_b}{L_b}+\frac{4EI_c}{L_c} & 0 & -\frac{6EI_b}{L_b^2} & \frac{2EI_b}{L_b} \\ -\frac{EA_b}{L_b} & 0 & 0 & \frac{EA_b}{L_b}+\frac{12EI_c}{L_c^3} & 0 & \frac{6EI_c}{L_c^2} \\ 0 & -\frac{12EI_b}{L_b^3} & -\frac{6EI_b}{L_b^2} & 0 & \frac{12EI_b}{L_b^3}+\frac{EA_c}{L_c} & -\frac{6EI_b}{L_b^2} \\ 0 & \frac{6EI_b}{L_b^2} & \frac{2EI_b}{L_b} & 0 & -\frac{6EI_b}{L_b^2} & \frac{4EI_b}{L_b}+\frac{4EI_c}{L_c} \end{bmatrix}$$

As a further simplification, the columns are assumed to be incompressible (axial deformations neglected) and the stiffness matrix is further reduced as shown below (removing the degrees of freedom associated with v_1 and v_2). The global equation of equilibrium becomes

$$\begin{bmatrix} \frac{EA_b}{L_b}+\frac{12EI_c}{L_c^3} & \frac{6EI_c}{L_c^2} & -\frac{EA_b}{L_b} & 0 \\ \frac{6EI_c}{L_c^2} & \frac{4EI_b}{L_b}+\frac{4EI_c}{L_c} & 0 & \frac{2EI_b}{L_b} \\ -\frac{EA_b}{L_b} & 0 & \frac{EA_b}{L_b}+\frac{12EI_c}{L_c^3} & \frac{6EI_c}{L_c^2} \\ 0 & \frac{2EI_b}{L_b} & \frac{6EI_c}{L_c^2} & \frac{4EI_b}{L_b}+\frac{4EI_c}{L_c} \end{bmatrix} * \begin{pmatrix} u_1 \\ \theta_1 \\ u_2 \\ \theta_2 \end{pmatrix} = \begin{bmatrix} F/2 \\ 0 \\ F/2 \\ 0 \end{bmatrix}$$

The diaphragm effect of the floor results in equal horizontal displacements ($u_1 = u_2 = u$) and by symmetry, one can deduce that $\theta_1 = \theta_2 = \theta$). From the second equation, we get

$$\frac{6EI_c}{{L_c}^2}u + \left[\frac{4EI_b}{L_b}+\frac{4EI_c}{L_c}\right]\theta + \left[\frac{2EI_b}{L_b}\right]\theta = 0 \qquad (eq\ 3.2)$$

Which is rewritten as,

$$\frac{EI_c}{L_c}\left[4\theta + \frac{6u}{L_c}\right] + \left[\frac{6EI_b}{L_b}\right]\theta = 0$$

If we denote,

$$\alpha = \frac{I_c/L_c}{I_b/L_b}$$

Then (ignoring the negative sign, since we are only interested in absolute values),

$$\theta = \left[\frac{6\alpha}{6+4\alpha}\right]\frac{u}{L_c} \qquad (eq\ 3.3)$$

Moments at the end of the beam can now be calculated as $M = 6EI_b/L_b * \theta$ from which the curvature is obtained as $M/(EI_b)$. For the beam to remain completely elastic, maximum curvature that is allowable is $2\ \varepsilon_y / D$ which implies

$$\left[\frac{36\ \alpha}{6+4\alpha}\right]\frac{u_{max}}{L_c L_b} \leq \frac{2\ \varepsilon_y}{D}$$

Substituting for u_{max} from equation (eq 3.1), we get

$$\left[\frac{1.44\ \alpha}{6+4\alpha}\right]\frac{e}{{L_b}^2} \leq \frac{\varepsilon_y}{D} \qquad (eq\ 3.4)$$

Similarly, the moments at the base of columns are also derived in terms of top displacements as follows.

$$\frac{12EI_c}{{L_c}^3}u + \frac{6EI_c}{{L_c}^2}\theta = \frac{F}{2} \qquad (eq\ 3.5)$$

Multiplying by $L_c/2$ on both sides, we get

$$\frac{6EI_c}{{L_c}^2}u + \frac{3EI_c}{L_c}\theta = \frac{F\ L_c}{4}$$

But from equation (eq 3.2), we have

$$\frac{6EI_c}{{L_c}^2}u + \left[\frac{4EI_b}{L_b} + \frac{4EI_c}{L_c}\right]\theta + \left[\frac{2EI_b}{L_b}\right]\theta = 0$$

Subtracting, we get (ignoring sign for now since we are only interested in absolute values of moments),

$$\left[\frac{6EI_b}{L_b} + \frac{EI_c}{L_c}\right]\theta = \frac{FL_c}{4}$$

From which θ can be found out as

$$\theta = \frac{1}{\left({EI_b}/{L_b}\right)} * \frac{\left({FL_c}/{4}\right)}{6+\alpha} \qquad (eq\ 3.6)$$

Both beam and column have the same joint rotation θ implying that moments at the beam ends must be same as moments at the top of columns (since no other moment loads are acting on the beam column joint). Hence

Moments at the base of column $= M_{Top} - FL_c/2$

$= 6\,(EI_b/L_b)\,\theta - FL_c/2$

Substituting for θ from equation (eq 3.5), we get

$$M_{Col.base} = \frac{6}{6+\alpha} * \frac{FL_c}{4} - \frac{FL_c}{2} = \left[\frac{3+\alpha}{6+\alpha}\right]\frac{FL_c}{2}$$

From equations (eq 3.3 and eq 3.6), on equating θ we get

$$\frac{FL_c}{2} = \left[\frac{12\alpha\,(6+\alpha)}{(6+4\alpha)}\right] * \frac{EI_b}{L_b} * \frac{u}{L_c}$$

Substituting for $FL_c/2$ in the previous equation, we obtain

$$M_{Col.base} = \left[\frac{12\alpha\,(6+\alpha)}{(6+4\alpha)}\right] * \frac{EI_b}{L_b} * \frac{u}{L_c} * \left[\frac{3+\alpha}{6+\alpha}\right] = \left[\frac{12\alpha\,(3+\alpha)}{(6+4\alpha)}\right] * \frac{EI_b}{L_b} * \frac{u}{L_c}$$

Curvature is calculated as M/EI_c and substituting for u as u_{max} we get

$$\left[\frac{12\,(3+\alpha)}{(6+4\alpha)}\right] * \frac{u_{max}}{{L_c}^2} \leq \frac{2\varepsilon_y}{D}$$

Or, in terms of the link length, e, we can rewrite the above expression as

$$\left[\frac{0.48\,(3+\alpha)}{(6+4\alpha)}\right] * \frac{e}{{L_c}^2} \leq \frac{\varepsilon_y}{D} \qquad (eq\ 3.7)$$

It should be noted that the above expressions (eq 3.4 and eq 3.7) only serve as a ballpark estimate of possible link lengths because the columns are subject to axial force (DL + 0.3 LL) in addition to seismic loads and the MRF has to remain elastic under the combination of vertical and lateral loads. It is noted that if the MRF is independent from the EBF then the axial stresses are nominal and it is a lot easier to satisfy the above criterion but in case the MRF and EBF are adjacent to each other (as is in the case study), the high axial force in the column common to MRF and EBF also has to be designed to remain elastic (which may require the use of higher strength steel grade). Hence a reserve margin is suggested when using the simple equation for preliminary assessment in order to avoid iterations in analysis.

It is also seen that reducing the link length has a direct impact on the possible maximum interstorey drift (umax) but it has been observed that reduction of link lengths can result in the structure being not ductile enough to meet the target roof displacement at near collapse (NC)

before failure of link elements. Although the presence of a moment resisting frame ensures the structure does not collapse, significant reduction in post-failure capacity of structure is observed. As will be shown during the case study, the dual frame does 'not' form a mechanism after the failure of the link but instead the moment resisting frame takes the lead. A mechanism is formed only after loss of stability in both MRF and EBF on the same floor. Although the presence of a moment resisting frame ensures the structure does not collapse, significant reduction in post-failure capacity of structure is observed. In order for the structure to remain ductile to reach target displacements at near collapse, maximum possible link lengths are recommended.

3.2.2. **Check for strength of MRF**

The MRF not only needs to be ductile enough to allow the maximum interstorey drifts due to EBF plastic rotations, but also needs to be stiff enough to have a higher restoring force than acting forces in in the deformed shape (after residual drifts) once the links are cut off.

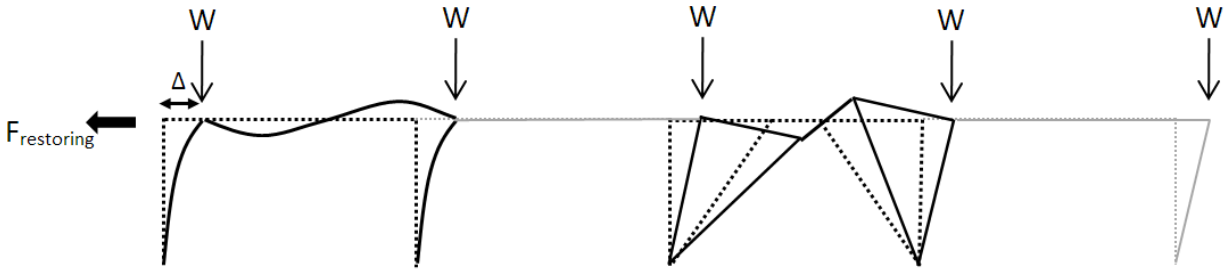

Figure 3.5 Residual drifts in a storey (due to EBF link plastic rotation)

Note: The forces 'W' denoted in the figure above are eccentric vertical forces on the whole storey and not just the loads on the frame under consideration (leaning column effect). Here, we can see that the destabilizing moments are calculated as

$M_{destabilizing}$ = Storey Weight * Residual drift

Whereas the restoring forces (due to MRF stiffness) is $F_{restoring}$.

The condition for the MRF to be able to pull back the mass of the floor is if

$F_{restoring} * h \geq$ Storey weight * u_{max}

It must be kept in mind that after an earthquake, all stories can have the maximum possible drift in the same direction (worst case scenario) where the forces due to upper stories pile up on the

lower ones. In other words, for a n-storey building, net destabilizing moment at storey i can be calculated (at worst) as

$$M_{destabilizing} = \sum_{i+1}^{n} W_i * \left(\sum_{i+1}^{n} \Delta_i \right) \qquad (eq\ 3.8)$$

3.2.3. **Reduction in residual displacements**

Inelastic yielding of the shear links inevitably causes permanent storey drifts. It is noted that mere replacement of shear links would definitely renew the frame's lateral load bearing capacity but the presence of permanent storey drifts would most likely result in reduced performance of the structure under future earthquakes and thereby even higher residual storey drifts after the next quake.

Presence of the elastic frame not only helps in bringing back the structure (after the links are cut for replacement) but also does it's work in reducing the residual interstorey drifts by a little, as shown below.

The stiffness of the MRF frame can be approximated as

From (eq 3.5),

$$\frac{12EI_c}{{L_c}^3} u + \frac{6EI_c}{{L_c}^2} \theta = \frac{F}{2}$$

Substituting for θ from (eq 3.3) with the negative sign, we get

$$\frac{12EI_c}{{L_c}^3} u + \frac{6EI_c}{{L_c}^2} * \left[\frac{-6\alpha}{6+4\alpha} \right] \frac{u}{L_c} = \frac{F}{2}$$

From which the stiffness (F/u) can be found as

$$K_{MRF} = K_1 = \frac{24EI_c}{{L_c}^3} \left[1 - \frac{3\alpha}{6+4\alpha} \right] \qquad (eq\ 3.9)$$

The stiffness of the EBF (for the K braced configuration), on the other hand can be found using the approximate relationship between storey shear and link shear force, and storey drift with link rotations, as shown below.

$$F_{storey} = V_{link} * \frac{L_b}{L_c}$$

Whereas (eq 3.1) gives

$$\Delta = \theta * L_c = \frac{\gamma * e * L_c}{L_b}$$

From the above two equations, the stiffness of the EBF bay can be approximated as

$$K_{EBF} = K_2 = \frac{F}{\Delta} = \frac{V_{link}}{\gamma\ e} * \left(\frac{L_b}{L_c}\right)^2 = \frac{G\ A_{sh}}{e} * \left(\frac{L_b}{L_c}\right)^2 \qquad (eq\ 3.10)$$

Where A_{sh} is the shear area of the link, (refer section 5.2.1).

After the shear link has undergone plastic deformations, the MRF would try to bring it back to its original position as far as it can, which is calculated as

$K_1 * (u_{max} - x) = K_2 * x$

Which gives the restoring displacement (x) equal to

$$x = \frac{K_1}{K_1 + K_2} * u_{max} \qquad (eq\ 3.11)$$

This is a direct reduction on the residual drift observed in the building immediately after the earthquake and as expected, depends directly on the stiffness of the MRF in the bay (relative to the stiffness of the EBF).

It is observed that the lateral stiffness from MRF comes from flexure (EI/L^3) whereas the lateral stiffness of the EBF comes from shear (GA/e) and the latter is significantly greater than the former, therefore in the elastic regime, it is expected that the EBF would take the majority of lateral load and the MRF would gain a better share of lateral load only after the shear links have yielded.

From the above, and (eq. 3.11), given how small K_1 is when compared to K_2, it is also concluded that the restoring displacement 'x' is small and therefore can be neglected. Therefore, full value of u_{max} is taken into account when checking for elasticity of the MRF frame.

Chapter 4 - Case Study

The conceptual seismic design of the dual frames is performed using the software package SAP2000 according to EN 1993-1-1 [1] and EN 1998-1-1 [2]. The steel frames used for case studies in the INNOSEIS project were selected to be designed as dual frames in order to assess their seismic performance. Three configurations for the steel buildings were chosen

- Low rise building (2 storey)
- Medium rise building (4 storey)
- High rise building (8 storey)

The basic geometry for the frames used in the study is shown below. The number of bays in the X and Y directions are 3, each 8m long. Storey heights are taken as 4m.

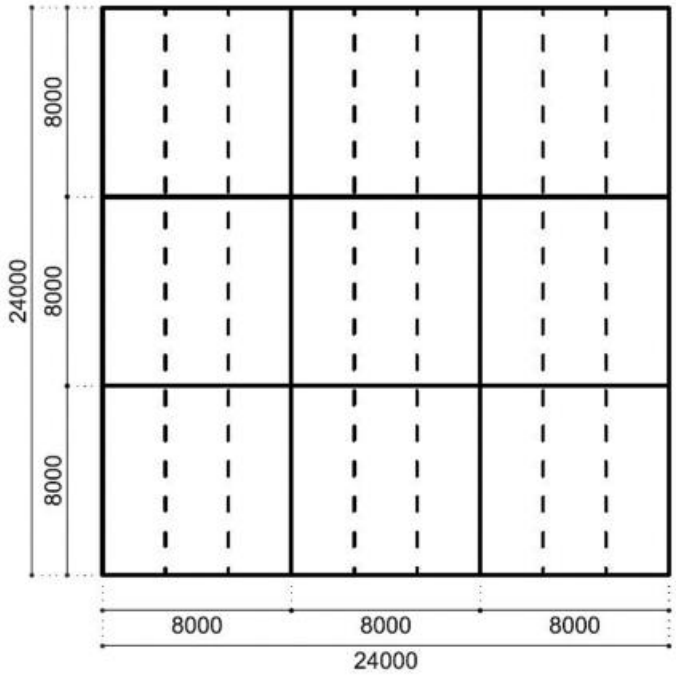

Figure 4.1 Plan configuration of the case study buildings

The buildings were designed as dual frames having one eccentrically braced frame and one moment resisting frame along each periphery in both X and Y directions. The third bay is designed as a gravity load resisting frame (simply supported).

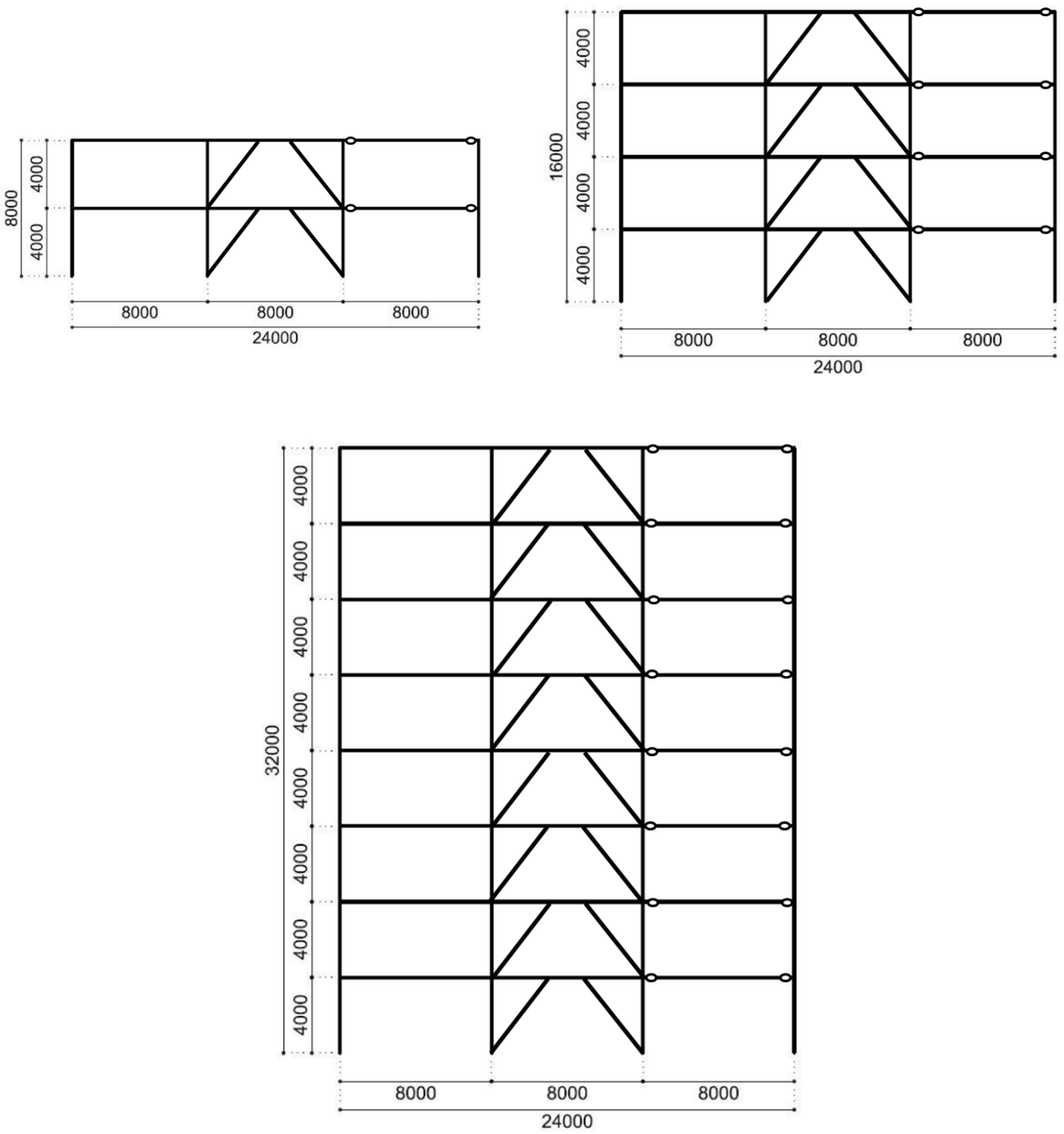

Figure 4.2 Side view (Elevation) of the case study buildings

The lateral load resisting frames in each direction are arranged in such a way in order to achieve independent structural behavior in the X and Y directions. A plan view of the arrangement of lateral load resisting system in the case study building is shown below.

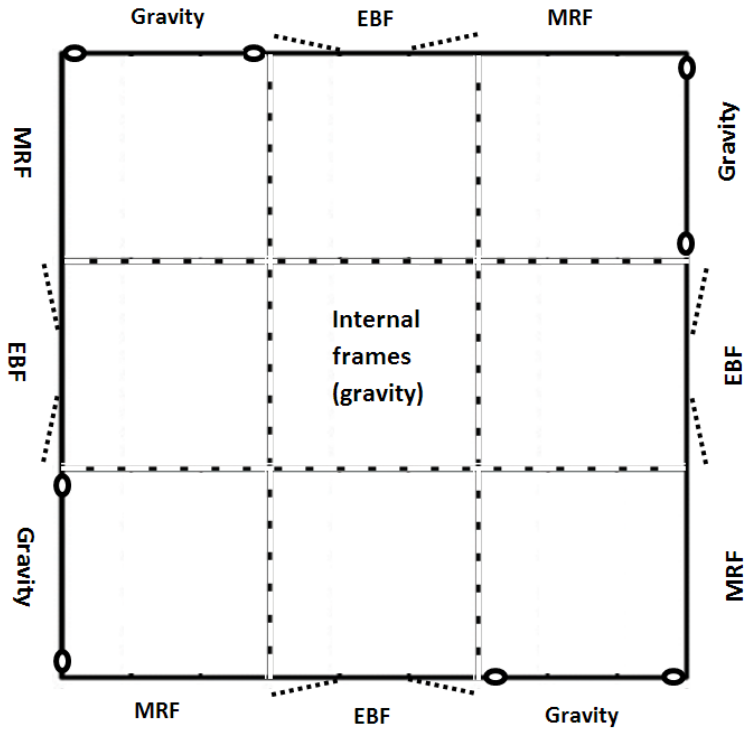

Figure 4.3 Arrangement of lateral load resisting system

4.1 Seismic design of case study frames

The dual frames are designed for the same loads (as per EN 1991-1-1, EN 1993-1-1 and EN 1998-1-1) as in the INNOSEIS project, which is briefly outlined below. It is noted that the behavior factor (q) for dual frames is taken as the same as that of ordinary eccentrically braced frames (EBF) as an initial estimate since the MRF is expected to remain elastic throughout and the ductility comes only from the eccentric braced frame deformations.

The loads considered for seismic design of the frame are

- Dead Loads: 2.75 kN/m^2
- Superimposed Dead Loads: 2.75 kN/m^2 (Floor level)
  2.75 kN/m^2 (Roof level)
  2.75 kN/m^2 (Perimeter walls load)
- Live Loads: 3.8 kN/m^2
- Seismic Loads
  - Importance factor: 1
  - Peak ground acceleration (PGA): 0.20 g
  - Soil type: C
  - Behavior factor (q): 6
  - Response spectrum parameters: S = 1.15
    T_B = 0.2 sec
    T_C = 0.6 sec
    T_D = 2.0 sec

S355 grade steel was chosen for all elements (except a few members where high strength steel (S460) was used, as will be denoted in the relevant sections). The response spectrum curve adopted for the design is shown below.

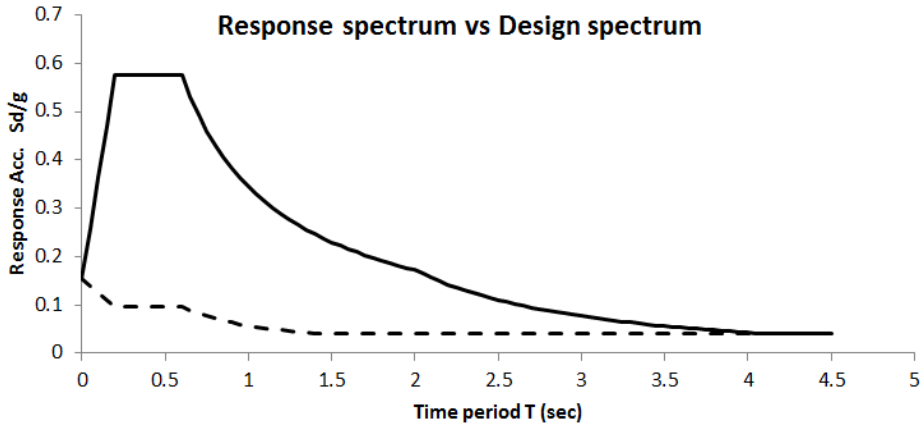

Figure 4.4 Response spectrum for the case study buildings (q=6)

The static and seismic design was performed in the program SAP2000. The member checks were performed directly in the software (SAP2000). Sample checks for the link proportioning and MRF elasticity checks are provided in Annexure A.
Different cases are considered in the arrangement of the dual frames, as denoted below

Case A) Dual frame (MRF + EBF + Gravity) – Reference case
Case B) Increased stiffness by an extra MRF (MRF + EBF + MRF)
Case C) Increased stiffness by stronger MRF (stiff MRF + Symmetric EBF + Gravity)

Two configurations are considered for each of the above cases

Case 1) Frames designed to be ductile enough to reach target displacement without failure of EBF at near collapse limit.
Case 2) Frames designed with very short links but which reaches target displacement at near collapse limit with failure of EBF links and activating reserve capacity in MRF.

Note: Since the idea behind the different cases is to study the effect of MRF on the post yield behavior of the EBF, and the MRFs are slender in comparison to the EBF, “minimal to no changes are made to the EBF bay” between the reference case A and cases B and C even though increasing the stiffness outside of EBF results in a slight decrease of forces in the links.
The design sections adopted for the different cases are shown below in the following sections. The primary steel grade (default) considered for the design was S355 but certain exceptions were made where high strength steel was used (S460). The sections using high strength steel are marked with an asterisk (*) to denote the use of HSS.

4.2 Design summary of case study frames (8 storey)

The final design (sections) of the buildings used for the case study (low, med and high rise) is summarized for all three cases (A, B and C) and configurations (1 and 2) in this section.

4.2.1. 8 Storey frame (case A1)

The results of eigenvalue analysis and static cum seismic design of the 8 storey 2D frame performed in SAP2000 are shown below.

Table 4.1 Eigenvalue results for 8 storey frame (case A1)

	Mode 1	Mode 2	Mode 3
Time Period	1.463462	0.513248	0.290036
Modal mass participation factor	0.76123	0.14754	3.90E-02

The design sections are shown below. (Steel grade: S355, S460 sections marked with *)

Table 4.2 Design cross sections - 8 storey frame (case A1)

A1	Columns			Beams			Link		
Stry.	Col 1	Col 2,3	Col 4	Span 1	Span 2	Span 3	Section	Length	Braces
1	HEB 260*	HEM 400*	HEB 260	IPE 360	HEB 260	IPE 450	HEB 180	1	HEB 260
2	HEB 260*	HEM 360*	HEB 260	IPE 360	HEB 260	IPE 450	HEB 200	1.1	HEB 260
3	HEB 260*	HEM 360*	HEB 260	IPE 360	HEB 260	IPE 450	HEB 180	1	HEB 260
4	HEB 260*	HEB 360*	HEB 260	IPE 360	HEB 240	IPE 450	HEB 180	1	HEB 240
5	HEB 260	HEB 360	HEB 260	IPE 360	HEB 220	IPE 450	HEB 160	0.9	HEB 220
6	HEB 260	HEB 320	HEB 260	IPE 360	HEB 220	IPE 450	HEA 180	0.9	HEB 200
7	HEB 260	HEB 300	HEB 260	IPE 360	HEB 220	IPE 450	HEB 140	0.8	HEB 180
8	HEB 260	HEB 300	HEB 260	IPE 360	HEB 220	IPE 450	HEB 100	0.56	HEB 160

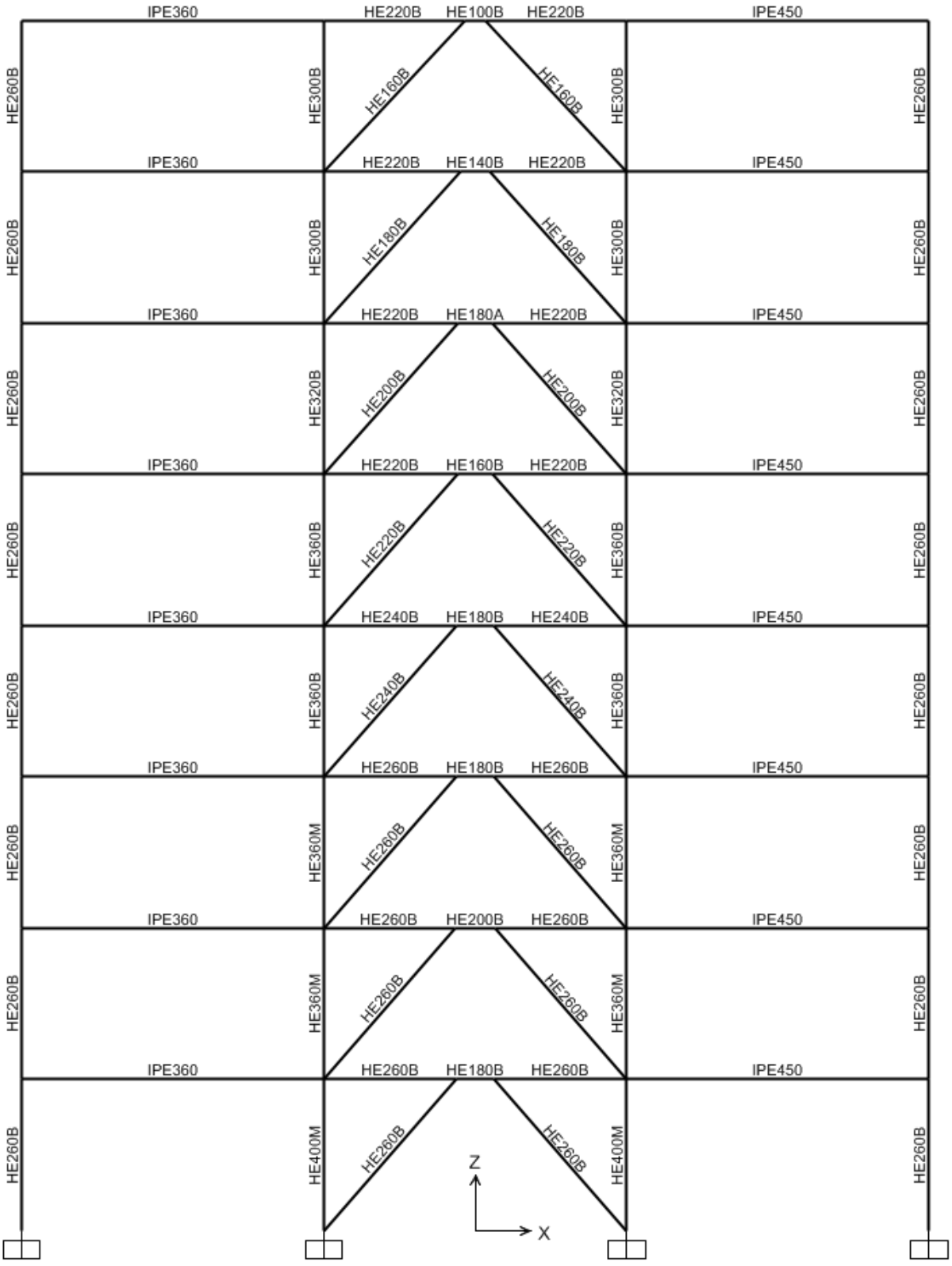

Figure 4.5 Design sections for 8 storey frame (case A1)

4.2.2. **8 Storey frame (case A2)**

The results of eigenvalue analysis and static cum seismic design of the 8 storey 2D frame performed in SAP2000 are shown below.

Table 4.3 Eigenvalue results for 8 storey frame (case A2)

	Mode 1	Mode 2	Mode 3
Time Period	1.193406	0.405907	0.227388
Modal mass participation factor	0.74142	0.16656	4.40E-02

The design sections are shown below.

Table 4.4 Design cross sections - 8 storey frame (case A2)

A2	Columns			Beams			Link		
Stry.	Col 1	Col 2,3	Col 4	Span 1	Span 2	Span 3	Section	Length	Braces
1	HEB 260	HEM 400	HEB 260	IPE 360	HEB 260	IPE 450	HEB 200	0.6	HEB 260
2	HEB 260	HEM 360	HEB 260	IPE 360	HEB 260	IPE 450	HEB 220	0.7	HEB 260
3	HEB 260	HEM 360	HEB 260	IPE 360	HEB 260	IPE 450	HEB 200	0.6	HEB 260
4	HEB 260	HEB 360	HEB 260	IPE 360	HEB 240	IPE 450	HEA 220	0.6	HEB 240
5	HEB 260	HEB 360	HEB 260	IPE 360	HEB 220	IPE 450	HEB 180	0.5	HEB 220
6	HEB 260	HEB 320	HEB 260	IPE 360	HEB 220	IPE 450	HEB 160	0.4	HEB 200
7	HEB 260	HEB 300	HEB 260	IPE 360	HEB 220	IPE 450	HEB 140	0.4	HEB 180
8	HEB 260	HEB 300	HEB 260	IPE 360	HEB 220	IPE 450	IPE 140	0.4	HEB 160

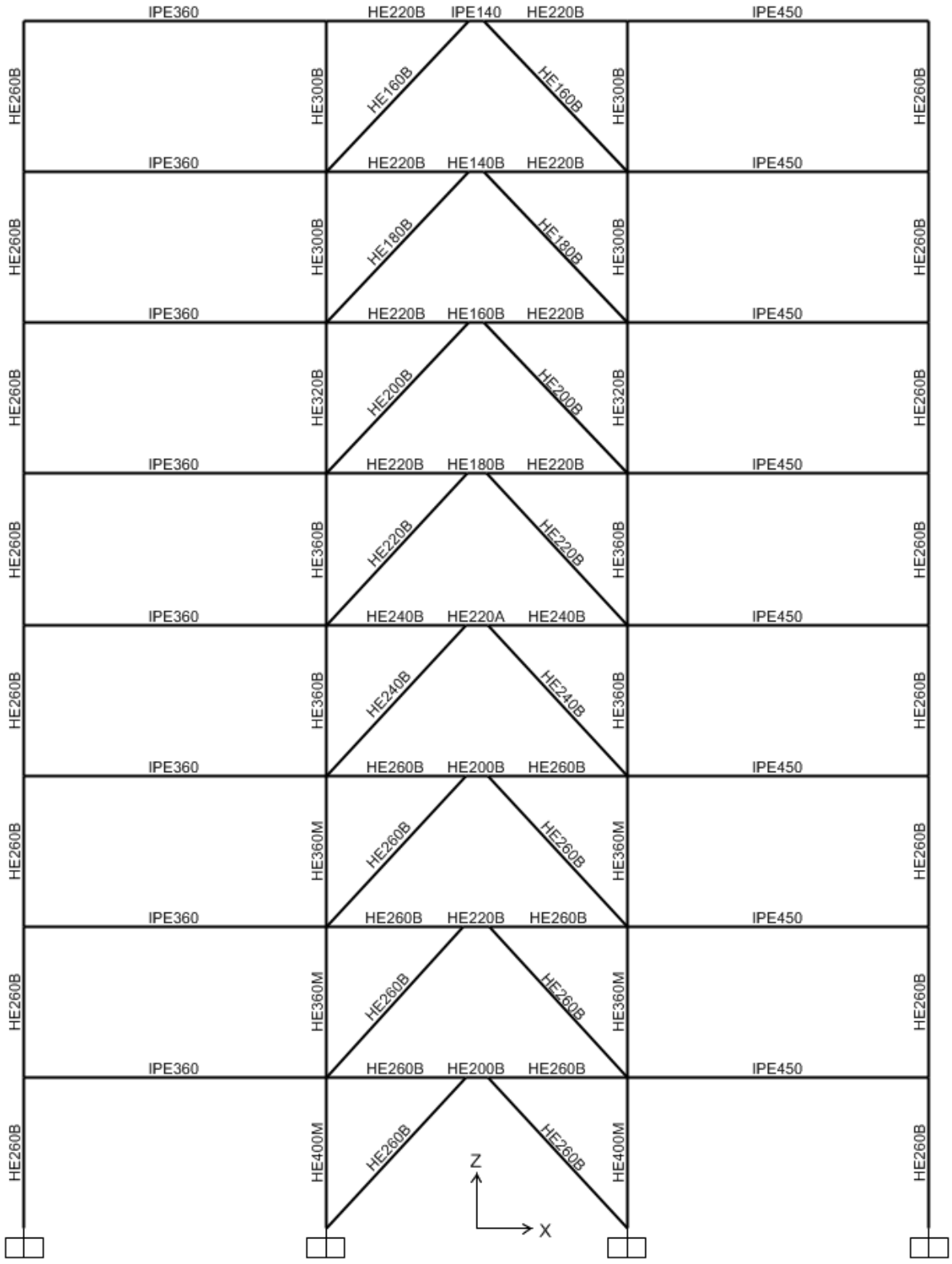

Figure 4.6 Design sections for 8 storey frame (case A2)

4.2.3. **4 Storey frame (case A1)**

The results of eigenvalue analysis and static cum seismic design of the 4 storey 2D frame performed in SAP2000 are shown below.

Table 4.5 Eigenvalue results for 4 storey frame (case A1)

	Mode 1	Mode 2	Mode 3
Time Period	0.796623	0.290602	0.180406
Modal mass participation factor	0.83949	0.1034	2.99E-02

Table 4.6 Design cross sections - 4 storey frame (case A1)

A1	Columns			Beams			Link		
Stry.	Col 1	Col 2	Col 3	Span 1	Span 2	Span 3	Section	Length	Braces
1	HEB 220	HEB 320	HEB 220	IPE 360	HEB 240	IPE 450	HEA 220	1.15	HEB 240
2	HEB 220	HEB 300	HEB 220	IPE 360	HEB 240	IPE 450	HEA 220	1.15	HEB 240
3	HEB 220	HEB 260	HEB 220	IPE 360	HEB 220	IPE 450	HEB 160	0.9	HEB 220
4	HEB 220	HEB 240	HEB 220	IPE 360	HEB 220	IPE 450	HEA 140	0.75	HEB 180

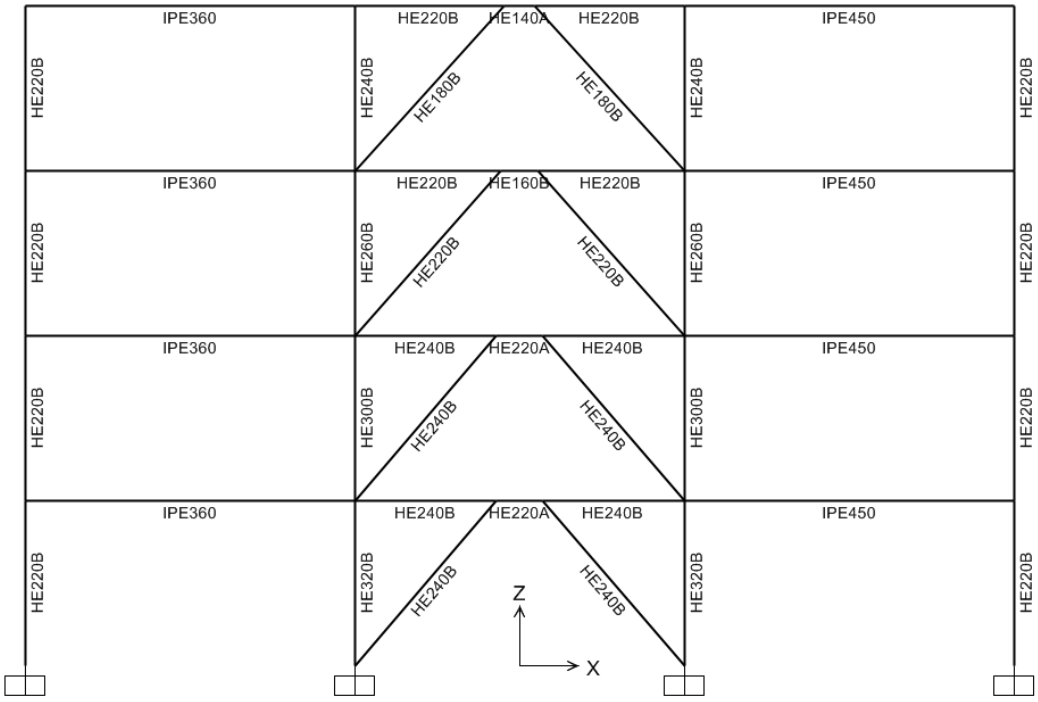

Figure 4.7 Design sections for 4 storey frame (case A1)

4.2.4. **4 Storey frame (case A2)**

The results of eigenvalue analysis and static cum seismic design of the 4 storey 2D frame (case A2) performed in SAP2000 are shown below.

Table 4.7 Eigenvalue results for 4 storey frame (case A2)

	Mode 1	Mode 2	Mode 3
Time Period	0.565714	0.211315	0.13076
Modal mass participation factor	0.8214	0.12812	0.00

Table 4.8 Design cross sections - 4 storey frame (case A2)

A2	Columns			Beams			Link		
Stry.	Col 1	Col 2	Col 3	Span 1	Span 2	Span 3	Section	Length	Braces
1	HEB 220	HEM 300	HEB 220	IPE 360	HEB 240	IPE 450	HEB 220	0.6	HEB 240
2	HEB 220	HEB 300	HEB 220	IPE 360	HEB 240	IPE 450	HEB 220	0.6	HEB 240
3	HEB 220	HEB 260	HEB 220	IPE 360	HEB 220	IPE 450	HEB 180	0.5	HEB 220
4	HEB 220	HEB 240	HEB 220	IPE 360	HEB 220	IPE 450	HEB 140	0.4	HEB 180

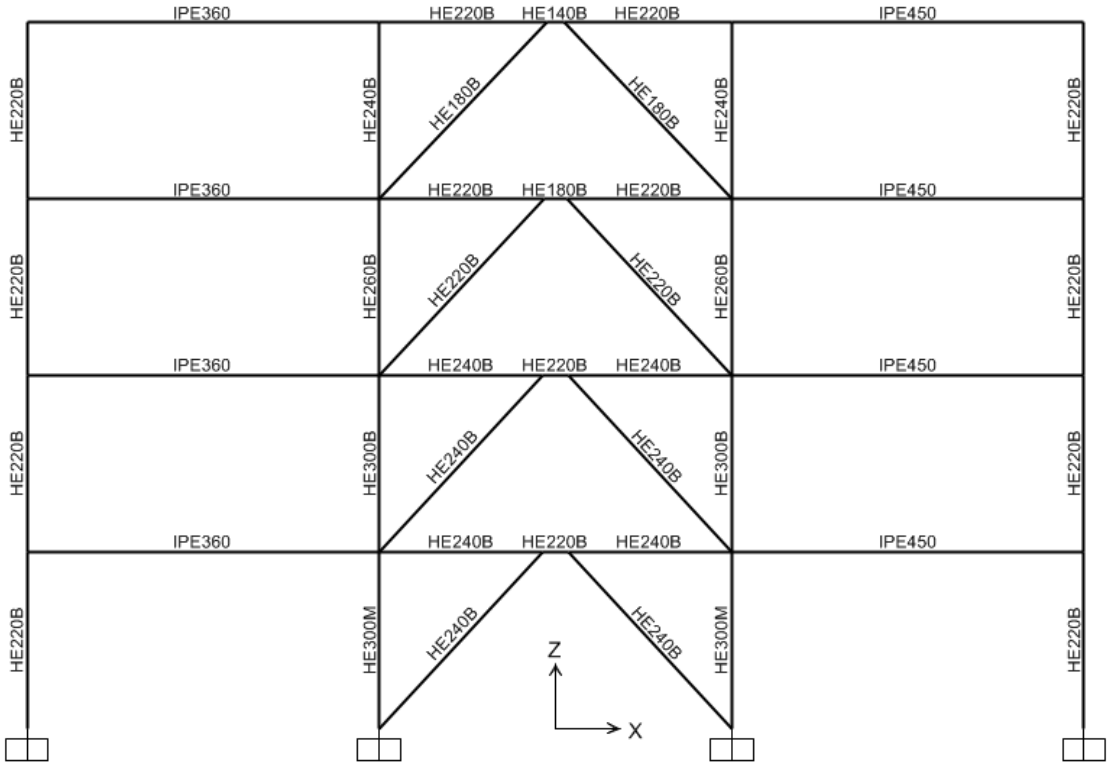

Figure 4.8 Design sections for 4 storey frame (case A1)

4.2.5. **2 Storey frame (case A1)**

The results of eigenvalue analysis and static cum seismic design of the 2 storey 2D frame (case A1) performed in SAP2000 are shown below.

Table 4.9 Eigenvalue results for 2 storey frame (case A1)

	Mode 1	Mode 2	Mode 3
Time Period	0.451714	0.180207	0.097871
Modal mass participation factor	0.86251	0.10468	0.00

Table 4.10 Design cross sections - 2 storey frame (case A1)

A1	Columns			Beams			Link		
Stry.	Col 1	Col 2, 3	Col 4	Span 1	Span 2	Span 3	Section	Length	Braces
1	HEB 220	HEB 220	HEB 220	IPE 360	HEB 240	IPE 450	HEA 200	1	HEB 240
2	HEB 220	HEB 220	HEB 220	IPE 360	HEB 200	IPE 450	HEA 180	0.95	HEB 200

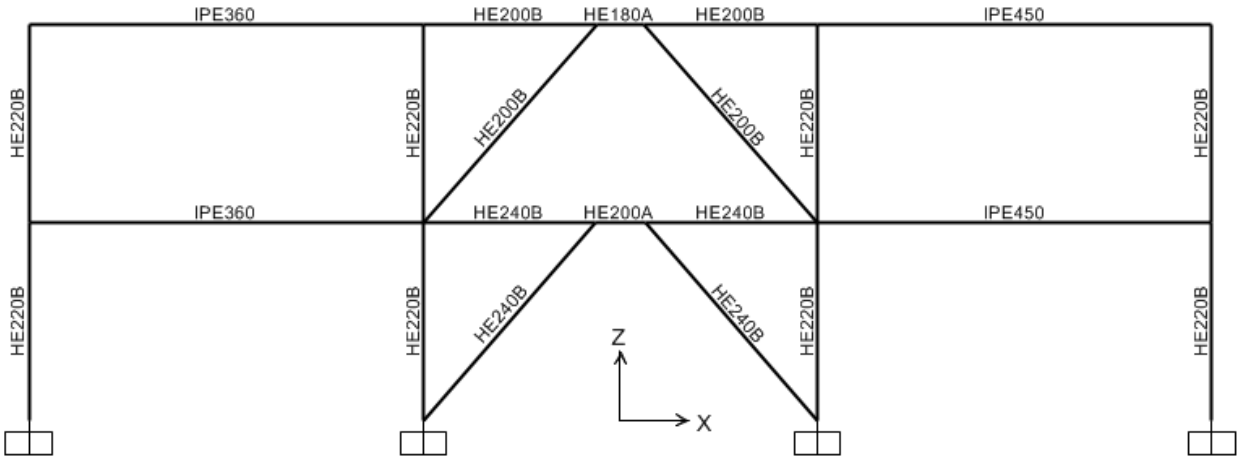

Figure 4.9 Design sections for 2 storey frame (case A1)

4.2.6. **2 Storey frame (case A2)**

The results of eigenvalue analysis and static cum seismic design of the 2 storey 2D frame (case A2) performed in SAP2000 are shown below.

Table 4.11 Eigenvalue results for 2 storey frame (case A2)

	Mode 1	Mode 2	Mode 3
Time Period	0.316823	0.124415	0.098357
Modal mass participation factor	0.88915	0.09457	0.00E+00

Table 4.12 Design cross sections - 2 storey frame (case A2)

A2	Columns			Beams			Link		
Stry.	Col 1	Col 2, 3	Col 4	Span 1	Span 2	Span 3	Section	Length	Braces
1	HEB 220	HEB 220	HEB 220	IPE 360	HEB 240	IPE 450	HEA 200	0.5	HEB 240
2	HEB 220	HEB 220	HEB 220	IPE 360	HEB 200	IPE 450	HEA 180	0.4	HEB 200

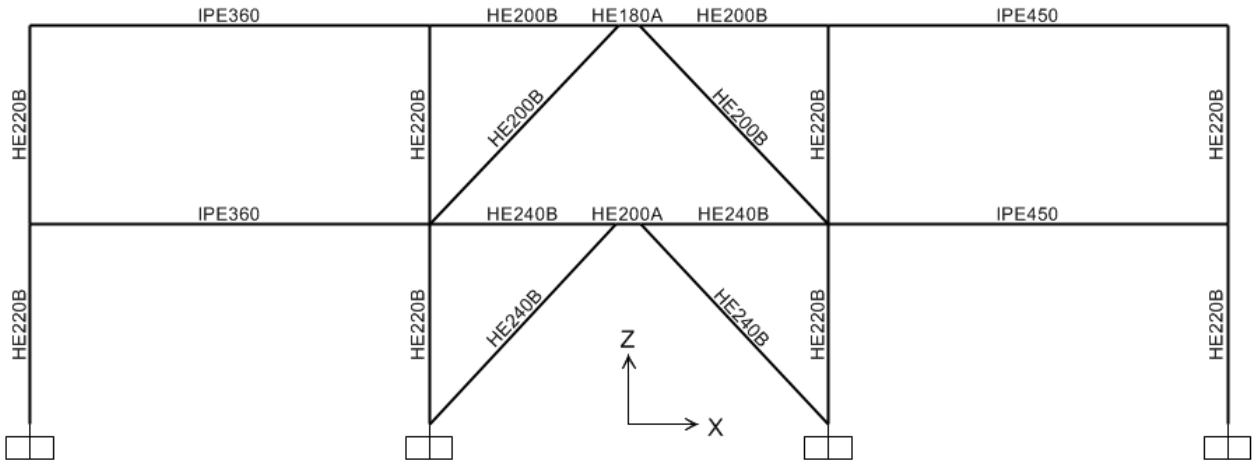

Figure 4.10 Design sections for 2 storey frame (case A2)

4.3 Design summary of variations in case study frames

Different modifications to the moment resisting frame part in the dual frames have been considered to study its effect on augmenting the seismic performance of the dual frames. Since the model geometries have been retained as in the case A, the other proposed geometries are summarized below (with the changes in sections marked in bold and underline).

As in the previous section, S355 grade of steel was used for all sections except the ones marked with an asterisk (*) where HSS (S460) was adopted.

Table 4.13 Design cross sections - 8 storey frame (case B1)

B1	Columns			Beams			Link		
Stry.	Col 1	Col 2,3	Col 4	Span 1	Span 2	Span 3	Section	Length	Braces
1	HEB 260*	HEM 400*	**HEB 260***	IPE 360	HEB 260	**IPE 360**	HEB 180	1	HEB 260
2	HEB 260*	HEM 360*	**HEB 260***	IPE 360	HEB 260	**IPE 360**	HEB 200	1.1	HEB 260
3	HEB 260*	HEM 360*	**HEB 260***	IPE 360	HEB 260	**IPE 360**	HEB 180	1	HEB 260
4	HEB 260*	HEB 360*	**HEB 260***	IPE 360	HEB 240	**IPE 360**	HEB 180	1	HEB 240
5	HEB 260	HEB 360	**HEB 260**	IPE 360	HEB 220	**IPE 360**	HEB 160	0.9	HEB 220
6	HEB 260	HEB 320	**HEB 260**	IPE 360	HEB 220	**IPE 360**	HEA 180	0.9	HEB 200
7	HEB 260	HEB 300	**HEB 260**	IPE 360	HEB 220	**IPE 360**	HEB 140	0.8	HEB 180
8	HEB 260	HEB 300	**HEB 260**	IPE 360	HEB 220	**IPE 360**	HEB 100	0.56	HEB 160

Table 4.14 Design cross sections - 8 storey frame (case B2)

B2	Columns			Beams			Link		
Stry.	Col 1	Col 2,3	Col 4	Span 1	Span 2	Span 3	Section	Length	Braces
1	HEB 260	HEM 400	**HEB 260**	IPE 360	HEB 260	**IPE 360**	HEB 200	0.6	HEB 260
2	HEB 260	HEM 360	**HEB 260**	IPE 360	HEB 260	**IPE 360**	HEB 220	0.7	HEB 260
3	HEB 260	HEM 360	**HEB 260**	IPE 360	HEB 260	**IPE 360**	HEB 200	0.6	HEB 260
4	HEB 260	HEB 360	**HEB 260**	IPE 360	HEB 240	**IPE 360**	HEA 220	0.6	HEB 240
5	HEB 260	HEB 360	**HEB 260**	IPE 360	HEB 220	**IPE 360**	HEB 180	0.5	HEB 220
6	HEB 260	HEB 320	**HEB 260**	IPE 360	HEB 220	**IPE 360**	HEB 160	0.4	HEB 200
7	HEB 260	HEB 300	**HEB 260**	IPE 360	HEB 220	**IPE 360**	HEB 140	0.4	HEB 180
8	HEB 260	HEB 300	**HEB 260**	IPE 360	HEB 220	**IPE 360**	IPE 140	0.4	HEB 160

Table 4.15 Design cross sections - 4 storey frame (case B1)

B1	Columns			Beams			Link		
Stry.	Col 1	Col 2	Col 3	Span 1	Span 2	Span 3	Section	Length	Braces
1	HEB 220	HEB 320	HEB 220	IPE 360	HEB 240	**IPE 360**	HEA 220	1.15	HEB 240
2	HEB 220	HEB 300	HEB 220	IPE 360	HEB 240	**IPE 360**	HEA 220	1.15	HEB 240
3	HEB 220	HEB 260	HEB 220	IPE 360	HEB 220	**IPE 360**	HEB 160	0.9	HEB 220
4	HEB 220	HEB 240	HEB 220	IPE 360	HEB 220	**IPE 360**	HEA 140	0.75	HEB 180

Table 4.16 Design cross sections - 4 storey frame (case B2)

B2	Columns			Beams			Link		
Stry.	Col 1	Col 2	Col 3	Span 1	Span 2	Span 3	Section	Length	Braces
1	HEB 220	HEM 300	HEB 220	IPE 360	HEB 240	**IPE 360**	HEB 220	0.6	HEB 240
2	HEB 220	HEB 300	HEB 220	IPE 360	HEB 240	**IPE 360**	HEB 220	0.6	HEB 240
3	HEB 220	HEB 260	HEB 220	IPE 360	HEB 220	**IPE 360**	HEB 180	0.5	HEB 220
4	HEB 220	HEB 240	HEB 220	IPE 360	HEB 220	**IPE 360**	HEB 140	0.4	HEB 180

Table 4.17 Design cross sections - 2 storey frame (case B1)

B1	Columns			Beams			Link		
Stry.	Col 1	Col 2, 3	Col 4	Span 1	Span 2	Span 3	Section	Length	Braces
1	HEB 220	HEB 220	HEB 220	IPE 360	HEB 240	**IPE 360**	HEA 200	1	HEB 240
2	HEB 220	HEB 220	HEB 220	IPE 360	HEB 200	**IPE 360**	HEA 180	0.95	HEB 200

Table 4.18 Design cross sections - 2 storey frame (case B2)

B2	Columns			Beams			Link		
Stry.	Col 1	Col 2, 3	Col 4	Span 1	Span 2	Span 3	Section	Length	Braces
1	HEB 220	HEB 220	HEB 220	IPE 360	HEB 240	**IPE 360**	HEA 200	0.5	HEB 240
2	HEB 220	HEB 220	HEB 220	IPE 360	HEB 200	**IPE 360**	HEA 180	0.4	HEB 200

Similarly, the models of case C were constructed based on the case A models by making the MRF bay stiffer (simulating the effect of having an interior MRF bay with stiff columns) and the design sections adopted are summarized below.

Table 4.19 Design cross sections - 8 storey frame (case C1)

C1	Columns			Beams			Link		
Stry.	Col 1	Col 2,3	Col 4	Span 1	Span 2	Span 3	Section	Length	Braces
1	**HEM 400***	HEM 400*	HEB 260	IPE 360	HEB 260	IPE 450	HEB 180	1	HEB 260
2	**HEM 360***	HEM 360*	HEB 260	IPE 360	HEB 260	IPE 450	HEB 200	1.1	HEB 260
3	**HEM 360***	HEM 360*	HEB 260	IPE 360	HEB 260	IPE 450	HEB 180	1	HEB 260
4	**HEB 360***	HEB 360*	HEB 260	IPE 360	HEB 240	IPE 450	HEB 180	1	HEB 240
5	**HEB 360**	HEB 360	HEB 260	IPE 360	HEB 220	IPE 450	HEB 160	0.9	HEB 220
6	**HEB 320**	HEB 320	HEB 260	IPE 360	HEB 220	IPE 450	HEA 180	0.9	HEB 200
7	**HEB 300**	HEB 300	HEB 260	IPE 360	HEB 220	IPE 450	HEB 140	0.8	HEB 180
8	**HEB 300**	HEB 300	HEB 260	IPE 360	HEB 220	IPE 450	HEB 100	0.56	HEB 160

Table 4.20 Design cross sections - 8 storey frame (case C2)

C2	Columns			Beams			Link		
Stry.	Col 1	Col 2,3	Col 4	Span 1	Span 2	Span 3	Section	Length	Braces
1	**HEM 400**	HEM 400	HEB 260	IPE 360	HEB 260	IPE 450	HEB 200	0.6	HEB 260
2	**HEM 360**	HEM 360	HEB 260	IPE 360	HEB 260	IPE 450	HEB 220	0.7	HEB 260
3	**HEM 360**	HEM 360	HEB 260	IPE 360	HEB 260	IPE 450	HEB 200	0.6	HEB 260
4	**HEB 360**	HEB 360	HEB 260	IPE 360	HEB 240	IPE 450	HEA 220	0.6	HEB 240
5	**HEB 360**	HEB 360	HEB 260	IPE 360	HEB 220	IPE 450	HEB 180	0.5	HEB 220
6	**HEB 320**	HEB 320	HEB 260	IPE 360	HEB 220	IPE 450	HEB 160	0.4	HEB 200
7	**HEB 300**	HEB 300	HEB 260	IPE 360	HEB 220	IPE 450	HEB 140	0.4	HEB 180
8	**HEB 300**	HEB 300	HEB 260	IPE 360	HEB 220	IPE 450	IPE 140	0.4	HEB 160

Table 4.21 Design cross sections - 4 storey frame (case C1)

C1	Columns			Beams			Link		
Stry.	Col 1	Col 2	Col 3	Span 1	Span 2	Span 3	Section	Length	Braces
1	**HEB 320**	HEB 320	HEB 220	IPE 360	HEB 240	IPE 450	HEA 220	1.15	HEB 240
2	**HEB 300**	HEB 300	HEB 220	IPE 360	HEB 240	IPE 450	HEA 220	1.15	HEB 240
3	**HEB 260**	HEB 260	HEB 220	IPE 360	HEB 220	IPE 450	HEB 160	0.9	HEB 220
4	**HEB 240**	HEB 240	HEB 220	IPE 360	HEB 220	IPE 450	HEA 140	0.75	HEB 180

Table 4.22 Design cross sections - 4 storey frame (case C2)

C2	Columns			Beams			Link		
Stry.	Col 1	Col 2	Col 3	Span 1	Span 2	Span 3	Section	Length	Braces
1	**HEM 300**	HEM 300	HEB 220	IPE 360	HEB 240	IPE 450	HEB 220	0.6	HEB 240
2	**HEB 300**	HEB 300	HEB 220	IPE 360	HEB 240	IPE 450	HEB 220	0.6	HEB 240
3	**HEB 260**	HEB 260	HEB 220	IPE 360	HEB 220	IPE 450	HEB 180	0.5	HEB 220
4	**HEB 240**	HEB 240	HEB 220	IPE 360	HEB 220	IPE 450	HEB 140	0.4	HEB 180

Table 4.23 Design cross sections - 2 storey frame (case C1)

C1	Columns			Beams			Link		
Stry.	Col 1	Col 2, 3	Col 4	Span 1	Span 2	Span 3	Section	Length	Braces
1	HEB 220	HEB 220	HEB 220	IPE 360	HEB 240	IPE 450	HEA 200	1	HEB 240
2	HEB 220	HEB 220	HEB 220	IPE 360	HEB 200	IPE 450	HEA 180	0.95	HEB 200

Table 4.24 Design cross sections - 2 storey frame (case C2)

C2	Columns			Beams			Link		
Stry.	Col 1	Col 2, 3	Col 4	Span 1	Span 2	Span 3	Section	Length	Braces
1	HEB 220	HEB 220	HEB 220	IPE 360	HEB 240	IPE 450	HEA 200	0.5	HEB 240
2	HEB 220	HEB 220	HEB 220	IPE 360	HEB 200	IPE 450	HEA 180	0.4	HEB 200

As we can see, the cases C1 and C2 are the same as cases A1 and A2 for the 2 storey frame and hence they are neglected. After the static and seismic design of the frames was performed, a non-linear static analysis was performed and the results are presented in the next chapter.

Chapter 5 - Non-linear Analysis

This chapter summarizes the modeling parameters used to perform the non-linear static and dynamic analyses on the case study frames and the results obtained so.

5.1 Analytical tool

The finite element analysis program Seismostruct [Seismosoft, 2004] is used to run all analysis. The package is able to predict large displacement behavior in all elements using the fiber modeling technique including geometric and material non-linearities.

In order to capture the post peak behavior of the link elements, one must model the shear (and flexural) non-linearities to the best possible accuracy while keeping a limit on computational demands. The fiber models of elements can accurately predict axial (and thereby flexural) stresses in elements but are not suitable to capture shear inelasticity. Hence, post-yield behavior of the shear links are captured by modeling it as shear springs at the ends of an otherwise elastic link member [REF]. The material model used to simulate the behavior of structural steel was the one proposed by Menegotto- Pinto (with the default parameters), as shown below.

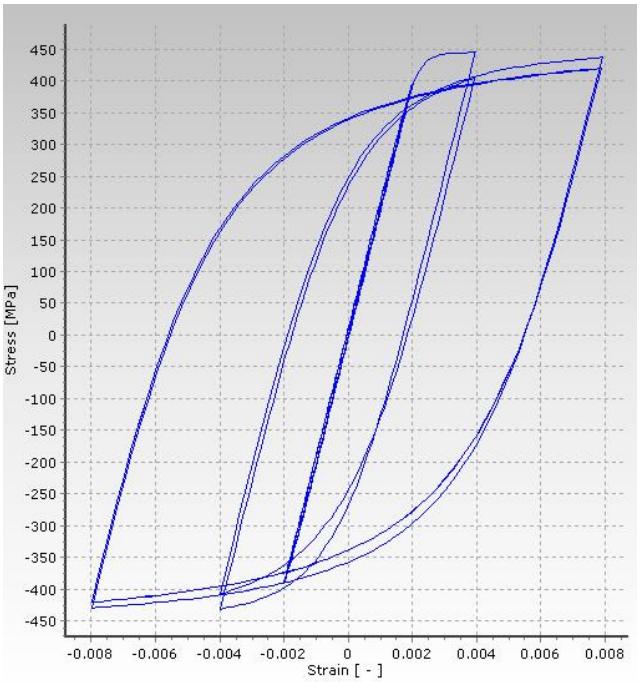

Figure 5.1 Menegotto-Pinto steel model (Seismostruct)

5.2 Modelling the link element

It is known that the behavior of EBF's are greatly influenced by the links (the primary and preferably the only source of hysteretic energy dissipation).The two main factors affecting the behavior of links are

- Cross section of the link element (i.e. Capacity)
- Length of the link element

The limiting values for link lengths, as provided in the Euro codes are already summarized in section 3.1.2. Since the link lengths are provided in such a way as to ensure the shear yielding of the links, the non-linear shear behavior is deemed to be more appropriate to be incorporated into the model rather than non-linearity in flexure.

As observed by the authors, a small drawback of the model is that it implicitly ignores the axial forces developed in the link element (as observed by [20, 21, 22]. But the effect of axial forces (tension) which develop in the link due to its elongation at large displacements (post yield behavior) are captured in the fiber model used by Seismostruct and hence this model was chosen as the most appropriate to model the link behavior both before and after yielding.

5.2.1. **Description of link model**

The link element as a whole consists of three segments

1. Flexural and Shear spring at one end
2. Elastic link element in the middle
3. Flexural and shear spring at the other end

Since the links under consideration are short links, flexural springs are not modeled explicitly and only shear springs are used to capture shear deformations of the element. It should be noted that ideally the elastic element used to model the link element should have appropriate flexural stiffness (EI) but infinite shear stiffness (GJ) to model the correct shear behavior. But this issue does not arrive in the Seismostruct since fiber modelling does not account for shear deformations. The basic link behavior as modeled in Seismostruct is shown below.

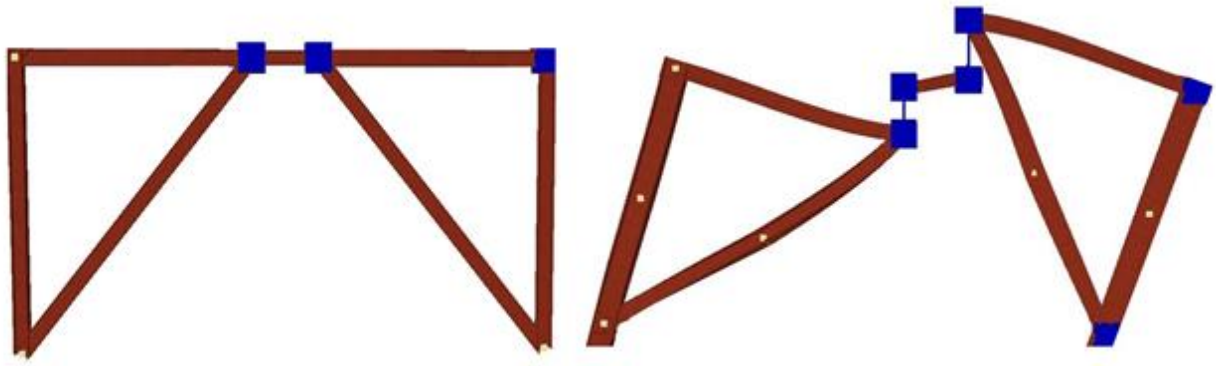

Figure 5.2 Link modelling in Seismostruct (initial and deformed shapes)

From the above figure, it can be seen that shear deformations are captured as spring elongations in the link elements situated at the ends of the link beam whereas flexural deformations are captured directly in the link element (fiber model).

The governing equations used to calculate the shear spring stiffness values are summarized below.

The reduction factor (χ) used to calculate the shear area was taken as

$$\chi = \frac{b * \left(d - t_f\right)^5}{240\ A\ i^4} * \left[15\frac{\eta^2}{\zeta} + 10\eta + 5\eta\frac{b^2}{\left(d - t_f\right)^2} + 2\zeta\right]$$

Where

b = width of the section

d = depth of the section

t_f = flange thickness

A = Area of the section

i = radius of gyration

η = stiffness parameter, given by $2t_f / (d - t_f)$

ζ = stiffness parameter, given by t_w/b

Since the link shear stiffness is modeled as a spring (force vs displacement), the stiffness of the spring was taken as

$$K_{L1,0} = \frac{G\ A}{\chi\ {}^{e}/_{2}}$$

The term (e/2) at the denominator signifies the link elongation over one half of the length of the link (since we are modelling two springs, one at each end).

Yield force limit was calculated as per Eurocode, taking only the shear capacity of the web, as

$V_y = 0.577 * f_y * A_{web}$

And ultimate shear capacity of the links was taken to be 50% higher than the yield force.

$V_u = 1.5 * V_y$

The post yield stiffness was calculated such that the ultimate capacity is reached at a plastic link rotation of 0.08 radians,

$$K_{L1,1} = \frac{V_u - V_p}{0.08 * \frac{e}{2} * K_{L1,0} + (V_u - V_p)} K_{L1,0}$$

The shear springs were modeled in Seismostruct using link elements as kinematic bilinear springs based on the following parameters

1) Initial stiffness ($K_{L1,0}$)
2) Yield force (V_P)
3) Post yield stiffness ratio ($K_{L1,1}$ / $K_{L1,0}$)

The material model used in Seismostruct for the link elements is shown below.

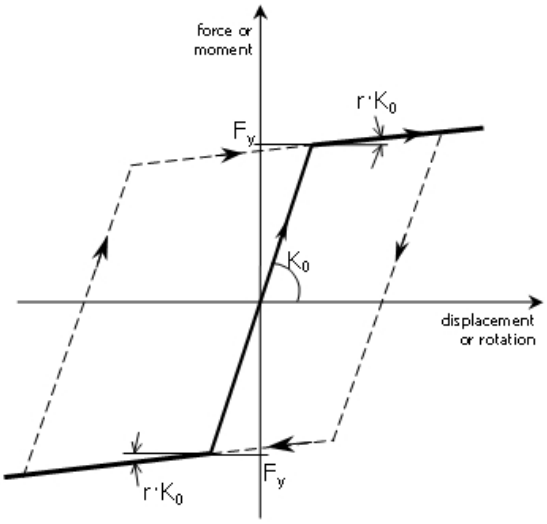

Figure 5.3 Link element (shear spring) model in Seismostruct

5.3 Non-linear Static Analysis (pushover)

Two kinds of lateral force distributions (as presented in the Eurocodes) are used to perform the pushover analyses of the structures; uniform and triangular. For both cases, it is checked whether the structure is ductile enough to withstand displacements corresponding to the three limit states of seismic action (Damage limitation, Significant Damage and Near Collapse).
Note: For the case 1 structures, even though the frame has a post peak capacity even after the failure of the shear link by the presence of the MRF, the reserve capacity is not taken into account.

The triangular and uniform pushover curves (with target displacements for the three limit states) for the 8,4 and 2 storey buildings for different cases are shown below. The target displacements are shown in the dotted vertical lines.

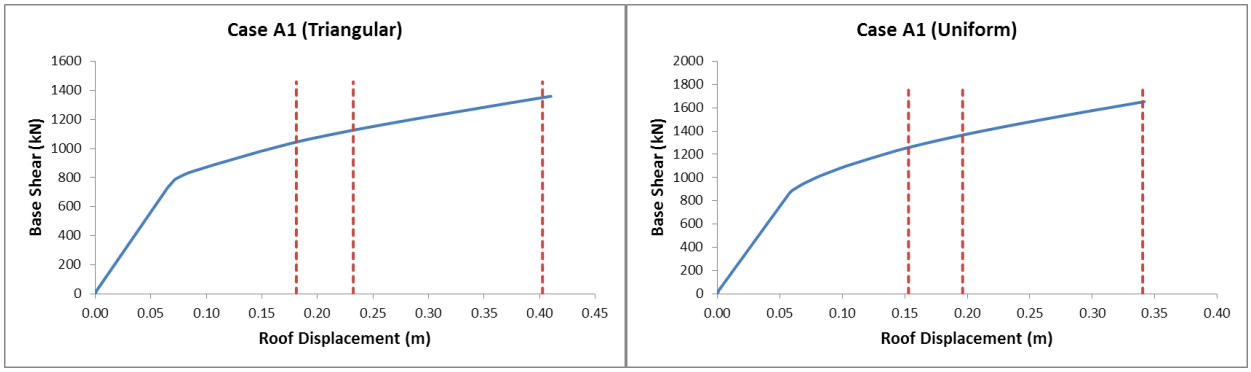

Figure 5.4 Pushover curves (case A1) for the 8 storey building

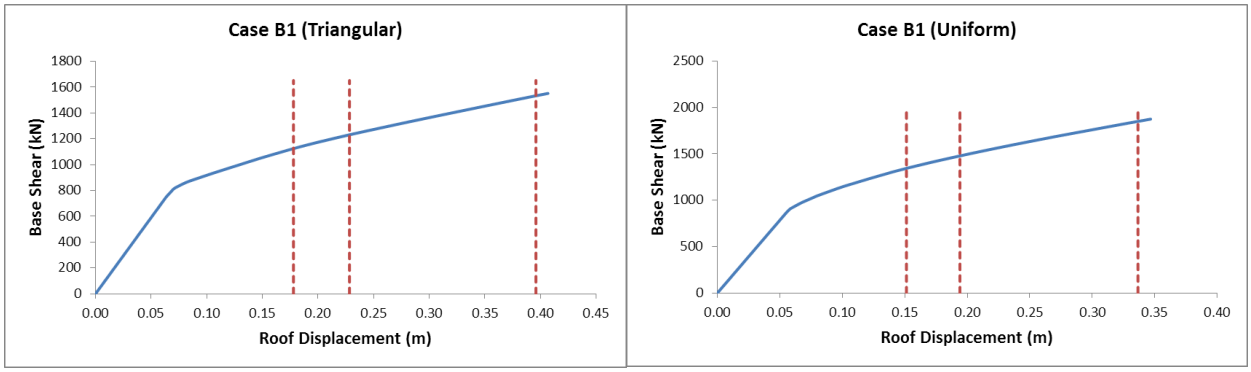

Figure 5.5 Pushover curves (case B1) for the 8 storey building

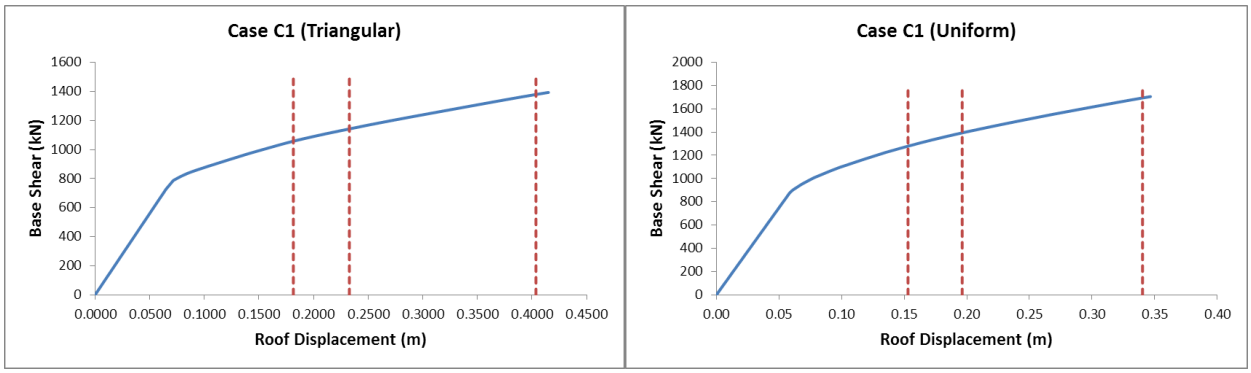

Figure 5.6 Pushover curves (case C1) for the 8 storey building

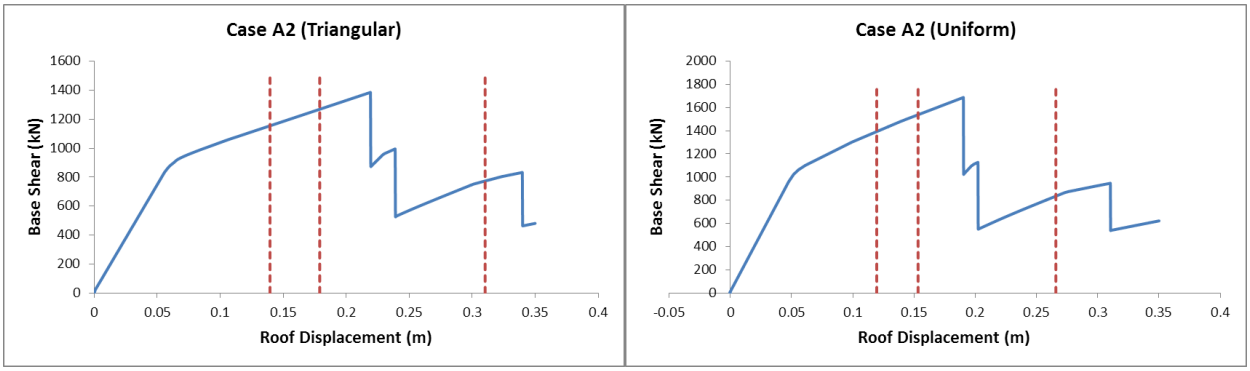

Figure 5.7 Pushover curves (case A2) for the 8 storey building

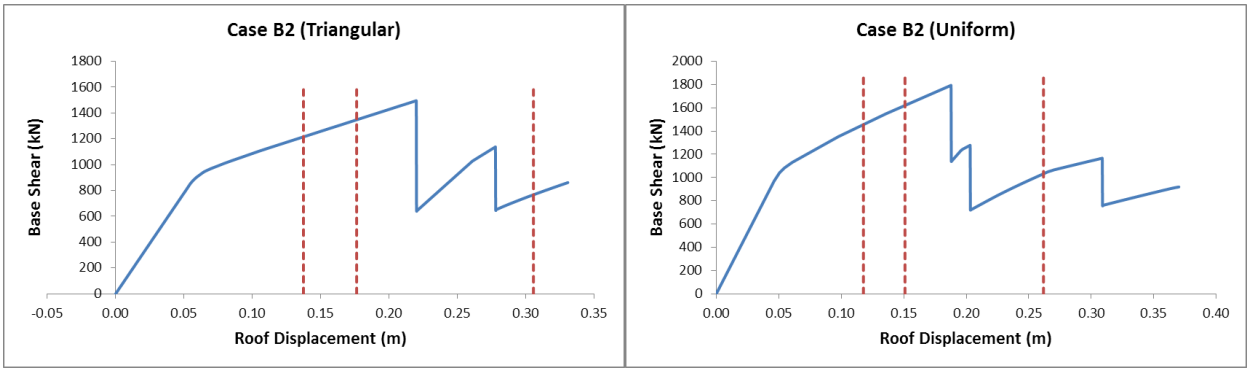

Figure 5.8 Pushover curves (case B2) for the 8 storey building

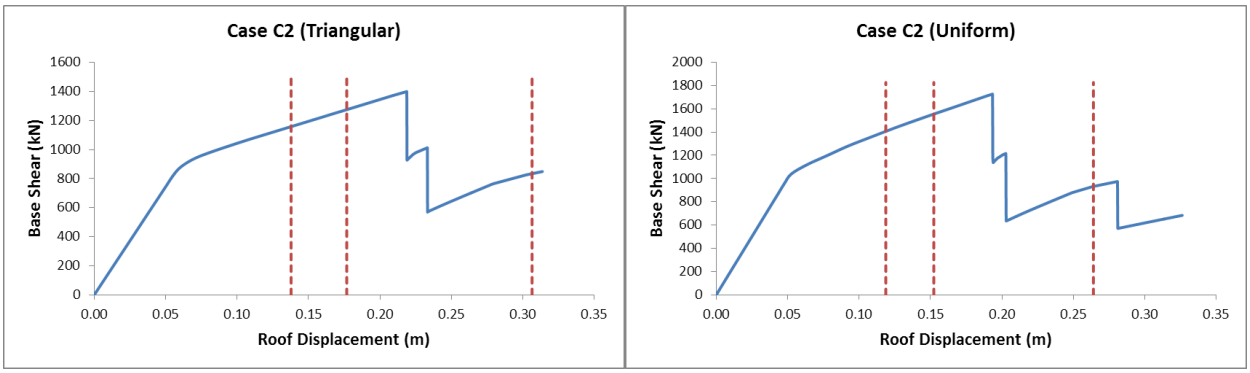

Figure 5.9 Pushover curves (case C2) for the 8 storey building

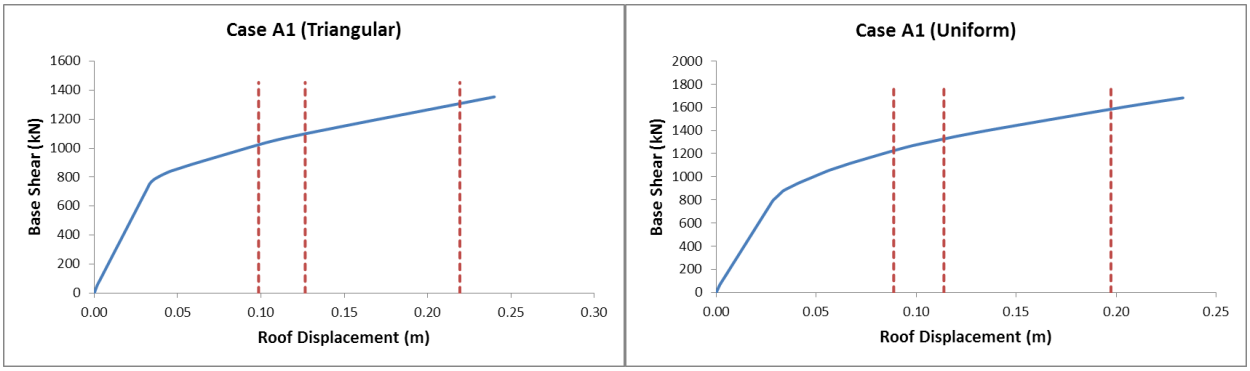

Figure 5.10 Pushover curves (case A1) for the 4 storey building

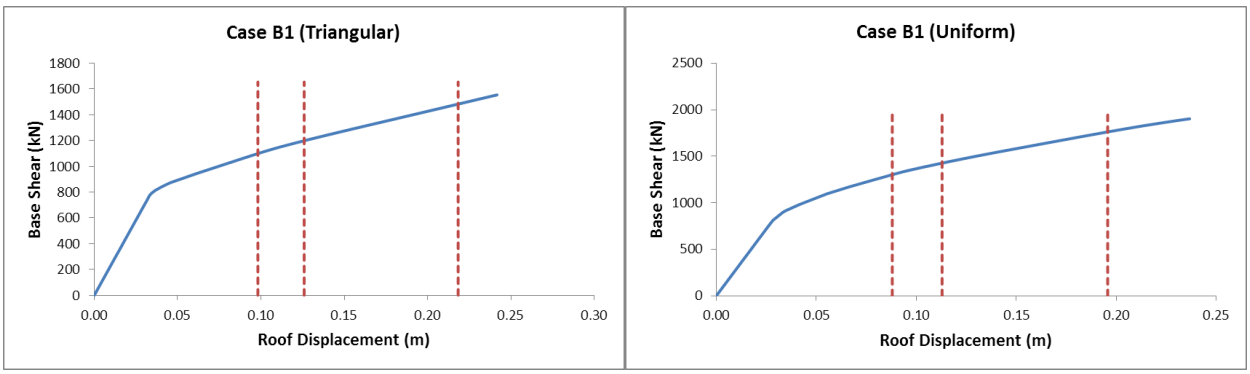

Figure 5.11 Pushover curves (case B1) for the 4 storey building

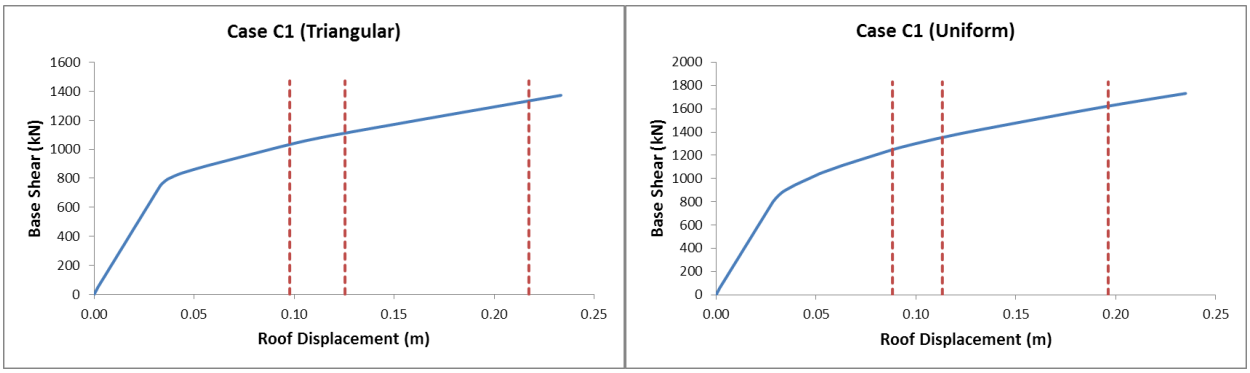

Figure 5.12 Pushover curves (case C1) for the 4 storey building

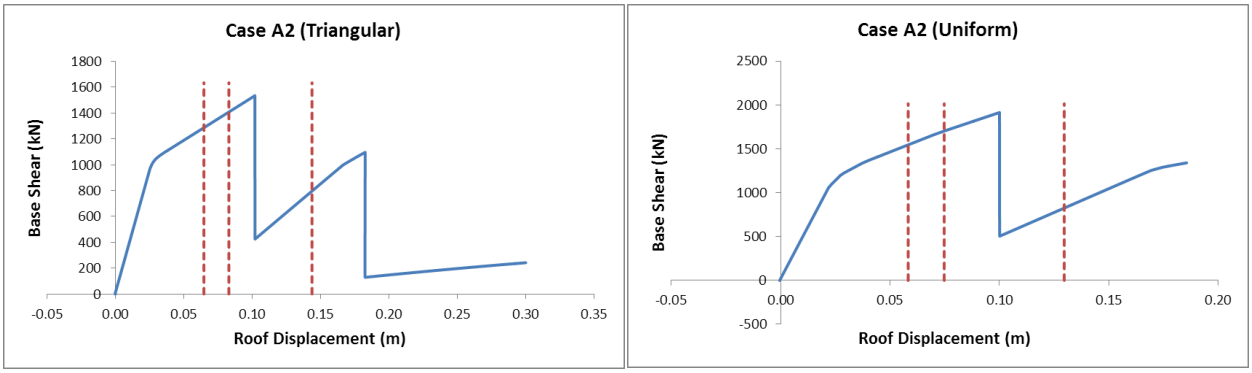

Figure 5.13 Pushover curves (case A2) for the 4 storey building

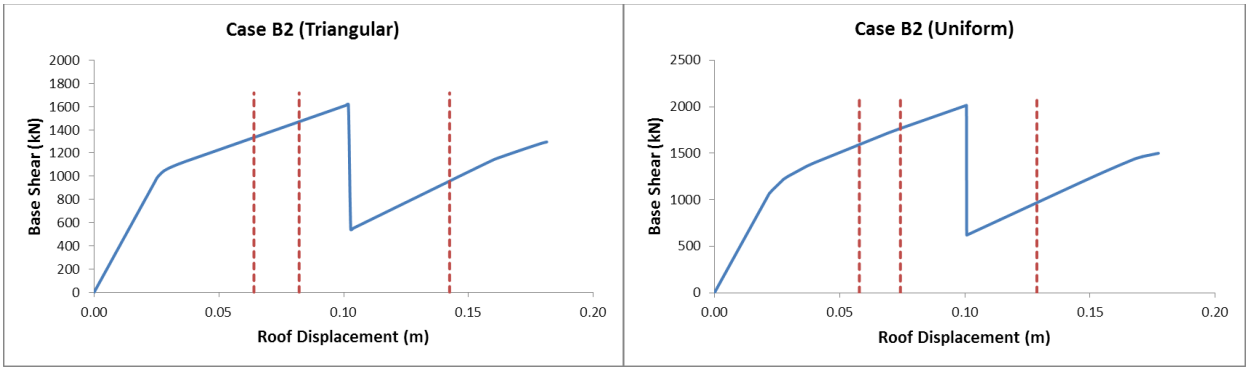

Figure 5.14 Pushover curves (case B2) for the 4 storey building

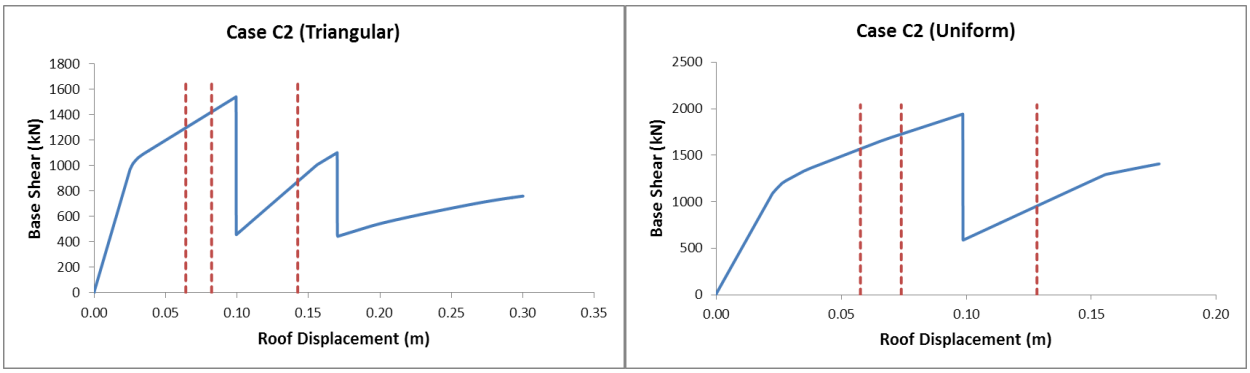

Figure 5.15 Pushover curves (case C2) for the 4 storey building

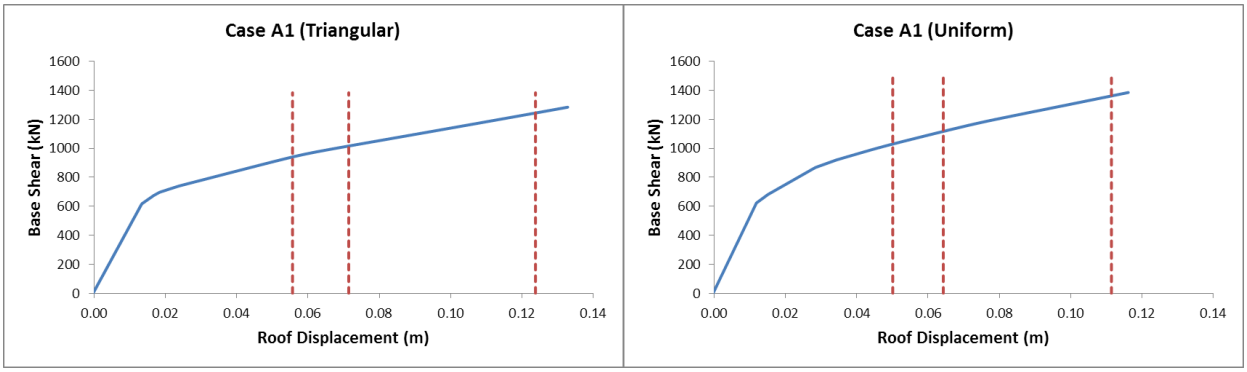

Figure 5.16 Pushover curves (case A1) for the 2 storey building

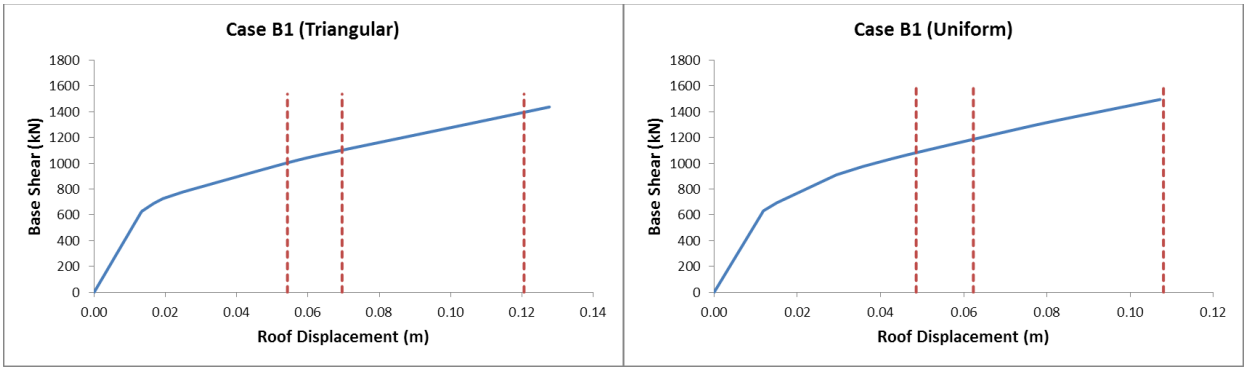

Figure 5.17 Pushover curves (case B1) for the 2 storey building

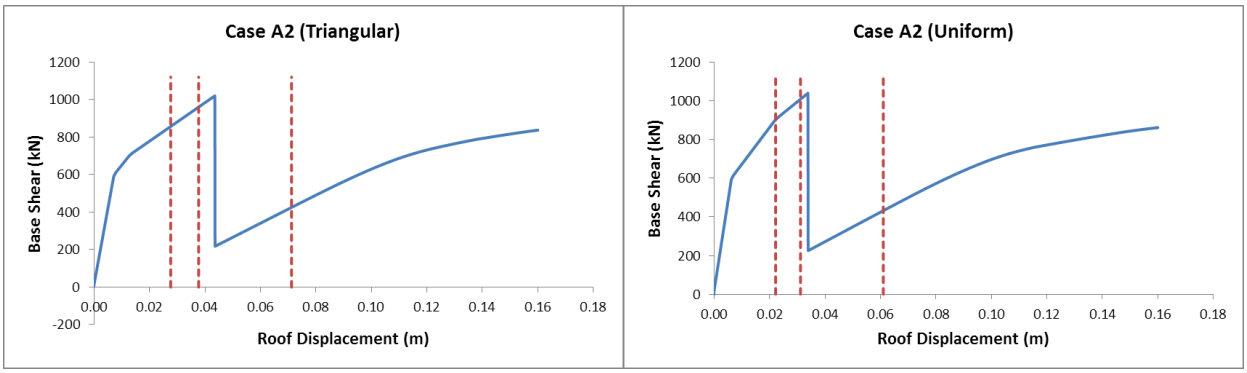

Figure 5.18 Pushover curves (case A2) for the 2 storey building

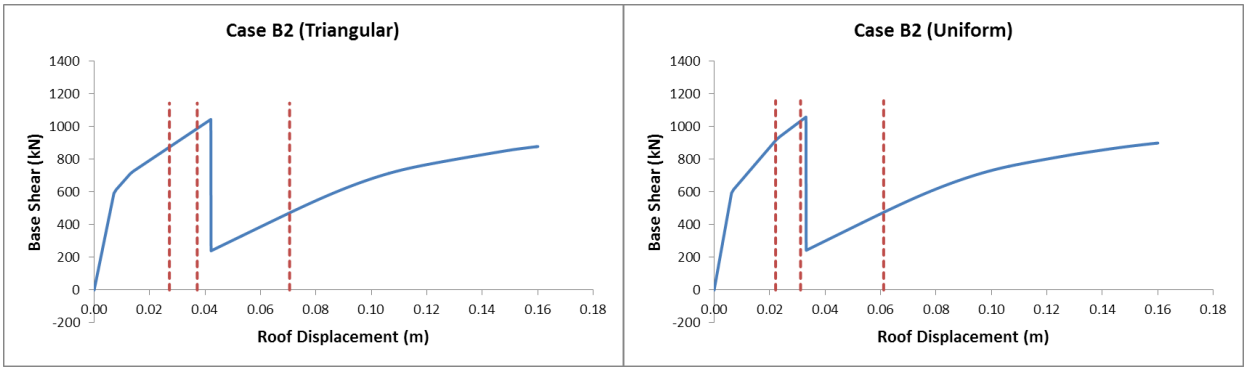

Figure 5.19 Pushover curves (case B2) for the 2 storey building

As we can see from the graphs above, the EBF's have been designed both with taking the reserve capacity of the MRF's and without. The primary advantage in case 2 is that since the reserve capacity of the MRF can ensure that target drifts are reached without structural collapse, smaller link lengths can be used. This in-turn results in lesser forces on the connections at the link ends and simpler connection details. But the primary drawback in adopting case 2 is that explicit checks have to be made during design stage to ensure that the structure does not collapse before target drift is reached due to a premature failure in both EBF and MRF in the same storey.

The pushover curves for the case 1 dual frames are now compared to those of the same buildings but having only an EBF as the lateral load resisting system.

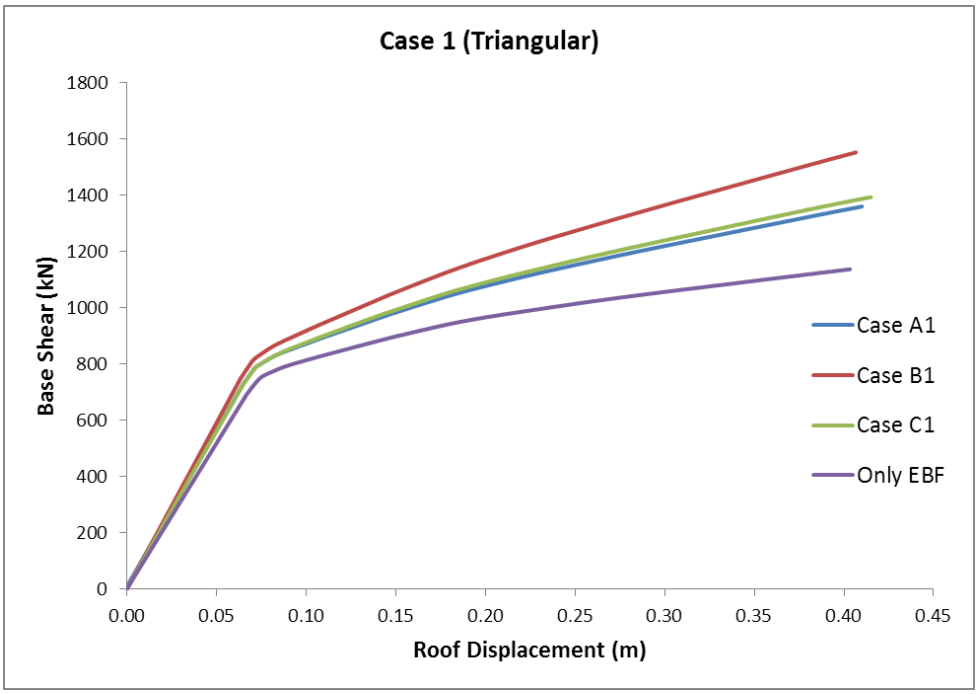

Figure 5.20 Pushover curves (case 1- Triangular) for the 8 storey building

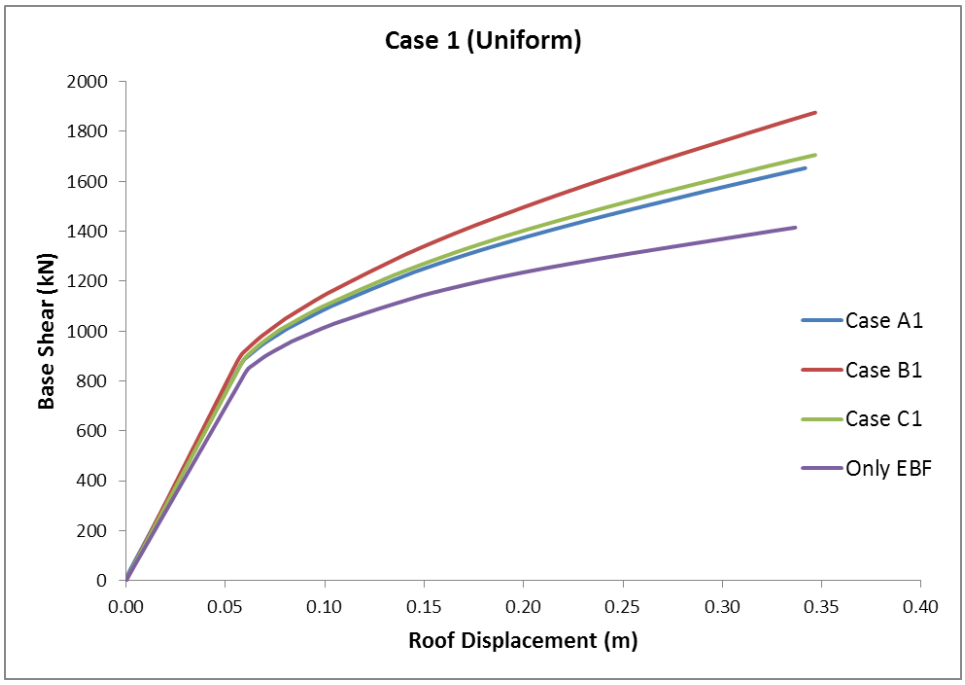

Figure 5.21 Pushover curves (case 1- Uniform) for the 8 storey building

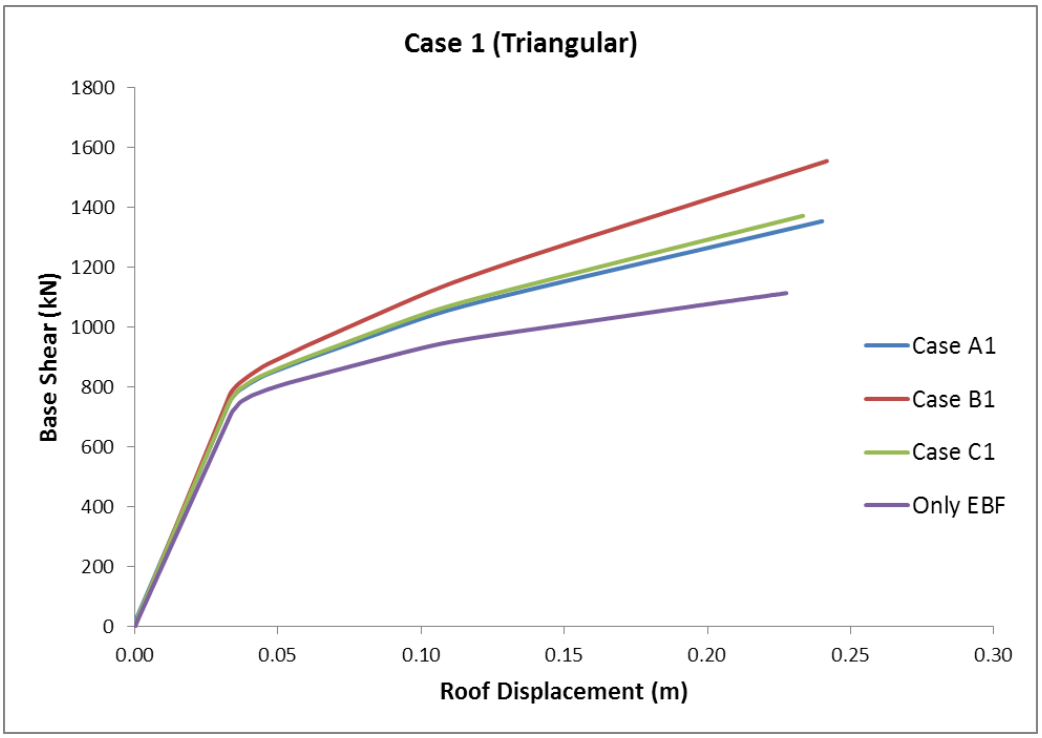

Figure 5.22 Pushover curves (case 1- Triangular) for the 4 storey building

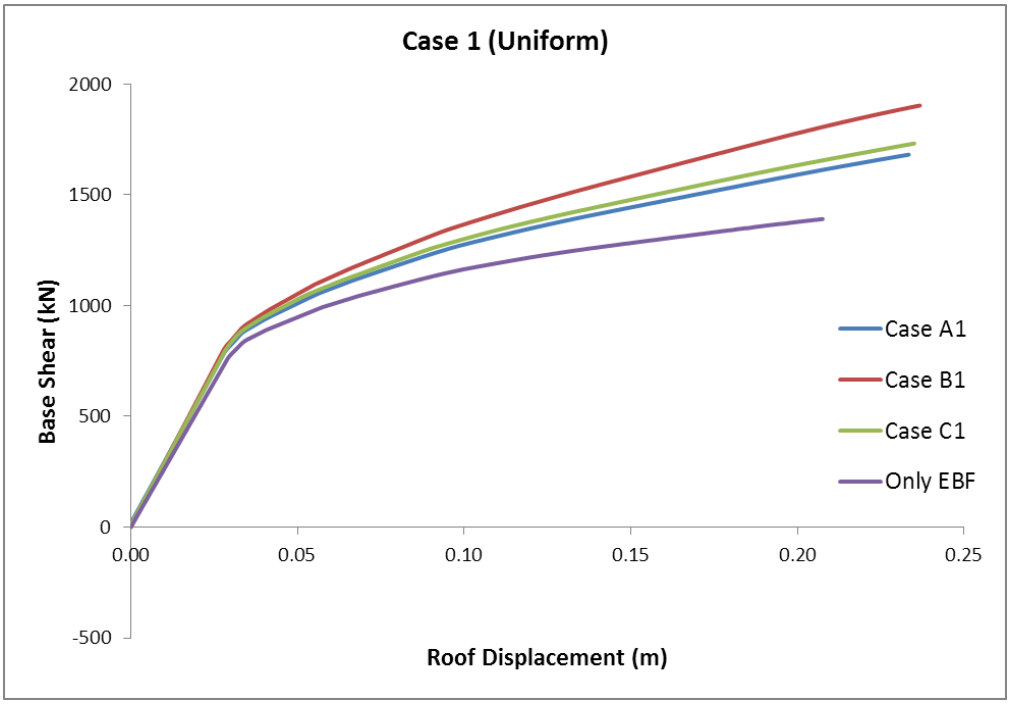

Figure 5.23 Pushover curves (case 1- Uniform) for the 4 storey building

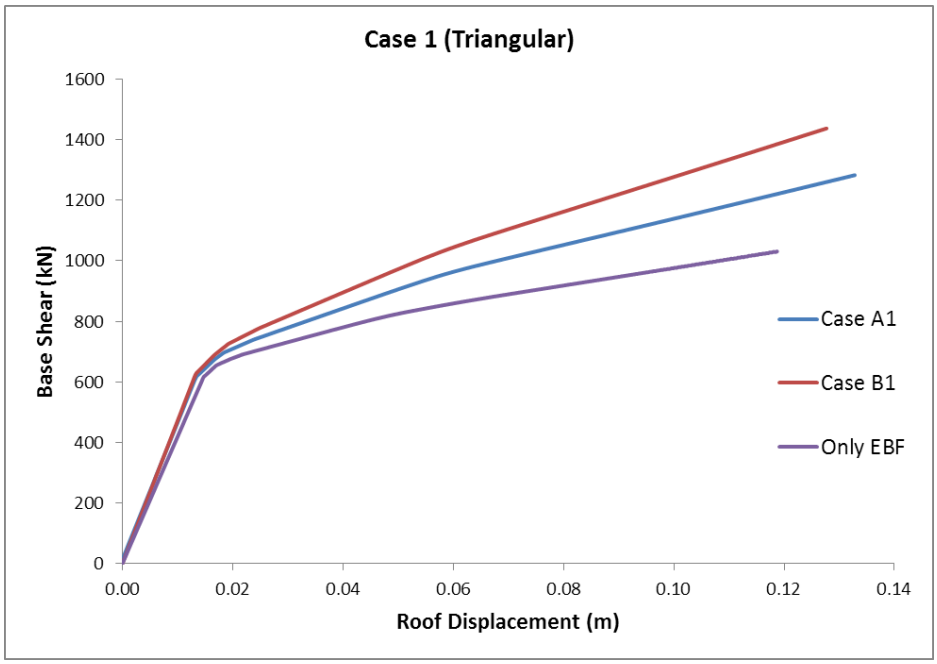

Figure 5.24 Pushover curves (case 1- Triangular) for the 2 storey building

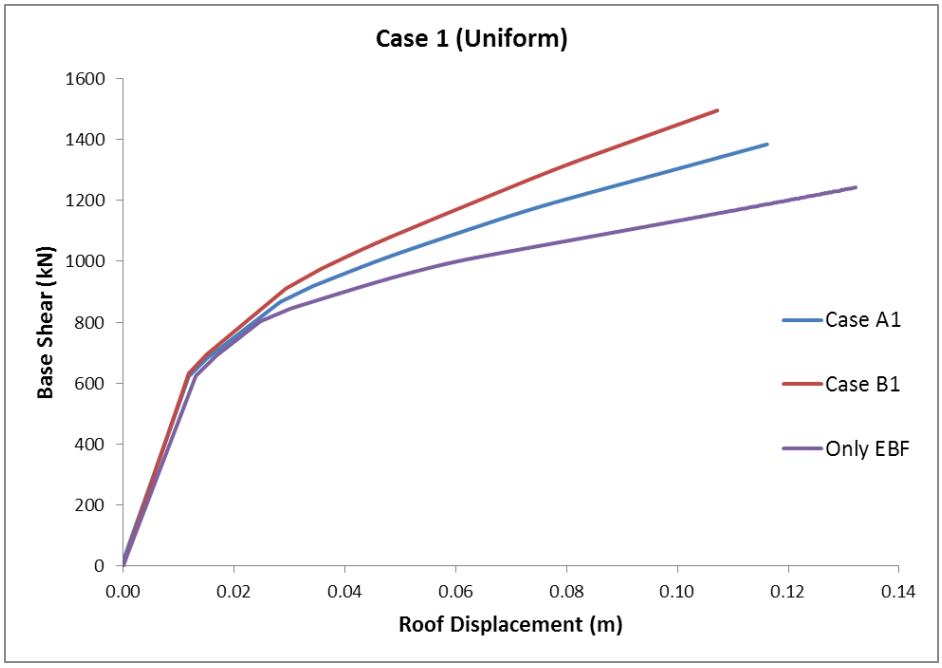

Figure 5.25 Pushover curves (case 1- Uniform) for the 2 storey building

From the above graphs, it can be clearly observed that the dual frames have a significantly better performance than EBFs in the post yield region. This further supports the initial observations with regards to stiffness of EBF and MRF.

From the Eurocode point of view, it can be said that dual frames have a significantly better ($\alpha u / \alpha 1$) than the EBF's because the post yield stiffness is the one which gets a significant buff due to the moment resisting frame. Therefore the ductility factor for dual frames is expected to be higher than that of EBFs. Therefore, the initial assumption of the ductility factor for the dual frames to be the same as that of the EBFs ($q = 6$) is found to be conservative.

Note: As noted in the literature review, researchers in the past have observed local failures and premature collapse of dual frames and so have used a lower ductility factor (5 and 4). But in the present study, due to the presence of removable links, the link sections have been carefully chosen to ensure near equal overstrength factors along the whole height of the building (10-15% variation in Ω). Also the braces were designed conservatively (using the full effective length). Therefore in the present study, premature structural collapse or events like brace buckling was avoided and the structures were able to completely mobilize the shear links. This is proven by the fact that the links yielding in all stories were observed prior to the ultimate shear capacity being reached in any link. Also the link yielding at all stories happened at almost the same time as can be seen in the almost bilinear pushover curves.

Therefore, the present system is deemed to be robust and capable to mobilize the ductility presented by shear links completely and hence the use of a higher ductility factor (=6) is justified.

5.3.1. **Axial forces in the links**

Shown below is the axial force development in one of the links during a pushover analysis.

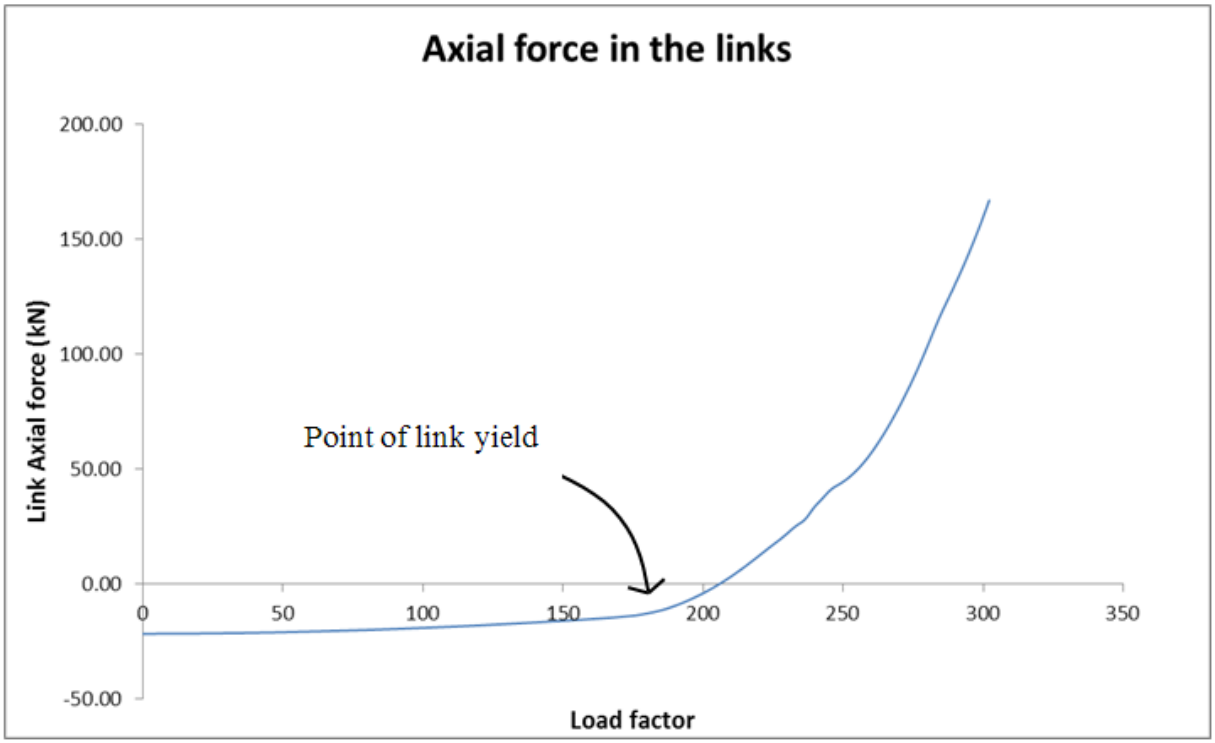

Figure 5.26 Development of axial forces in the shear links

Similar curves are obtained when plotting axial force diagrams in the links at all levels in all cases. This leads to the conclusion that once the link yields, due to the large displacements involved, inevitably some axial force tends to start developing in it, which affects its ultimate capacity. It is observed that this axial force, occurring at large displacements must be researched in greater detail because this force needs to be taken into account during the connection design for the replaceable links.

5.4 Non-linear Dynamic Analysis (THA)

Time history analysis was also performed in the software Seismostruct (Seismosoft) for an artificial accelerogram, scaled to the design seismic peak ground acceleration of 0.2g. The accelerogram (accelerations, velocities and displacements) are plotted as shown below.

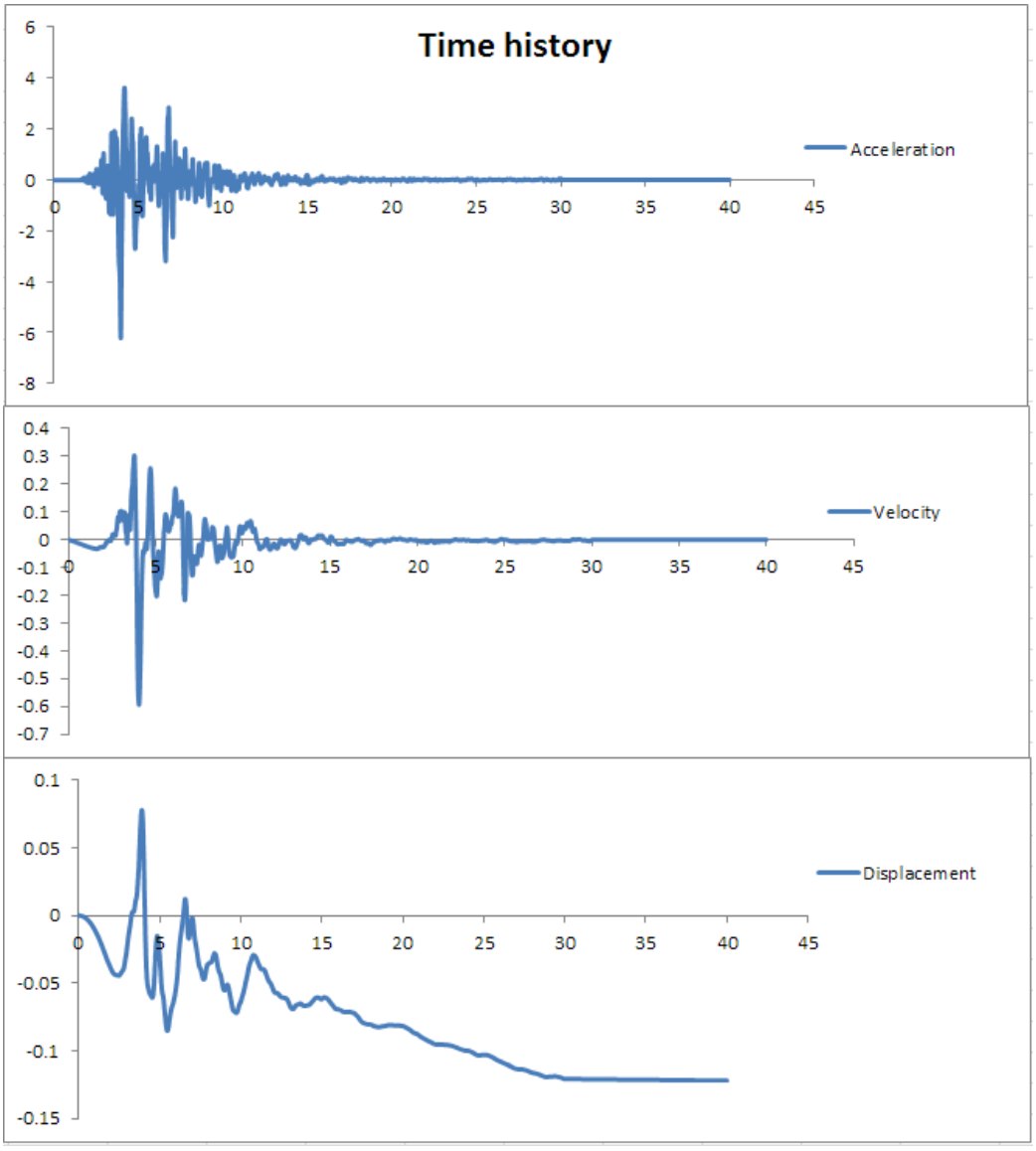

Figure 5.27 Artificial accelerogram (scaled to 0.2g PGA)

The response spectrum of the accelerogram and the design response spectrum are shown in the figure below.

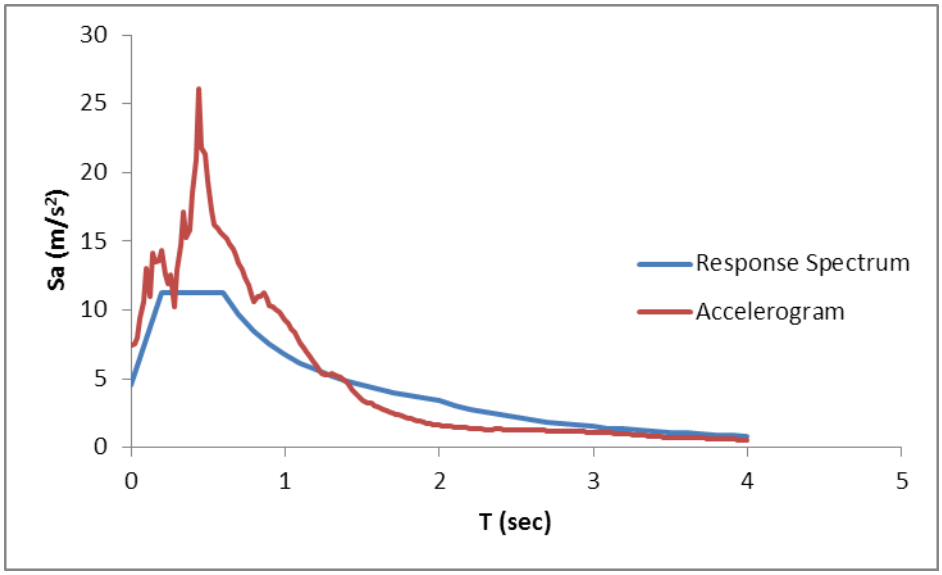

Figure 5.28 Response spectrum (design vs accelerogram)

Time history analysis is run for all the models (cases 1,2 and A,B and C) of the 2,4 and 8 storey buildings and once the seismic excitation is over, the links are removed one by one (deactivated) to check if the elastic MRF is capable of recentering itself. Two criterions are checked:

- Links removed from bottom to top
- Links removed from top to bottom

For the analysis, Rayleigh damping (with tangent stiffness) is adopted and is set to be equal to 2% damping for the first and second modes of vibration. The roof displacements are plotted against time for the different scenarios analyzed and the results are shown below.

5.4.1. 8 storey frame (THA – links removed from top to bottom)

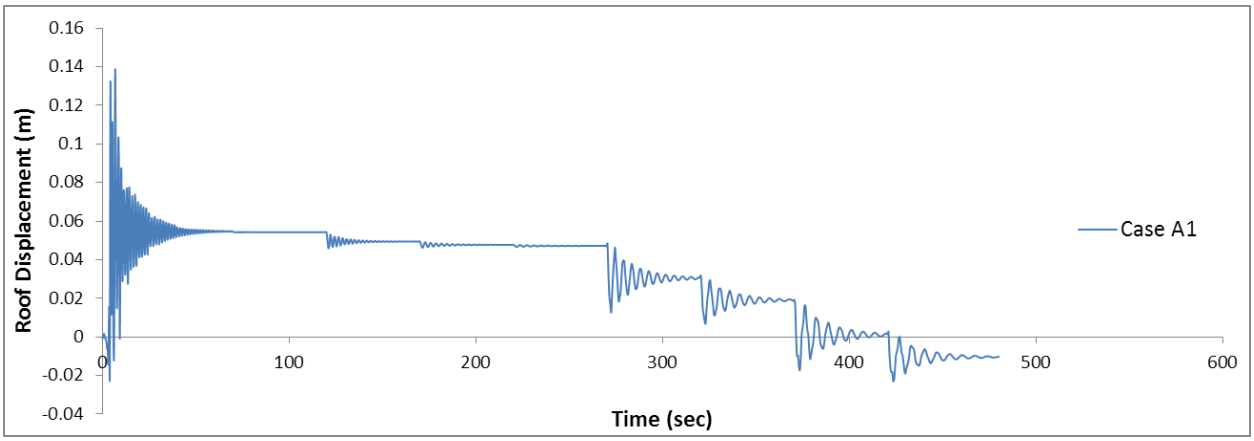

Figure 5.29 THA 8 storey frame case A1 (Links removed from Top)

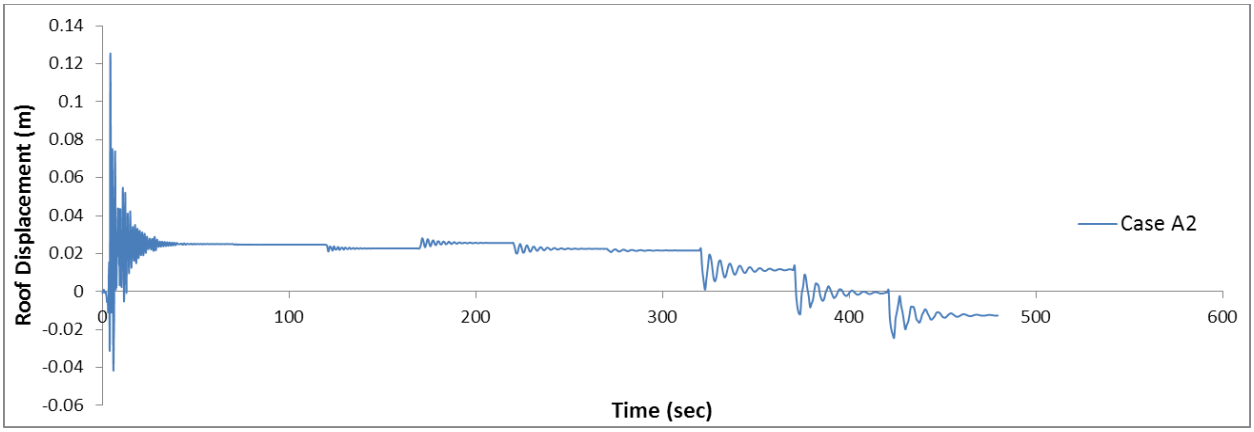

Figure 5.30 THA 8 storey frame case A2 (Links removed from Top)

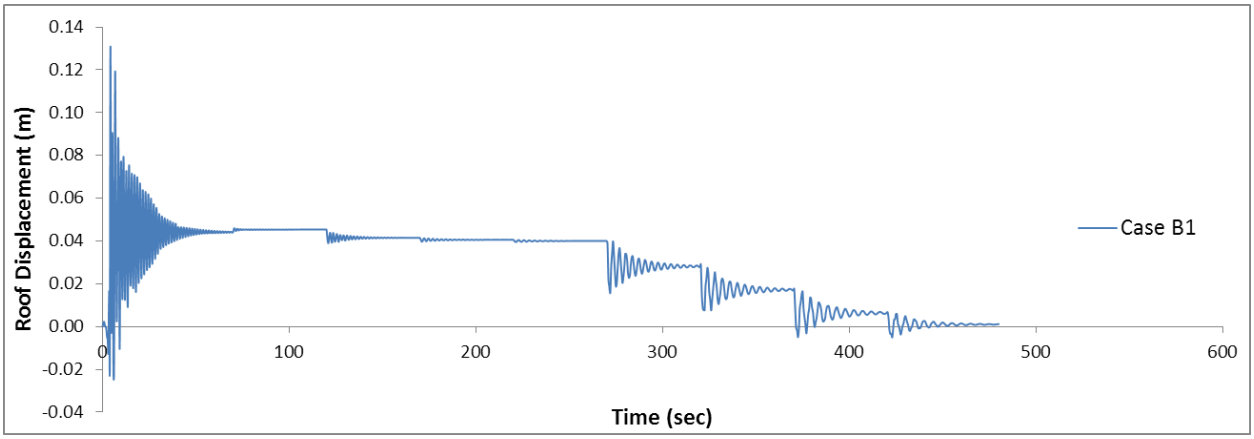

Figure 5.31 THA 8 storey frame case B1 (Links removed from Top)

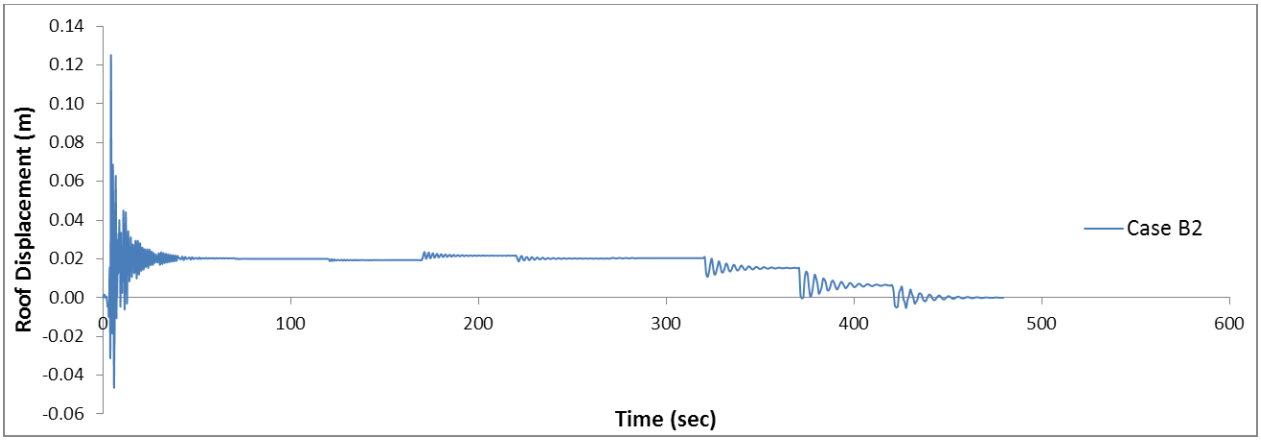

Figure 5.32 THA 8 storey frame case B2 (Links removed from Top)

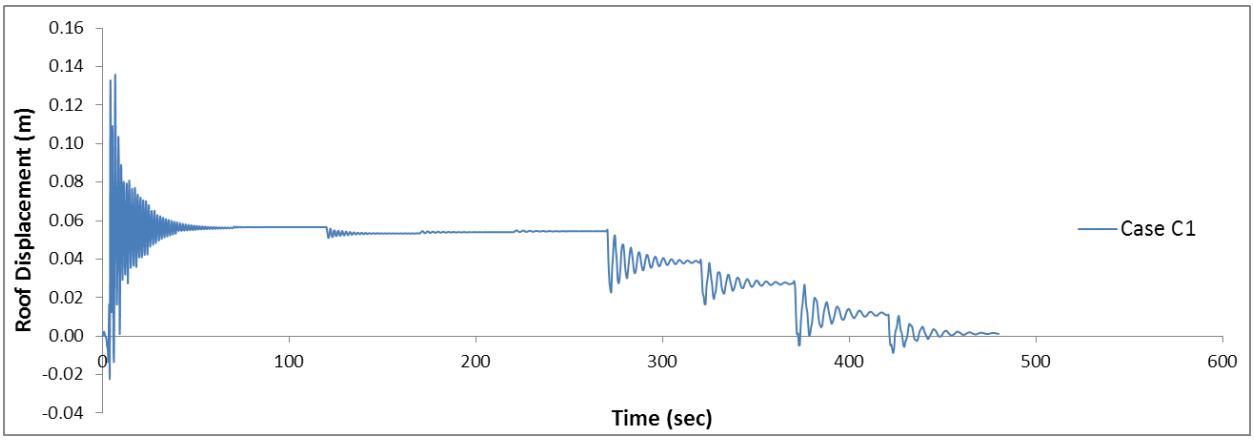

Figure 5.33 THA 8 storey frame case C1 (Links removed from Top)

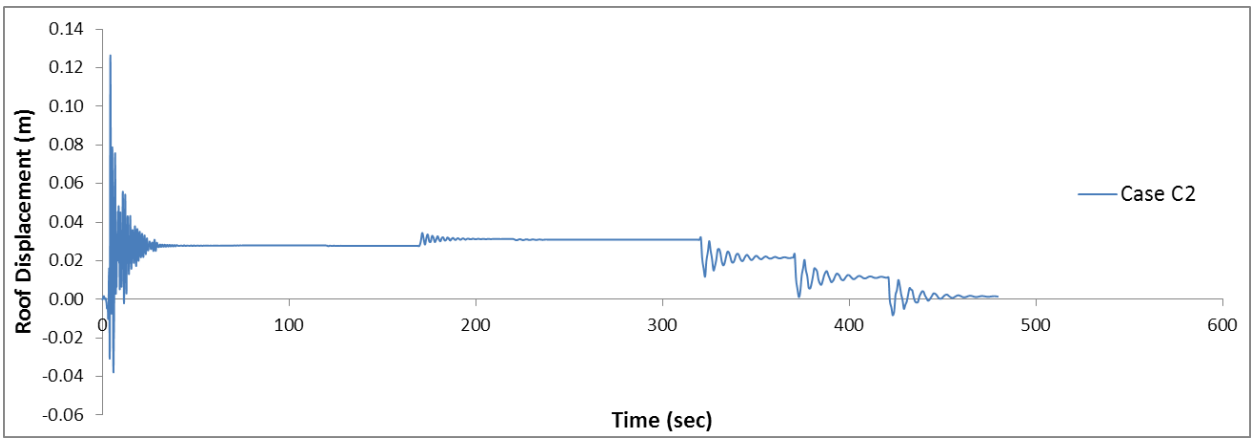

Figure 5.34 THA 8 storey frame case C2 (Links removed from Top)

5.4.2. 8 storey frame (THA – links removed from bottom to top)

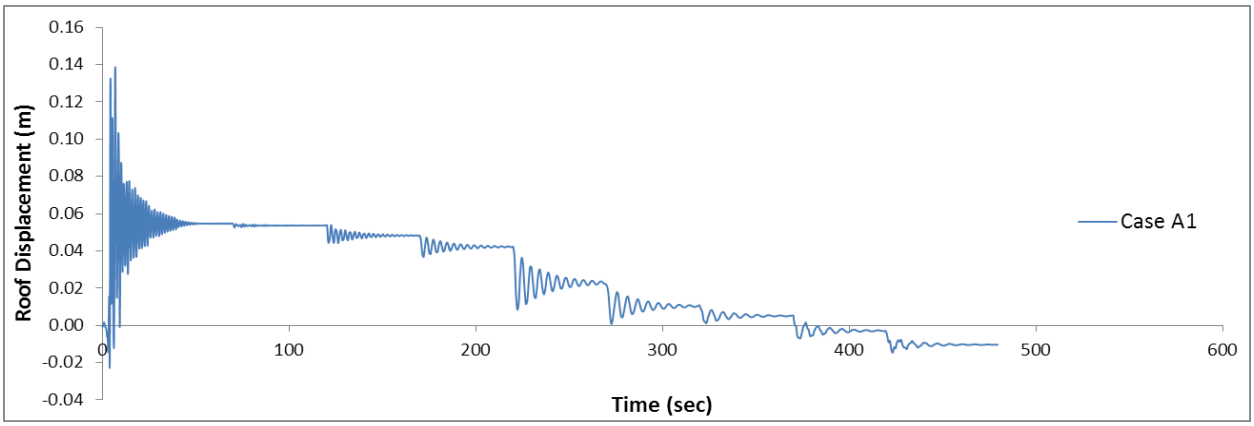

Figure 5.35 THA 8 storey frame case A1 (Links removed from Bottom)

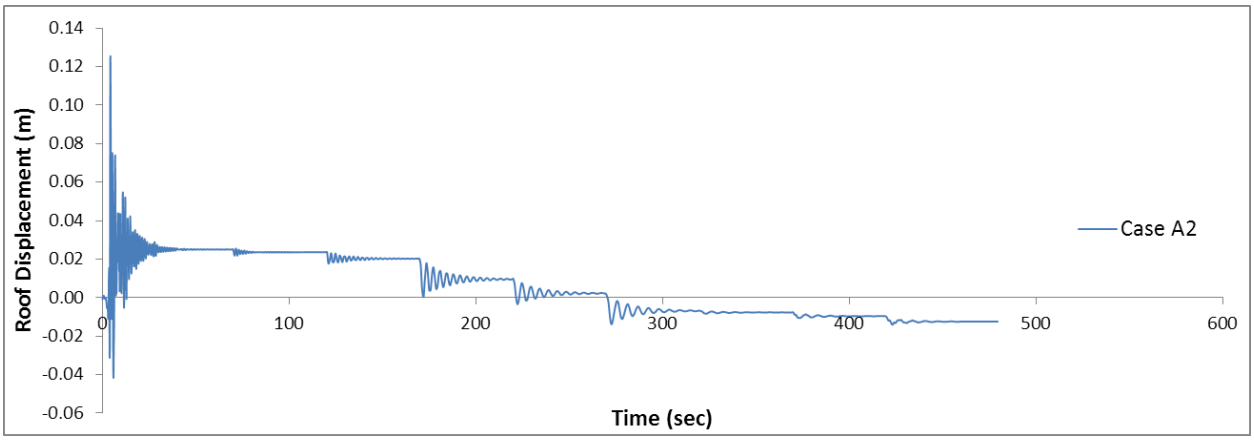

Figure 5.36 THA 8 storey frame case A2 (Links removed from Bottom)

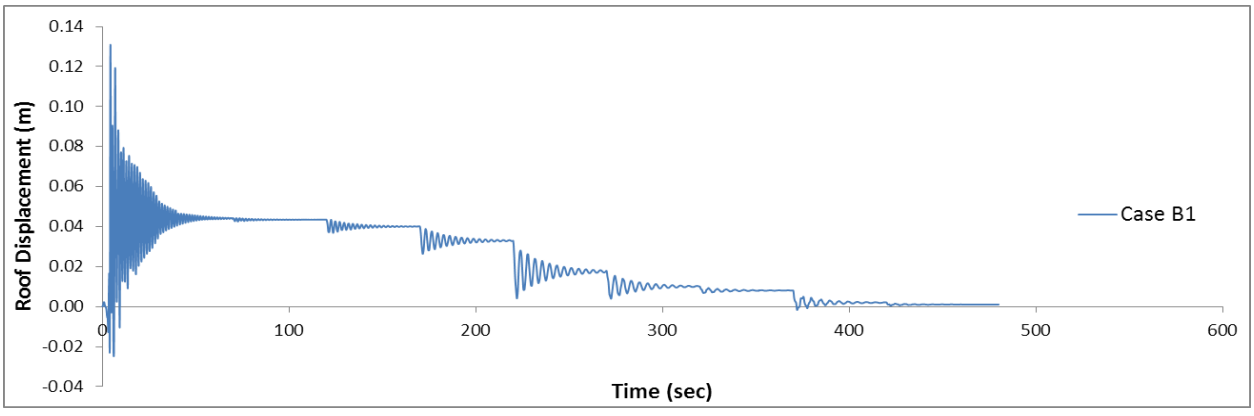

Figure 5.37 THA 8 storey frame case B1 (Links removed from Bottom)

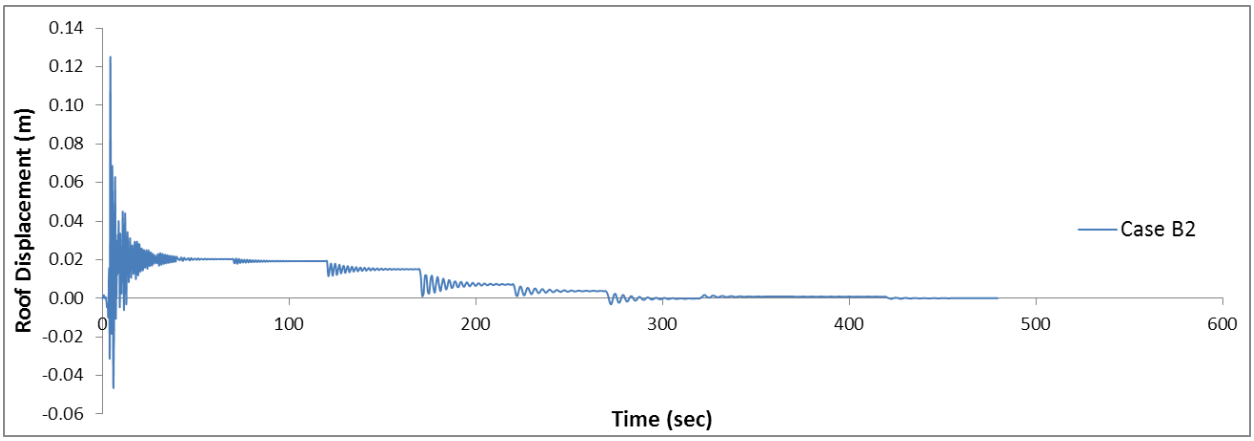

Figure 5.38 THA 8 storey frame case B2 (Links removed from Bottom)

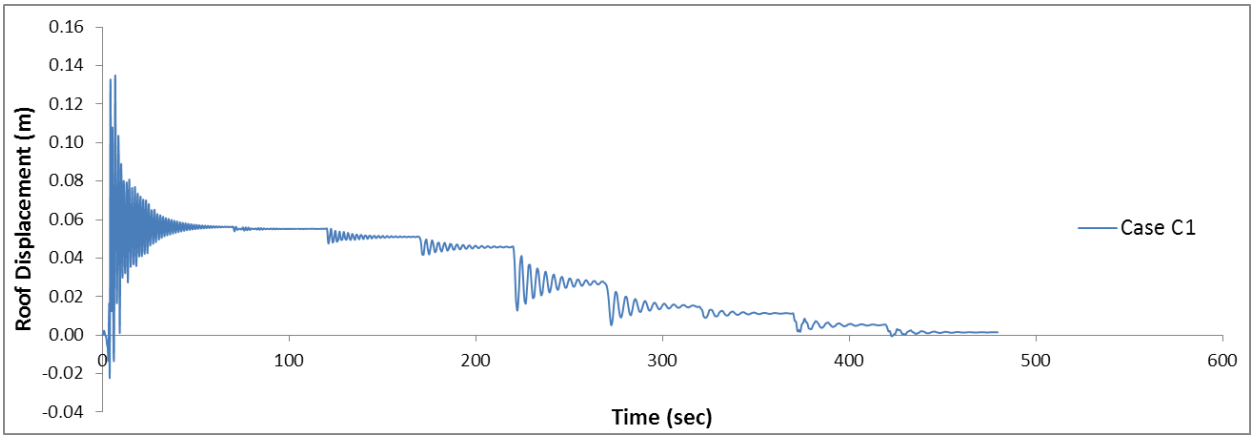

Figure 5.39 THA 8 storey frame case C1 (Links removed from Bottom)

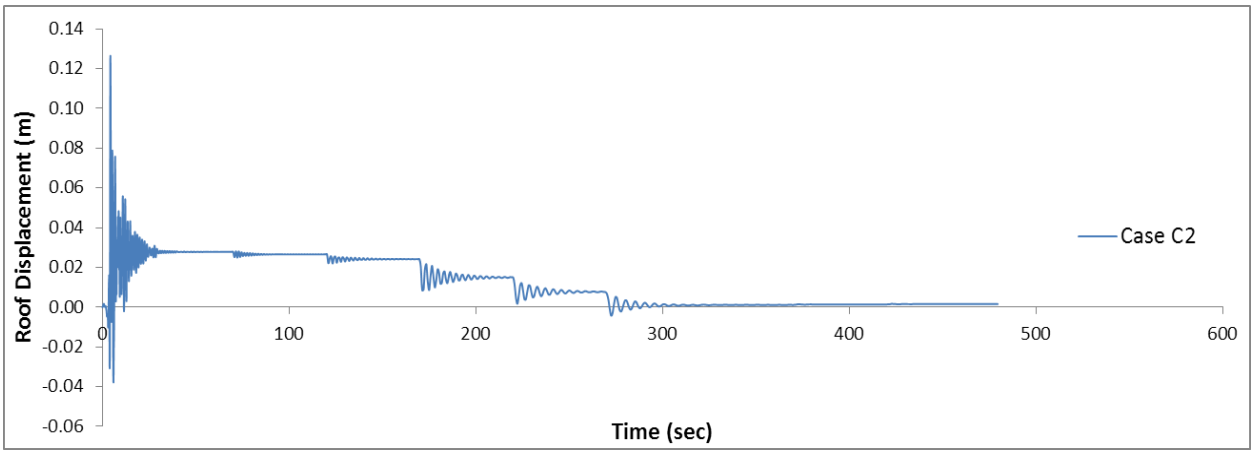

Figure 5.40 THA 8 storey frame case C2 (Links removed from Bottom)

5.4.3. **4 storey frame (THA – links removed from top to bottom)**

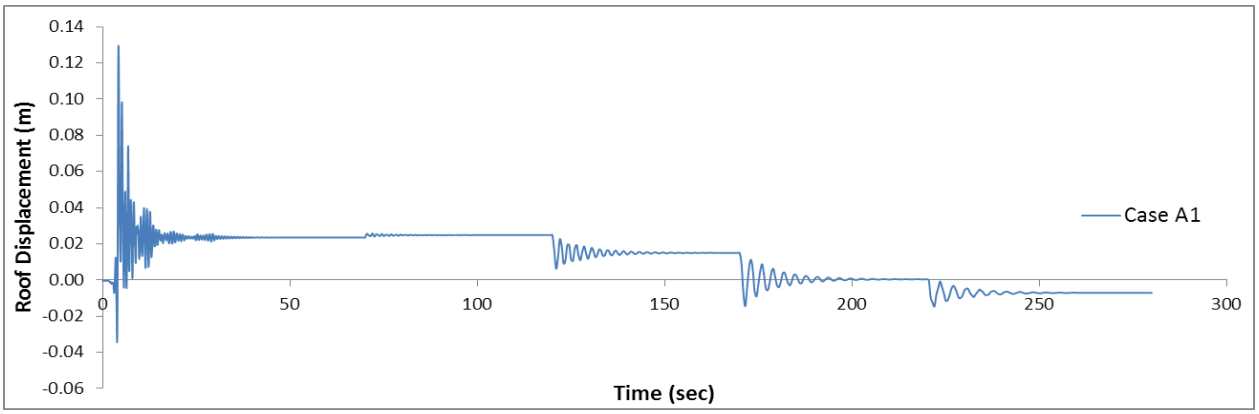

Figure 5.41 THA 4 storey frame case A1 (Links removed from Top)

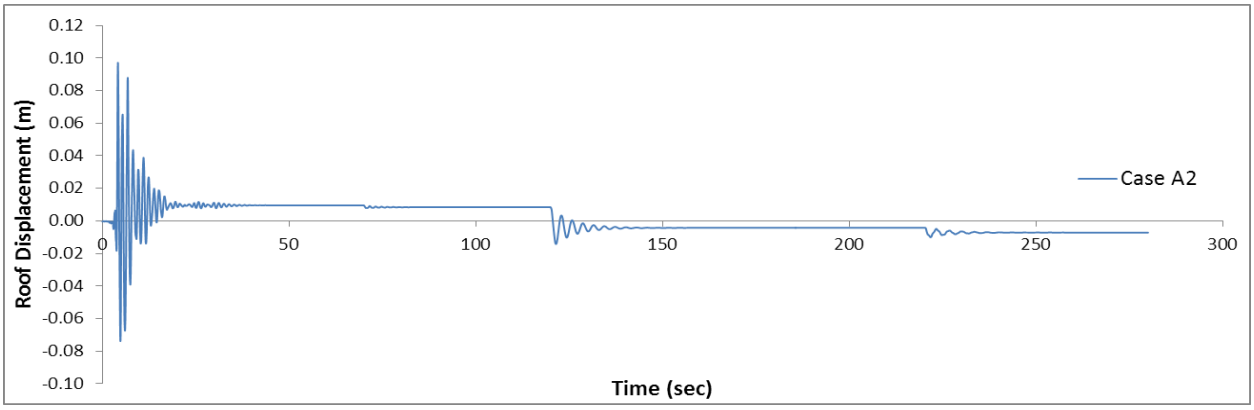

Figure 5.42 THA 4 storey frame case A2 (Links removed from Top)

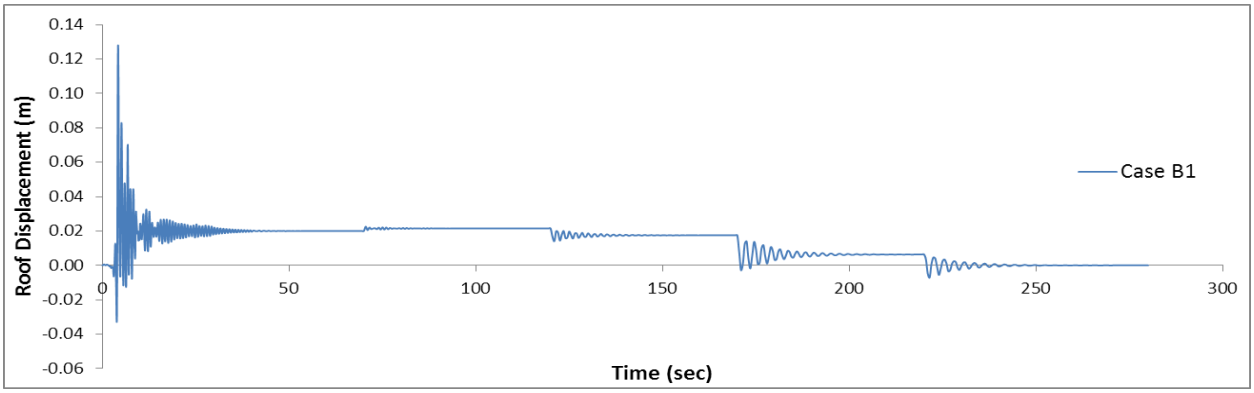

Figure 5.43 THA 4 storey frame case B1 (Links removed from Top)

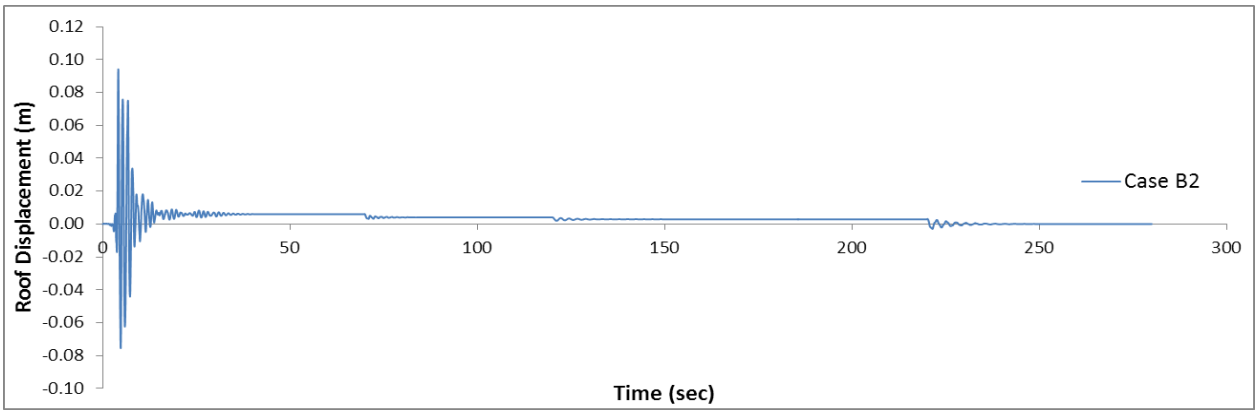

Figure 5.44 THA 4 storey frame case B2 (Links removed from Top)

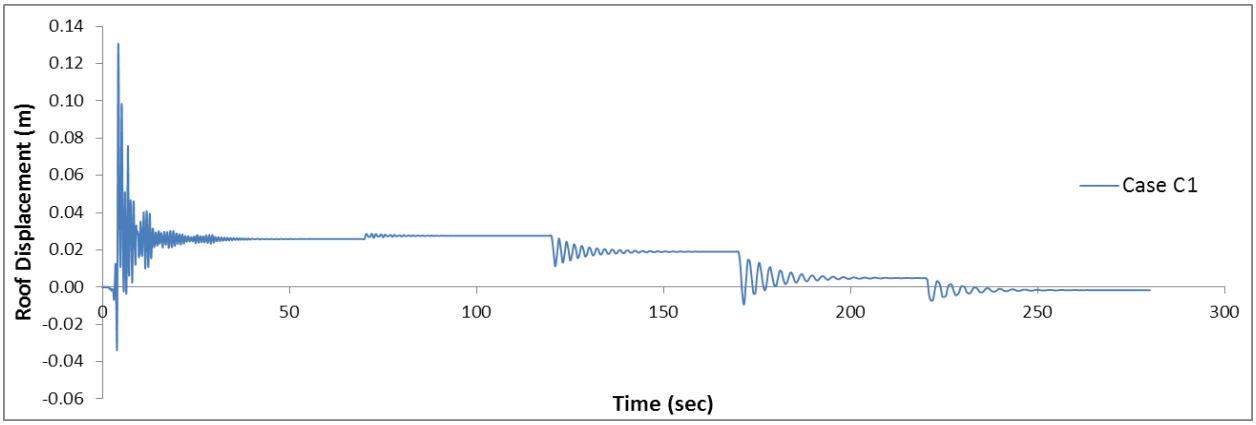

Figure 5.45 THA 4 storey frame case C1 (Links removed from Top)

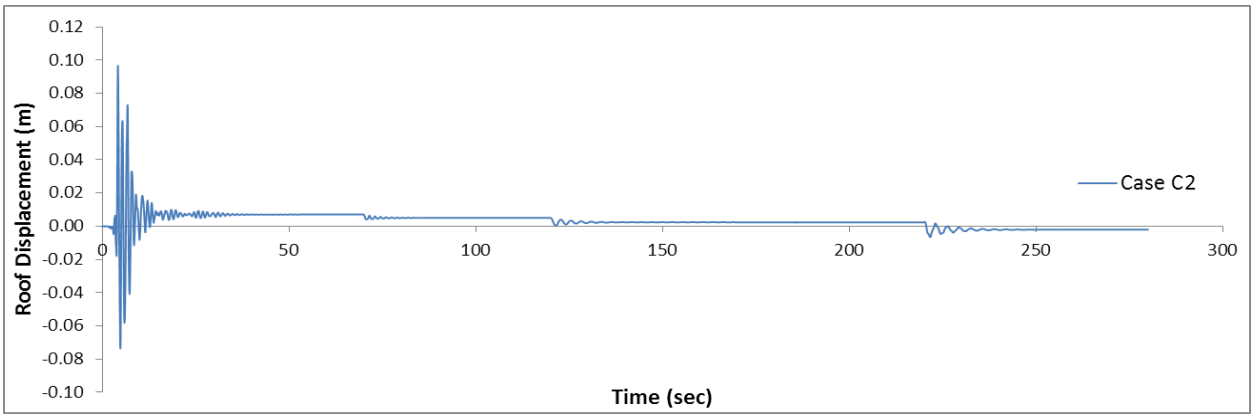

Figure 5.46 THA 4 storey frame case C2 (Links removed from Top)

5.4.4. **4 storey frame (THA – links removed from bottom to top)**

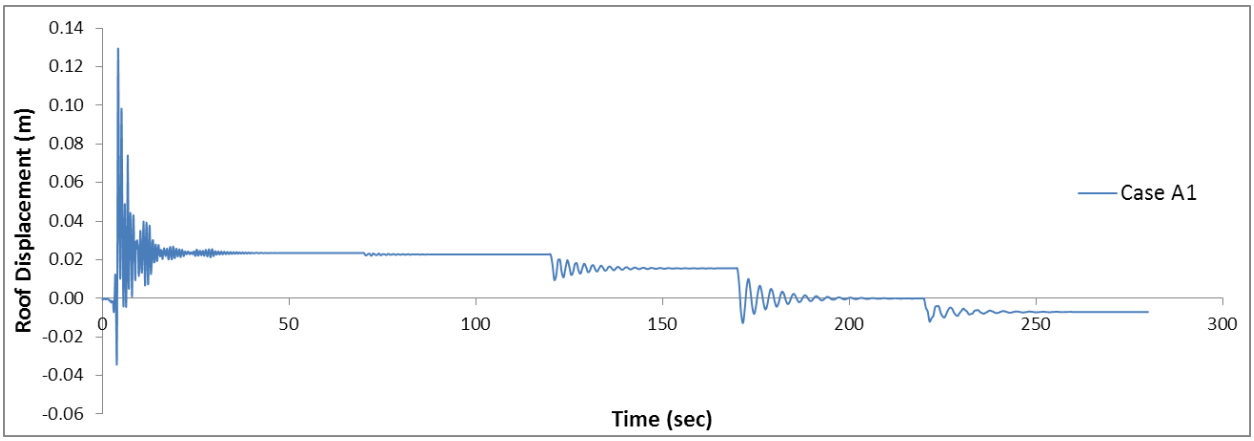

Figure 5.47 THA 4 storey frame case A1 (Links removed from Bottom)

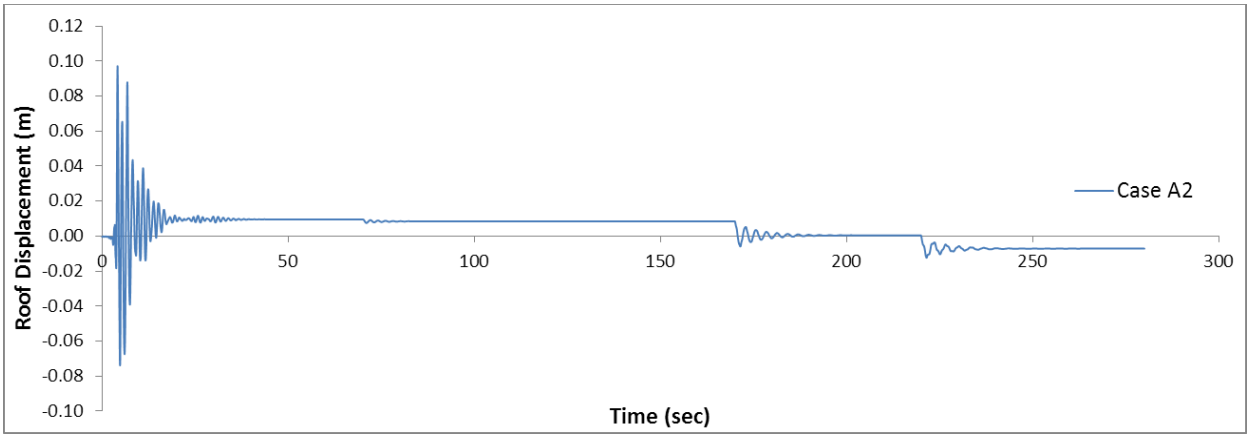

Figure 5.48 THA 4 storey frame case A2 (Links removed from Bottom)

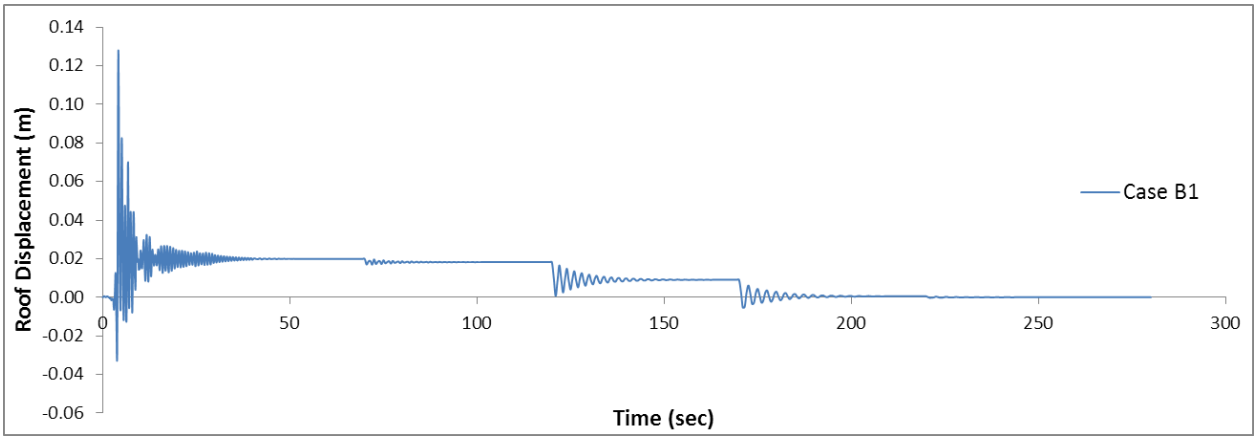

Figure 5.49 THA 4 storey frame case B1 (Links removed from Bottom)

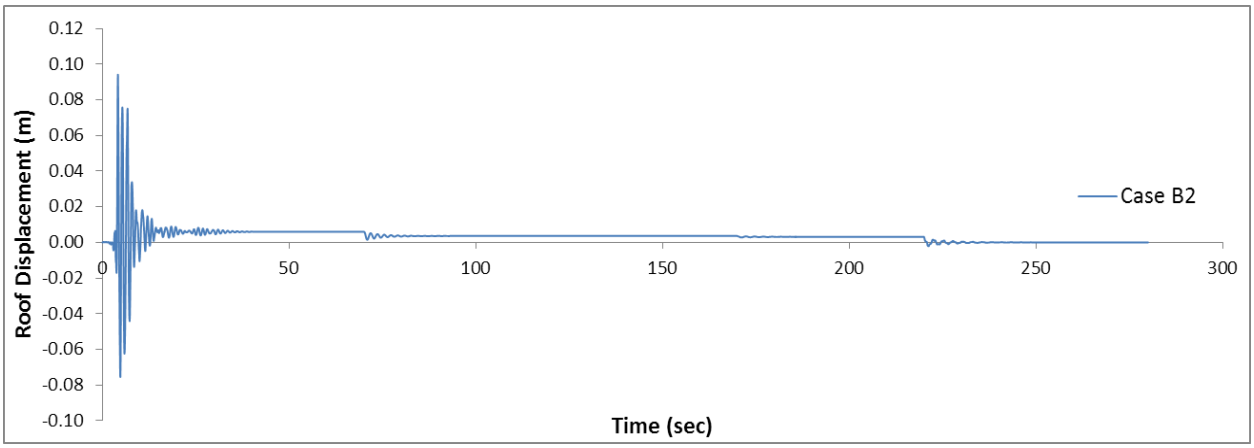

Figure 5.50 THA 4 storey frame case B2 (Links removed from Bottom)

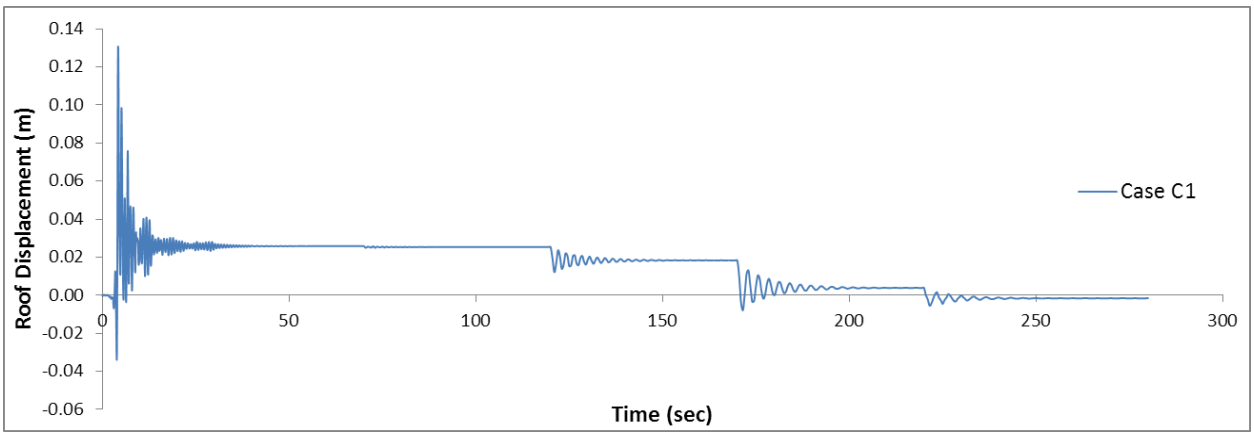

Figure 5.51 THA 4 storey frame case C1 (Links removed from Bottom)

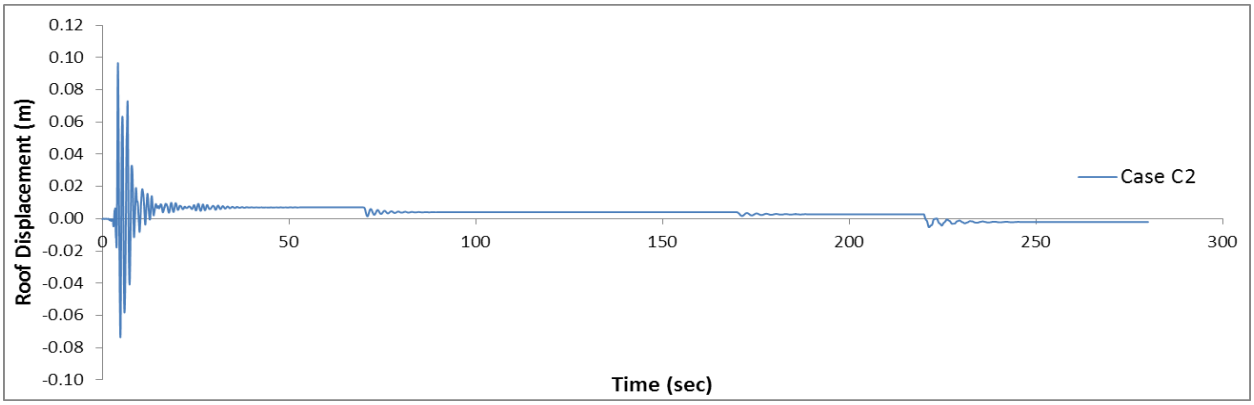

Figure 5.52 THA 4 storey frame case C2 (Links removed from Bottom)

5.4.5. 2 storey frame (THA – links removed from top to bottom)

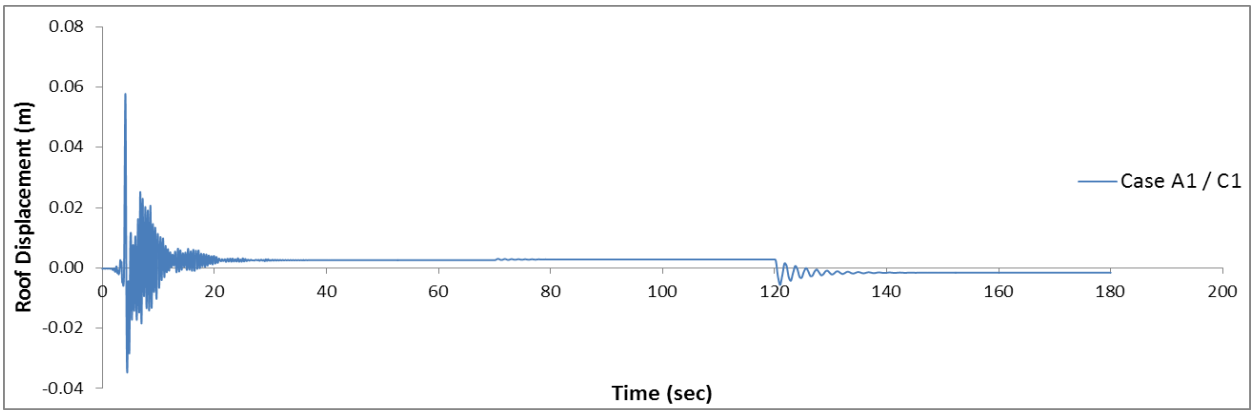

Figure 5.53 THA 2 storey frame case A1 / C1 (Links removed from Top)

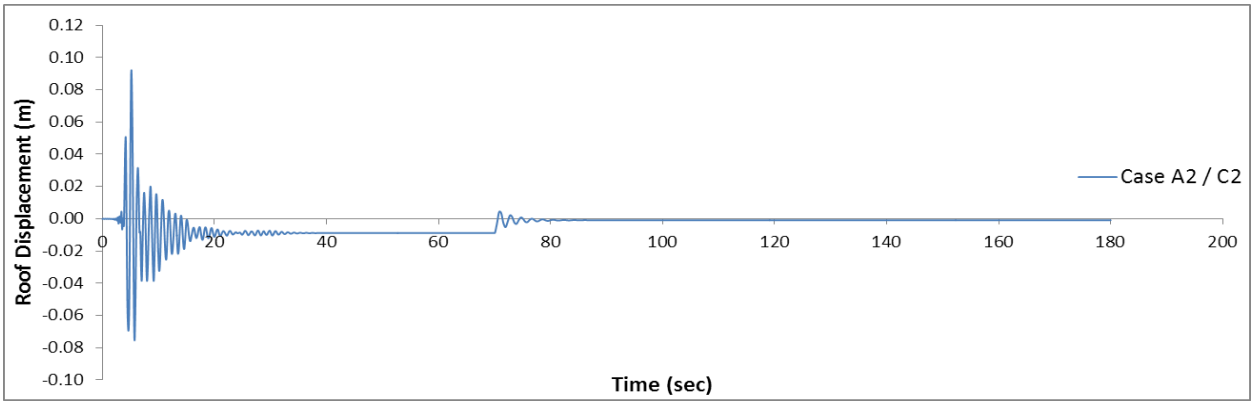

Figure 5.54 THA 2 storey frame case A2 / C2 (Links removed from Top)

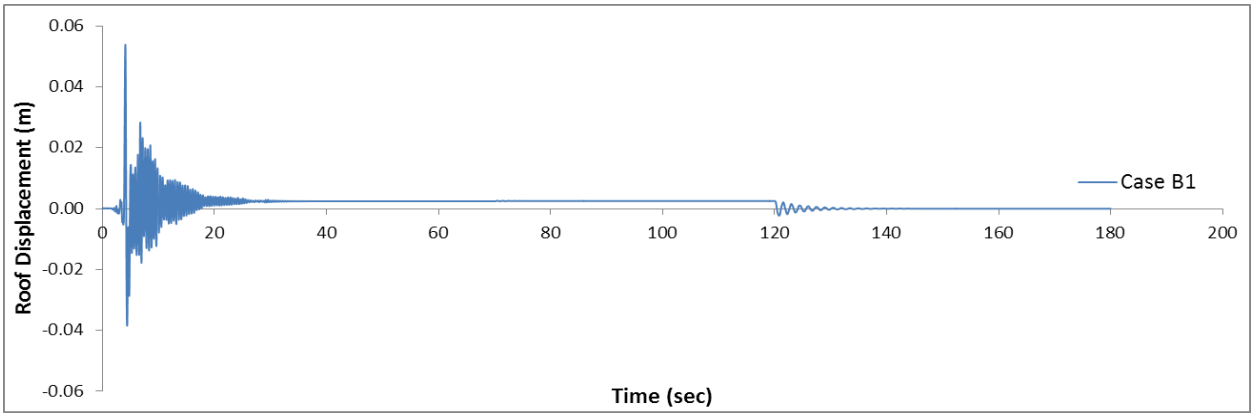

Figure 5.55 THA 2 storey frame case B1 (Links removed from Top)

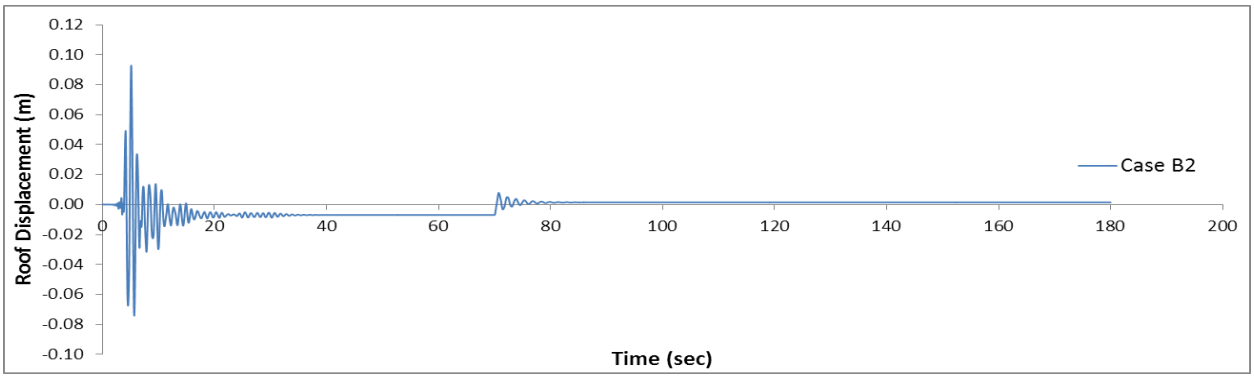

Figure 5.56 THA 2 storey frame case B2 (Links removed from Top)

5.4.6. 2 storey frame (THA – links removed from bottom to top)

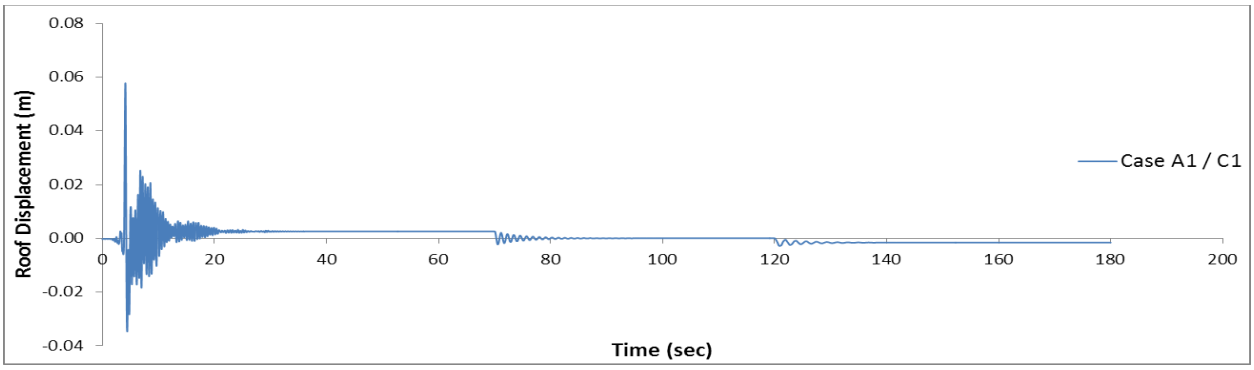

Figure 5.57 THA 2 storey frame case A1 / C1 (Links removed from Bottom)

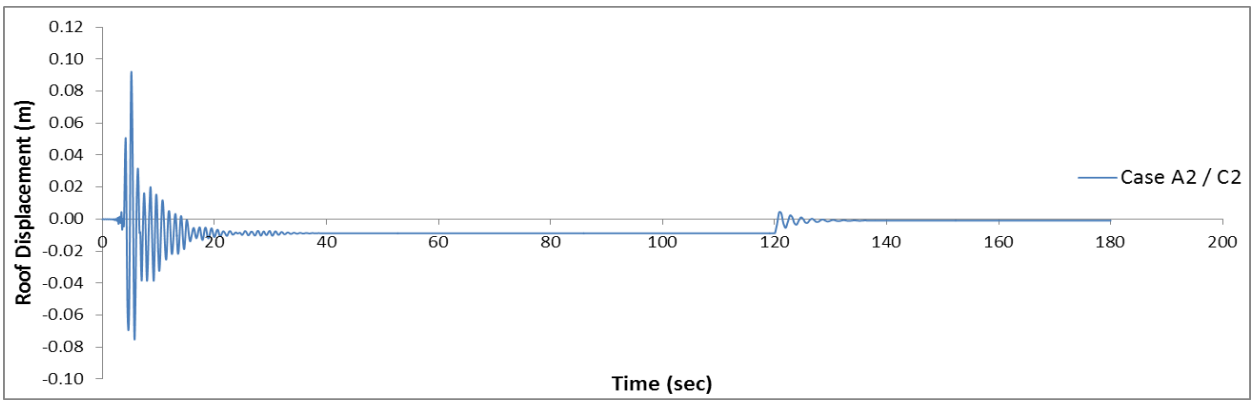

Figure 5.58 THA 2 storey frame case A2 / C2 (Links removed from Bottom)

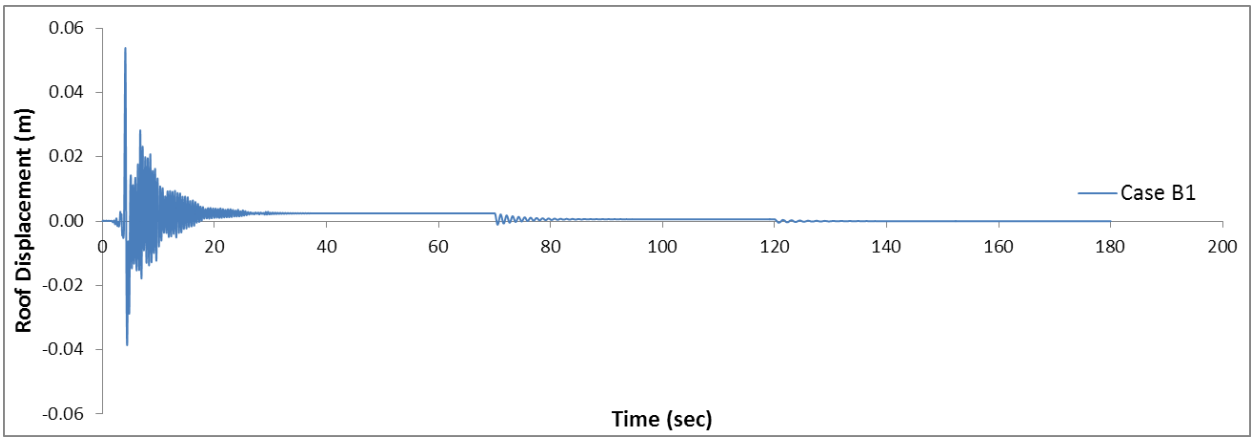

Figure 5.59 THA 2 storey frame case B1 (Links removed from Bottom)

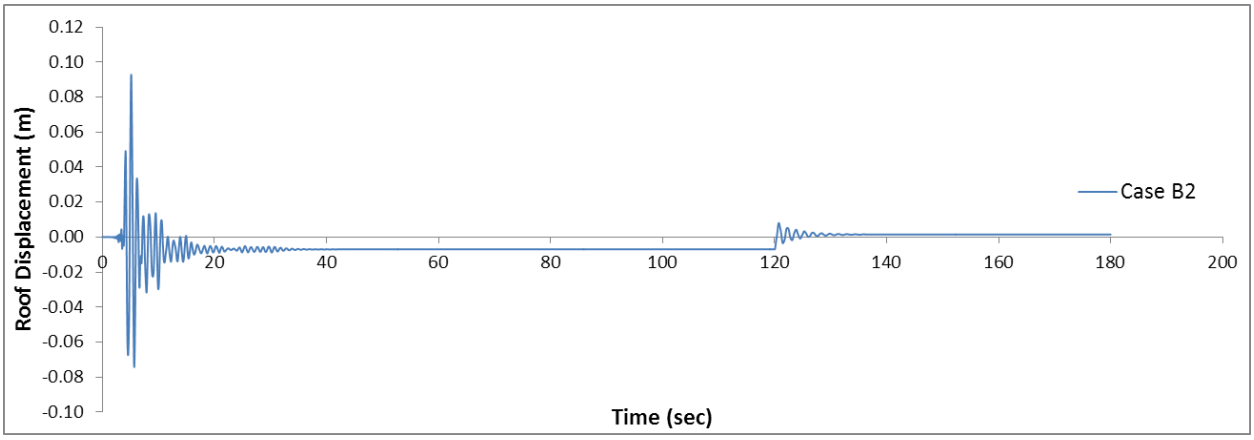

Figure 5.60 THA 2 storey frame case B2 (Links removed from Bottom)

From the calculated roof displacement time histories, the following observations are made

1) The case B frames performed much superior to cases A and C with 0 residual drift after link removal
2) Order of link removal (starting from top or bottom) resulted in nearly same performance level
3) Only in the case of 2 storey building, the observed displacements for case 2 (shorter links = stiffer frames) are higher than those of case 1. In these cases, link failure at storey 1 was observed. This resulted in the MRF taking over and thus higher storey drifts. Although the buildings were designed for no failure of MRF for the limit state Damage Limitation (DL), the response spectrum of the used accelerogram is also much higher

than the design response spectrum (especially at shorter periods corresponding to low rise buildings) and so a higher level of seismic load is supposed to be applied.

As can be seen in the pushover curves for the case 2 of the 2 storey buildings (Figure 5.18 and Figure 5.19), the target drift for limit state Significant Damage (SD) is almost reaching the drift at which the link at storey 1 fails. As the applied accelerogram has a bit higher response spectrum, it is understandable that the drifts exceeded those corresponding to 0.08 radians of plastic rotation in the link at storey 1 and thus the MRF got activated. The authors note that this design can be potentially disastrous as ideally one does not want to use the MRF frame to resist seismic loads but instead to use it for re-centering. Any yielding in the MRF frame sections will seriously hinder its recentering properties and also make the whole idea behind recentering frames as not applicable. Therefore, the authors feel that although case 1 design has potentially higher peak displacements and transient drifts, it is fail proof and thus can be employed with confidence in the MRF remaining elastic for frequent earthquakes.

Chapter 6 - Conclusions

From the static and seismic analysis of dual frames performed in the study, the following conclusions are made.

1) Design of MRF component of the dual frames for overstrength has to be incorporated into the Eurocodes based on the suggestions by [8] and [12] and also observed by the author.
2) It is best to avoid coupling between the two subsystems (MRF and EBF) in dual frames for the simple reason that the applied response spectrum and utilized behavior factor are the same. Indeed, as long as the EBFs are elastic, the MRFs will only take a minor chunk of the seismic lateral load and therefore it is realistic to expect bigger numbers of over-strength factors. But if the MRFs and EBFs share a common column, MRF over-strength factor cannot be used to design the columns of the MRF because axial force in the common columns come from both EBF (governing) and MRF. This would result in unrealistically high loads on the MRF columns based on the overstrength of MRF beams (while the load comes from EBF braces).
3) The dual frames are found to be significantly superior to EBFs because of their greater energy dissipation capacity (higher area under the pushover curve, especially after links are yielded). This results in significantly lower transient drifts which are further reduced once the links are removed.
4) A little bit of care is to be taken if the dual frames are designed as case 2 (MRF reserve strength is utilized) especially as case A or C. This is because, after the link fails, there is but a single bay of MRF in the storey and formation of plastic hinges can quickly result in structure collapse. Also if uniform distribution of link overstrength across all stories is not achieved and realized through pushover analyses, it might be better to adopt a lower value of behavior factor.
5) Recentering of the dual frames has been observed and documented for different design scenarios in the present study. The author feels that the case B systems (MRF + EBF + MRF) are able to restore themselves completely after link removal. Partly this is attributed to the symmetry in the system.

   The columns and beams of the MRF in cases A and C also remain elastic

throughout the time history analysis but they tend to sway towards the left due to inherent asymmetry (Case A MRF frames are asymmetric with stiffer columns on the right, whereas in Case C, the MRF frame is symmetric but the system as a whole is not, which results in small values of residual drifts).

Scope for future research:

The study confirms the possibility of achieving a 2D frame which can completely restore its original shape after small earthquakes with cheaper and minimal intervention. But the 3D effects of the same need to be investigated (torsional effects, if any, due to building sway, as seen in cases A and C). The influence of order of link removal in plan on a 3D building (torsional effects) should also be studied in more detail.

During the course of the study, it was confirmed that axial forces develop in the links at large displacements (after the link has yielded). This axial force must be taken into account in the design of connections for the links and therefore must be investigated in greater detail.

Behavior factor (q) for dual frames with removable links and elastic MRF components is found to be higher than those of the EBFs in the present study but has to be confirmed through non-linear incremental dynamic analyses.

Design recommendations in the Eurocodes for MRF-EBF dual frames in scope of having an elastic MRF for recentering capabilities in the frame must be investigated in greater detail and confirmed with the preliminary design checks made in this study.

Bibliography

1) Eurocode EN 1993-1-1, Eurocode 3 – Design of steel structures – Part 1-1: General rules and rules for buildings

2) Eurocode EN 1998-1-1, Eurocode 8 – Design of structures for earthquake resistance – Part 1: General rules, seismic actions and rules for buildings.

3) Seismosoft [2014] "SeismoStruct v7.0 – A computer program for static and dynamic nonlinear analysis of framed structures," available from *http://www.seismosoft.com*.

4) Sina KA, Topkaya C (2017) "A review of research on steel eccentrically braced frames" Journal of constructional steel research 128, pp 53-73.

5) Nabil Mansour (2010), PhD Thesis, "Development of the design of eccentrically braced frames with replaceable shear links", University of Toronto.

6) Dubina D, Aurel Stratan, Dinu F, "Recentering capacity of dual-steel frames", Steel Construction 4 (2011) 10.1002/stco.201110011.

7) Dubina D, Stratan A, Ioan A, "Recentering Dual eccentrically braced frames with removable links" Proceedings of the Romanian Academy, Series A, Volume 17, Number 2/2016, pp. 167-177.

8) Stratan A, Dubina D (2013), "Numerical simulation of bolted links removal in eccentrically braced frames", Pollack Periodica, DOI: 10.1556/Pollack.8.2013.1.2

9) Elgazouli AY (2009)"Assessment of European seismic design procedures", Bulletin of Earthquake Engineering, 8: 65-89.

10) Hjelmstad KD, Popov EP (1983). "Cyclic behavior and design of link beams". Journal of Structural Engineering, ASCE 1983;109 (10):2387-403

11) Bosco M, Marino E M, Rossi P R (2015). "Critical review of the EC8 design provisions for buildings with eccentric braces" Earthquakes and Structures, Vol 8, No. 6, pp 1407-1433

12) Bosco M, Ghersi A, Marino E M, Rossi P R (2014). "Seismic response and behavior factor of dual eccentrically braced frames designed by Eurocode 8", Second European conference on Earthquake Engineering and Seismology

13) Bosco M, Marino E M, Rossi O R (2016). "A design procedure for dual eccentrically braced – moment resisting frames in the framework of Eurocode 8", Engineering structures 10.1016/j.engstruct.2016.09.059

14) Duscika P, Itani AM, Buckle IG (2010). "Cyclic behavior of shear links of various grades of plate steel" Journal of structural engineering – ASCE 2010:136(4):370-8

15) Mazzolani FM, Della Corte G, D'Aniello M (2009). "Experimental analysis of steel dissipative bracing systems for seismic upgrading". Journal of Civil Engineering and Management 2009;15(1):7-19

16) Okazaki T, Arce G, Ryu HC, Engelhardt MD (2005), "Experimental study of local buckling, overstrength and fracture of links in eccentrically braced frames" Journal of Structural Engineering 2005:131(10): 1526-35

17) Fussell AJ, Clifton GC, Mago N (2014) "Development and research of eccentrically braced frames with replaceable active links"

18) Della Corte G, D'Aniello M, Landolfo R (2013). "Analytican and numerical study of plastic overstrength of shear links" Journal of Constructional Steel Research 82 (2013),pp 19-32

19) Ramadan T, Ghobarah A (1995). "Analytical model for shear link behavior" Journal of Structural Engineering, 1995;121:1574:1580

20) Bosco M, Marino EM, Rossi PR (2016) "Influence of modelling of steel links on seismic response of EBFs". Engineering structures 127 (2016) 459-474.

21) Bosco M, Marino EM, Rossi PR (2015) "Modelling of steel link beams of short, intermediate or long length". Engineering structures 84 (2015) 406-418.

22) Bosco M, Ghersi A, Marino EM, Rossi PR (2015) "Importance of link element in the assessment of the seismic response of multi storey EBFs designed by EC8" International Journal of Earthquake Engineering Num 3 (2015) Anno XXX111.

Appendix A - Design checks for 8 storey frame (Case A)

Project Name: Preliminary Design of Eccentrically Braced Frame
Title of calculations: Pre-design of shear links
Revision: 0
Made by: N. Aravind **Date:** 2/12/2017
Checked by: **Date:**

Material properties of shear link:

										(units)
Cross section of link:		=	HE 180 B	HE 200 B	HE 180 B	HE 180 B	HE 160 B	HE 180 A	HE 140 B	HE 100 B	
Section properties:	b	=	180	200	180	180	160	180	140	100	mm
	d	=	180	200	180	180	160	171	140	100	mm
	t_f	=	14	15	14	14	13	9.5	12	10	mm
	t_w	=	8.5	9	8.5	8.5	8	6	7	6	mm
	A	=	6530	7810	6530	6530	5430	4530	4300	2600	mm^2
	i	=	76.6	85.4	76.6	76.6	67.8	74.5	59.3	41.6	mm
Yield strength (mean strength)	f_y	=	443	443	443	443	443	443	443	443	MPa
Youngs Modulus	E	=	200	200	200	200	200	200	200	200	GPa
Shear modulus	G	=	76.92	76.92	76.92	76.92	76.92	76.92	76.92	76.92	GPa

Section capacity

Plastic section capacity in flexure	M_p	=	213.2602	284.6275	213.2602	213.2602	156.822	143.9307	108.7122	46.1606	kNm
Plastic section capacity in shear	V_p	=	**330.2494**	**391.0848**	**330.2494**	**330.2494**	**274.015**	**233.1172**	**207.5561**	**122.6933**	kN
Optimum link length		=	1.03	1.16	1.03	1.03	0.92	0.99	0.84	0.60	m
Provided link length	e	=	1.00	1.10	1.00	1.00	0.90	0.90	0.80	0.56	m

Stiffness properties

Parameters	η	=	0.169	0.162	0.169	0.169	0.177	0.118	0.188	0.222	
	ξ	=	0.047	0.045	0.047	0.047	0.050	0.033	0.050	0.060	
Shear coefficient	χ	=	4.966	4.966	4.966	4.966	4.906	4.843	5.143	5.074	
Shear stiffness	$k_{L0,1}$	=	GA/(x e/2)								
		=	202286.8	219939.2	202286.8	202286.8	189196.7	159885.7	160791.5	140760.7	kN/m
Post yield stiffness	$k_{L1,1}$	=	894.1075	972.1315	894.1075	894.1075	836.2495	706.695	710.6986	622.1623	
Ultimate shear capacity	V_u	=	$1.5\,V_p$								
		=	**495.3741**	**586.6272**	**495.3741**	**495.3741**	**411.0225**	**349.6758**	**311.3342**	**184.0399**	kN
Equivalent post yield kinematic stiffness	K_{L1}	=	$K_{L0,1} * (V_u - V_p) / (0.08\,K_{L0,1}\,e/2 + V_u - V_p)$								
		=	4045.559	4356.125	4045.559	4045.559	3730.719	3173.475	3178.947	2686.421	kN/m

Seismostruct automatically takes flexural hinges into account in the material model.

INPUT #1 -- Initial stiffness		=	202286.8	219939.2	202286.8	202286.8	189196.7	159885.7	160791.5	140760.7	kN/m
INPUT#2 -- Yield shear		=	**330.2494**	**391.0848**	**330.2494**	**330.2494**	**274.015**	**233.1172**	**207.5561**	**122.6933**	kN
INPUT #3 -- Post yield K ratio		=	0.019999	0.019806	0.019999	0.019999	0.019719	0.019848	0.019771	0.019085	

Project Name:	Preliminary Design of Eccentrically Braced Frame		
Title of calculations:	Elasticity checks for MRF Frame		
Revision:	0		
Made by:	N. Aravind	**Date:**	2/12/2017
Checked by:		**Date:**	

		1	2	3	4	5	6	7	8
Cross section of beam		IPE 360	IPE 360	IPE 360	IPE 360	IPE 360	IPE 360	IPE 360	IPE 360
Cross section of Column 1		HE 260 B	HE 260 B	HE 260 B	HE 260 B	HE 260 B	HE 260 B	HE 260 B	HE 260 B
Cross section of Column 2		HE 400 M	HE 360 M	HE 360 M	HE 360 B	HE 360 B	HE 320 B	HE 300 B	HE 300 B
Columns Steel Grade		460	460	460	460	355	355	355	355
Link length in EBF	e	1	1.1	1	1	0.9	0.9	0.8	0.56
Max deflection of storey	u_{max}	**0.04**	**0.044**	**0.04**	**0.04**	**0.036**	**0.036**	**0.032**	**0.0224**
Obs deflection under 100 kN		0.0064	0.0073	0.0073	0.0104	0.0104	0.012	0.013	0.013
Beam peak moment (obs)		42	47	47	63	63	68	71	71
Scaled up (for umax)		263	283	258	242	218	204	175	122
Beam elastic capacity		416	416	416	416	321	321	321	321
		OK	OK	OK	OK	OK	OK	OK	OK
Column 1 peak moment (obs)		51	49	49	83	83	96	102	102
Scaled up (for umax)		319	295	268	319	287	288	251	176
Column 1 elastic capacity		528	528	528	528	408	408	408	408
		OK	OK	OK	OK	OK	OK	OK	OK
Column 1 axial force (DL + 0.3LL)		734	642	547	454	361	268	174	80
Extreme fiber stress (P/A + M/Z)		339.65004	311.4899	280.0784	316.4202	280.7579	273.5062	233.4041	159.8524
		OK	OK	OK	OK	OK	OK	OK	OK
Column 2 peak moment (obs)		264	250	250	193	193	170	155	155
Scaled up (for umax)		1650	1507	1370	742	668	510	382	267
Column 1 elastic capacity		2217	1977	1977	1104	852	684	596	596
		OK	OK	OK	OK	OK	OK	OK	OK
Column 2 axial force (DL + 0.3LL)		1512	1308	1106	904	707	512	320	135
Extreme fiber stress (P/A + M/Z)		388.73249	391.7036	353.4878	359.3502	317.5127	296.5396	248.839	168.2182
		OK	OK	OK	OK	OK	OK	OK	OK

Check for stiffness of MRF (capability to take storey shear)

Total storey weight (kN) (DL + 0.3 LL)	1445.5	1445.5	1445.5	1445.5	1445.5	1445.5	1445.5	1520.4
Eccentricity (inter storey)	0.040	0.044	0.040	0.040	0.036	0.036	0.032	0.022
Destabilizing moment	2054.7	1589.1	1140.6	790.7	498.6	287.8	129.0	34.1
Obs deflection under 100 kN lateral force	0.0064	0.0073	0.0073	0.0104	0.0104	0.0120	0.0130	0.0130
Lateral force corresponding to max drift	625.0	602.7	547.9	384.6	346.2	300.0	246.2	172.3
Restoring force	625.0	602.7	547.9	384.6	346.2	300.0	246.2	172.3
Lever arm	4.0	4.0	4.0	4.0	4.0	4.0	4.0	4.0
Restoring moment	2500.0	2411.0	2191.8	1538.5	1384.6	1200.0	984.6	689.2
	OK	OK	OK	OK	OK	OK	OK	OK